2019

Temporal and spatial dynamics of submersed macrophytes and water temperatures in shallow flow-through wetlands

Jacob Scott Eeling
Iowa State University

Temporal and spatial dynamics of submersed macrophytes and water temperatures in shallow flow-through wetlands

by

Jacob S. Eeling

A thesis submitted to the graduate faculty

in partial fulfillment of the requirements for the degree of

MASTER OF SCIENCE

Major: Ecology and Evolutionary Biology

Program of Study Committee:
William G. Crumpton, Co-major Professor
Arnold G. van der Valk Co-major Professor
Thomas W. Jurik

The student author, whose presentation of the scholarship herein was approved by the program of study committee, is solely responsible for the content of this thesis. The Graduate College will ensure this thesis is globally accessible and will not permit alterations after a degree is conferred.

Iowa State University

Ames, Iowa

2019

TABLE OF CONTENTS

ACKNOWLEDGMENTS

I would like to thank my committee chair, William Crumpton, and my committee members, Arnold van der Valk and Thomas Jurik, for their guidance, support, and patience throughout the course of this research.

In addition, I would also like to thank my friends, colleagues, and the department faculty and staff for making my time at Iowa State University a wonderful experience. Specifically, I want to also offer my appreciation to David Green, Blake Sunkle, and Alex Andera, without whom this thesis would not have been possible.

Finally, I would like to thank my wife, Megan Eeling, for her continued love, patience, and support during the research and writing of this thesis.

ABSTRACT

Temperature dynamics and stratification within the water column of shallow flow-through constructed wetlands have a significant influence on their ecology and water quality. Recent research has shown that shallow water bodies are more thermally complex and more commonly exhibit complex temperature regimes than previously thought. The patterns of temperature dynamics and stratification alongside submersed macrophyte abundance and distribution were investigated in two shallow flow-through wetlands in central Iowa, USA. Sensor arrays in the water column recorded temperatures at 10-minute intervals, beginning before submersed macrophytes had become established to after submersed macrophyte senescence. Submersed macrophytes were surveyed bi-weekly using a 0.25 m^2 quadrat to estimate percent cover on a per species basis. Submersed macrophyte surveys were interpolated to provide cover estimates over the entire wetland site. Complex diel temperature patterns were observed at both wetlands, with diurnal stratification followed by nocturnal mixing being by far the most common thermal regime. Increases in submersed macrophyte cover coincided with an increase in diurnal stratification. Submersed macrophyte cover appears to enhance diurnal stratification but does not significantly inhibit nocturnal mixing.

CHAPTER 1. GENERAL INTRODUCTION

General Introduction

Shallow water bodies have long been considered to be isothermal systems (Branco & Torgensen, 2009). However, recent research has demonstrated that shallow water bodies can exhibit more complex temperature regimes, including long and short-term stratification (Condie and Webster, 2001; Herb and Stefan, 2005; Chimney *et al*., 2007 Andersen, 2017). Additionally, this research has shown that dynamic and complex temperature regimes in shallow water bodies are more common than previously thought. Complex temperature regimes have been shown to exist in both artificially and natural shallow water bodies.

The ecology and water quality of shallow water bodies is significantly impacted by temperature regimes (Condie and Webster, 2002). Most prior research of temperature in shallow waterbodies have studied natural water bodies such as lakes and ponds (Rose, 1996; Rose and Crumpton, 1996; Herb and Stefan, 2005; Andersen, 2017) and constructed treatment wetlands (Kadlec and Wallace, 2009). However, wetlands used for intercepting and treating non-point source loads have had much less research conducted into their water temperature dynamics and stratification. These systems generally exhibit ecological and hydraulic characteristics of both constructed and natural wetlands and likely also exhibit complex temperature dynamics similar to other shallow waterbodies.

Therefore, this study was designed to document and describe the spatial and temporal dynamics of submersed vegetation, water temperatures, and controlling environmental factors in two shallow flow-through wetlands receiving unregulated, non-point source loads. This data will inform an understanding of the spatiotemporal temperature dynamics of these shallow flow-

through constructed wetlands and the relationships between temperature, submersed macrophytes, and other environmental factors.

Thesis Organization

Chapter 2 is a paper anticipated to be submitted to the journal *Wetlands*. Jacob S. Eeling will be the first author, David I. Green will be the second author, and William G. Crumpton will be the third author. This paper details the results of a one-year comprehensive field study documenting the spatial and temporal dynamics of submersed vegetation and temperatures in two shallow flow-through surface water wetlands. The final chapter provides a general summary of the work and conclusions presented in Chapter 2.

References

Andersen, M. R., Sand-Jensen, K., Woolway, R. I., & Jones, I. D. (2017). Profound daily vertical stratification and mixing in a small, shallow, wind-exposed lake with submerged macrophytes. *Aquatic Sciences*, *79*(2), 395-406.

Branco, B. F., & Torgersen, T. (2009). Predicting the onset of thermal stratification in shallow inland waterbodies. *Aquatic Sciences-Research Across Boundaries*, *71*(1), 65-79.

Chimney, M. J., Wenkert, L., & Pietro, K. C. (2006). Patterns of vertical stratification in a subtropical constructed wetland in south Florida (USA). *Ecological engineering*, *27*(4), 322-330.

Condie, S. A., & Webster, I. T. (2001). Estimating stratification in shallow water bodies from mean meteorological conditions. *Journal of Hydraulic Engineering*, *127*(4), 286-292.

Condie, S. A., & Webster, I. T. (2002). Stratification and circulation in a shallow turbid waterbody. *Environmental Fluid Mechanics*, *2*(3), 177-196.

Gu, R., & Stefan, H. G. (1995). Stratification dynamics in wastewater stabilization ponds. *Water Research*, *29*(8), 1909-1923.

Herb, W. R., & Stefan, H. G. (2005). Model for wind-driven vertical mixing in a shallow lake with submersed macrophytes. *Journal of hydraulic engineering*, *131*(6), 488-496.

Kadlec, R. H., & Wallace, S. (2009). *Treatment wetlands*. CRC press.

Rose, C. 1996. Effects of emergent vegetation on wetland microbial processes. Ph.D. Thesis. Iowa State University, Ames, IA, USA.

Rose, C. and W. G. Crumpton. 1996. Effects of emergent macrophytes on dissolved oxygen dynamics in a prairie pothole wetland. Wetlands 16:495–502.

CHAPTER 2. TEMPORAL AND SPATIAL DYNAMICS OF SUBMERSED MACROPHYTES AND WATER TEMPERATURES IN SHALLOW FLOW-THROUGH WETLANDS

A paper to be submitted to the Journal *Wetlands*

Jacob S. Eeling, David I. Green, William G. Crumpton

Abstract

Temperature dynamics and stratification within the water column of shallow flow-through constructed wetlands have a significant influence on their ecology and water quality. Recent research has shown that shallow water bodies are more thermally complex and more commonly exhibit complex temperature regimes than previously thought. The patterns of temperature dynamics and stratification alongside submersed macrophyte abundance and distribution were investigated in two shallow flow-through wetlands in central Iowa, USA. Sensor arrays in the water column recorded temperatures at 10-minute intervals, beginning before submersed macrophytes had become established to after submersed macrophyte senescence. Submersed macrophytes were surveyed bi-weekly using a 0.25 m^2 quadrat to estimate percent cover on a per species basis. Submersed macrophyte surveys were interpolated to provide cover estimates over the entire wetland site. Complex diel temperature patterns were observed at both wetlands, with diurnal stratification followed by nocturnal mixing being by far the most common thermal regime. Increases in submersed macrophyte cover coincided with an increase in diurnal stratification. Submersed macrophyte cover appears to enhance diurnal stratification but does not significantly inhibit nocturnal mixing.

Introduction

Recent research has shown that shallow surface water bodies, such a wetlands, lakes, ponds, and wastewater treatment basins, can exhibit dynamic spatiotemporal variations in water column temperatures, including both short and long-term thermal stratification (e.g. Condie and Webster, 2001; Herb and Stefan, 2005; Chimney *et al*., 2007 Andersen, 2017), and that this behavior is more common than previously thought. For example, Gu and Stefan (1995) showed that shallow (1 – 2 m) wastewater stabilization ponds in Minnesota will, in addition to isothermal conditions, frequently exhibit periods of daytime stratification followed by nocturnal mixing of the water column. Alternatively, these systems might also demonstrate consecutive periods of both day and nighttime stratification. In both cases, these researchers showed that the occurrence of these conditions is strongly affected by both wind shear and advective currents. Likewise, Herb and Stefan (2005) for a shallow lake in Minnesota, Chimney *et al*. (2007) for a constructed treatment wetland in Florida, and Andersen (2017) for a shallow lake in Sweden each have shown that such dynamic stratification conditions are likely to exist within shallow natural water bodies as well. Additionally, these researchers have independently shown that the likelihood of occurrence of stratification in these systems is strongly affected by the spatial (vertical and horizontal) distribution and biomass of submersed macrophytes in addition to atmospheric and current effects.

The temperature dynamics of shallow waterbodies can have significant influences on their ecology and water quality (Condie and Webster, 2002), and for those systems used for wastewater treatment, their nutrient removal performance (Kadlec and Reddy, 2001). Most prior studies of temperatures in shallow water bodies have focused on natural lakes, ponds and

wetlands (Rose 1996; Rose and Crumpton 1996; Herb and Stefan, 2005; Andersen, 2017), and on constructed treatment wetlands (Kadlec and Wallace, 2009).

In contrast, wetlands used for intercepting and treating non-point source loads have been the subject of considerably fewer studies of water temperature dynamics and stratification. These wetlands are subjected to uncontrolled environmental conditions and receive unregulated flows from upslope areas. As such, these systems generally exhibit ecological and hydraulic characteristics of both constructed and natural wetlands, including the seasonal growth and senescence of large communities of submersed macrophytes (Green, 2016), and are thus likely to also exhibit spatiotemporal temperature dynamics that are similar to other shallow waterbodies. However, to-date, the temperature dynamics of these types of systems and controlling environmental factors have not been explored in-depth.

This study was designed to document and describe the spatial and temporal dynamics of submersed vegetation, water temperatures and controlling environmental factors in two shallow flow-through wetlands receiving unregulated, non-point source loads. The objectives of this study are to: 1) document submersed macrophyte cover and spatial distributions within each wetlands from the onset of growth through senescence; 2) concurrently document spatial and temporal patterns in temperatures at high vertical resolutions within each wetland; 3) concurrently document hydrological and atmospheric conditions for each wetland; and 4) assess temporal and spatial patterns in stratification with respect to changes in monitored environmental variables and submersed macrophyte characteristics.

Materials and Methods

Study Sites

This study was conducted on two shallow flow-through surface water wetlands (referred to herein as KS and RS) located in Story County in central Iowa, USA (Figures 1 and 2). These wetlands were created by impounding channels below the outlets of small, tile-drained agricultural watersheds to mitigate nutrient loads as part of the Iowa Conservation Reserve Enhancement Program (CREP, http://www.iowaagriculture.gov/waterResources/CREP.asp). The KS wetland was 1.34 ha with an average depth of 0.54 m, and the RS wetland was 2.4 ha with an average depth of 0.7 m (Table 1). Each wetland is fed by subsurface tile drainage and surface runoff from upslope agricultural catchments ranging from 740 acres (KS) to 1162 acres (RS). Flows are delivered to each wetland through a single inflow channel that gradually opens into a larger and deeper seasonally vegetated pool, characterized by a deeper (>1 m) central area bordered by shallow (<1 m) littoral regions. The basins impounded existing surface channels, the remnants of which are still distinctly present in the RS wetland (Figure 2). Each site is surrounded by a restored prairie buffer ranging from 18 acres (KS) to 40 acres (RS).

Atmospheric and Flow Monitoring

Atmospheric conditions were monitored with Vantage Vue weather stations (Davis Instruments, Hayward, California) deployed at each study site. Weather stations recorded rainfall, wind speed, wind direction, humidity, and temperature every 30 minutes from April 23rd to December 31st. Hourly solar radiation data was obtained from the Iowa State University Soil Moisture Network (https://mesonet.agron.iastate.edu/) for the Iowa State University Horticulture Farm (site AEEI4). Flow monitoring was conducted as part of a broader long-term study of Iowa

CREP wetland nutrient removal performance by researchers at Iowa State University (Crumpton and Stenback 2016).

Temperature Monitoring

Water temperatures were monitored using horizontally distributed stationary, vertical temperature sensor arrays. Eleven arrays were installed at the KS wetland, and 12 were installed at the RS wetland (Figures 1 and 2). The arrays were constructed with 1-inch PVC pipe onto which HOBO Pendant Temperature/Alarm 8K Data Logger sensors were attached (UA-001-08; Onset Corporation, Bourne, Massachusetts). Sensors were attached at even vertical intervals along the length of each array, spanning from approximately 2 cm below the water surface to approximately 2 cm above the sediment-water interface (Figure 3). Three arrays at each wetland were also fitted with an atmospheric sensor and radiation shield to record temperatures directly above the surface of the water.

Each array was fitted over a sunken galvanized metal pipe driven into the sediment to maintain stability in the water column. The number of sensors per array was determined by the local water depth at the location of the array, with the aim of establishing a spacing between sensors of between five and 10 cm, depending on water depth and the number of sensors on each given array. This interval was specific to each array, ranging from 3 sensors at the shallowest location, to 11 sensors at the deepest.

The sensor arrays were positioned throughout each wetland so that the number of arrays placed in shallow water areas (< 1 m) and in deep water areas (> 1 m) was proportional to the percentages of shallow and deep water area for each wetland (Tables 1 and 6, and Figures 1 and 2).

Inlet and outlet temperatures were measured throughout the study. Outlet temperatures at each wetland were measured with a single sensor located halfway through the water column at each respective wetland outlet. Inlet temperatures at RS were monitored as a part of the flow monitoring installations discussed previously. Inlet temperatures at KS were initially measured with an array with a single sensor, similar to the outlet arrays. Due to a technical issue, however, data for the KS inlet array was irretrievable after June 14th. Data for this sensor beyond this date was estimated from temperatures measured at the inlet of the RS wetland (data not shown).

Temperatures were measured at 10-minute intervals for each array sensor from before the onset of submersed macrophyte growth in mid-April and early May to at least two weeks after senescence in mid-November 2016. Temperatures were monitored for 235 days at KS beginning on April 1st and ending on November 21st, and for 195 days at RS beginning on April 29th and ending on November 9th. Monitoring over this period allowed temperatures to be recorded before vegetation became established, during various stages of vegetative growth throughout the growing season, and after senescence.

Vegetation Surveys

Submersed macrophyte cover surveys were conducted on each of the wetlands at approximately bi-weekly intervals beginning in mid-May corresponding to the onset of submersed macrophyte growth, and ending in late October, after senescence. During this period, 10 and nine surveys were conducted on the KS and RS wetlands, respectively. Each survey entailed the use of a 0.25 m^2 quadrat to document the percent cover of submersed macrophyte species at approximately 10 m intervals along transects running perpendicular to the primary flow direction from each respective wetland inlet to outlet, closely following the methods of

Titus *et al.* (2004). Emergent macrophytes were generally absent from each wetland pool except for very thin patches on the basin margins for sites KS and RS, and each wetland is almost completely dominated by submersed macrophytes. Therefore, surveys neglected documenting percent cover in emergent-dominated areas.

Surveys were conducted from small boats to minimize disturbance of vegetation and sediment. Percent cover at each survey location was assigned based upon a modified Daubenmire classification scheme (Daubenmire, 1959) using class intervals of 5%. Total percent cover of species was measured from 0 to 100 percent. The coordinates of each survey point were recorded using a Differential GPS unit (GeoXT model, Trimble, Sunnyvale CA). Approximately 100-250 data points were recorded for each survey.

Spatial Interpolation of Vegetative Cover

Kriging was used to interpolate measured submersed macrophyte percent cover measurements to represent vegetative cover data from each survey as a continuous surface for subsequent estimation of percent cover values at each array. To establish covariance for each kriging routine, semivariograms were fitted to each survey to model the relationship between variance and distance between points using measured percent cover estimates. This model was then used to interpolate to a 1 m^2 grid across the entire area of each wetland. Universal kriging was decided to be the most appropriate interpolation method due to possible anisotropy in the data. Interpolation was conducted using the R statistical computing language (R Core Team, 2015).

Kriging was also used to interpolate individual species percent cover values to represent percent cover by species through the growing season. The same kriging routines were used to

estimate species-specific percent cover as total percent cover. Species-specific percent cover shows the changes in species abundance and dominance throughout the year throughout each wetland. A given species of submersed macrophyte may be more or less likely to influence temperature regimes in wetlands than other species of submersed macrophytes. Therefore, species-specific cover values can be used inform the understanding of temperature regimes when abundance of each species is known for each array location. The semivariograms developed during the kriging process are given in Appendix D.

Results

Spatiotemporal Vegetation Patterns

The onset of submersed macrophyte growth at both wetlands began in middle to late May, followed by a period of sustained development during the summer months, and, ultimately, senescence between the middle of October and early November. Three species of submersed macrophytes were observed within the study sites: *Ceratophyllum demersum* (*C. demersum*), *Stuckenia pectinata* (*S. pectinata*), and *Chara vulgaris* (*C. vulgaris*); species that were also documented by Green (2016) within the KS wetland during surveys conducted in 2010 and 2011.

During the early part of the growing season, submersed macrophytes tended to become established primarily in the shallow sections of each wetland (Figures 4 and 5). This growth phase was followed by a differential rapid expansion of both percent cover and spatial extent into the deeper sections of each wetland pool, with *S. pectinata* occurring mostly within shallow areas (typically less than 0.5 m depth), and *C. demersum* occupying deeper section of each pool (typically 0.5 to greater than 1 m depth). Figures 4 and 5 show seasonal changes over the course

of the growing season for both wetlands for selected survey dates. Maps of interpolated percent vegetative cover for all vegetation surveys for both wetlands are provided in Appendix B.

In general, early season growth was observed to be comprised primarily of *S. pectinata* at both study sites. For the KS wetland, *S. pectinata* and *C. demersum* followed similar growth patterns from the early stages of development starting in mid-May, maximum growth in early to mid-July, and wetland-wide senescence in mid to late October (Figure 6). *C. vulgaris* began to become more prevalent within this wetland beginning at the peak of the growth cycle for *S. pectinata* and *C. demersum* and remained the dominant species for the remainder of the study period (Figure 6). In contrast, *S. pectinata* was observed to be the most prevalent species in the RS wetland between the onset of vegetative growth in mid-May and early September, when *C. demersum* became dominant (Figure 7).

For the KS wetland, wetland-wide mean peak percent cover for *S. pectinata* and *C. demersum* both reached approximately 28% in late June and early July. Similarly, for the RS wetland, *S. pectinata* reached a peak wetland-wide average percent cover of 59% during early July, while *C. demersum* reached peak growth during late August to early September, with an average percent cover of approximately 18%. Complete fall senescence was observed to occur approximately one month earlier at the RS wetland at the end of September while submersed macrophyte cover persisted into the month of October at the KS wetland (Figures 4 and 5). Interpolated submersed macrophyte cover for each array location can be found in Table 2 (KS) and Table 3 (RS).

Flow and Weather Conditions

In general, non-storm related flows gradually declined from the start of the study period, or were nearly constant, and rarely exceeded 1000 m^3d^{-1} at both wetlands. Periodic high-flow events occurred in late May, early June, and the middle of September at the KS wetland, and in the middle of August at the RS wetland (bottom panels of Figures 8 and 9), resulting from several successive late-season rain events. Mean daily flow rates for the KS and RS wetlands were 2,726 and 5670 $m^3\ d^{-1}$, respectively.

Short-wave solar radiation (W m^{-2}), the principal source of heat inputs into these systems, increased throughout the spring, peaked at the summer solstice, and slowly diminished throughout the remainder of the year, following annual solar cycles (middle panels of Figures 8 and 9). Day-to-day variability in mean daily solar radiation throughout the study period is mostly likely attributable to day-to-day variability in cloud cover.

Daily average wind speeds over the course of the monitoring period were approximately 1.69 and 2.29 m s^{-1} for the KS and RS wetlands, respectively (bottom panels of Figures 8 and 9), and tended to remain below 2 m s^{-1}. However, on a few occasions, particularly during brief storm events, wind speeds occasionally exceeded 4 m s^{-1}. As has also been observed by Andersen (2017) among others, wind speeds at both wetlands exhibited distinct diurnal patterns, with highest winds occurring during daylight hours, generally followed by decreased speeds during nighttime hours.

Seasonal Temperature Dynamics

As would be expected for the mid-continental temperate climate of central Iowa, seasonal changes in water temperatures in both wetlands closely followed seasonal changes in air

temperature and solar radiation inputs (Figures 8 and 9). In general, daily average water column temperatures within both wetlands tended to be equal to or below, equal to or exceeding, and above daily average air temperatures during spring, summer, and fall months, respectively.

As observed in Figures 10 and 11 and enumerated in Tables 4 and 5, from April (KS only) through the middle of May (KS and RS), prior to the beginning of vegetation growth, mean water column temperatures were approximately 11.1 ºC in April and 13.2 ºC in May for the KS wetland, and 15.1 ºC in May for the RS wetland. During this same period, average surface and bottom temperatures at the KS wetland ranged from approximately 11.8 to 10.4 ºC in April and 14.5 to 12.3 ºC in May, respectively. Surface and bottom temperatures at the RS wetland ranged from approximately 17.6 to 12.3 ºC in May, respectively. In both wetlands during early to late spring months air temperatures ranged from -4 to 28 ºC, and were, in general, approximately equal to mean depth-average and surface temperatures, and slightly higher than bottom temperatures, with significant temporal deviations related to inter-month variability in weather patterns. Average and maximum mean water column temperatures also tended to remain between 4 and 6 ºC above influent temperatures, indicating significant atmospheric heating during this part of the year (Figures 10 and 11).

By June and July, submersed macrophytes had become established, occurring throughout both wetlands at all water depths. Depth-average mean temperatures at the KS wetland were 21 and 22.5 ºC in June and July respectively. Depth-average June and July mean temperatures the RS wetland were similar, with temperatures of 21.4 and 22.7 ºC, respectively. Surface and bottom temperatures for the KS and RS wetlands ranged from 23.6 to 18.7 ºC, and 26.1 to 14.5 ºC in June and 25.1 to 20.7 ºC, and 26.8 to 17 ºC in July, respectively (Tables 4 and 5, and Figures 10 and 11). The mean depth-average, surface, and bottom water temperatures during

these two months tended to be equal to or slightly lower than average air temperatures. However, by July temperatures at the surface of the water columns of both wetlands tended to greatly exceed both air temperatures and bottom temperatures, in some cases by as much as 10 ^{o}C, indicating significant thermal stratification. During both months, mean depth-average, surface, and bottom temperatures tended to be above influent temperatures, sometimes by between 8 and 10 ℃. This difference was markedly higher in the KS wetland, with an increase in influent temperatures from June to July of nearly 8 ^{o}C, compared with only a 2 ^{o}C increase over this same period for the RS wetland.

In late summer and early fall months, during peak vegetation growth in both wetlands, depth-average mean water temperatures in the months of August and September decreased in both wetlands to 19.4 and 17.2 ℃ for KS, 18.8 and 14.5 ℃ for RS. Similarly, average surface temperatures had cooled dramatically compared to early summer, and during this period remained, on average, 2 to 4 ^{o}C warmer than ambient air temperatures. Depth-average surface temperatures at KS were 21.2 ℃ in August and 17.5 ℃ in September, marking a drop of almost 8 ℃ from July. Surface temperatures at RS saw a similar drop, with averages in August of 23.3 ℃, and in September of 20 ℃. Temperatures at the bottom of the water column remained much more consistent than temperatures at the surface. At KS, average bottom temperatures in August were 18.3 ℃ and 16.9 ℃ in September, while average bottom temperatures at RS in August were 18 ℃ and 17.7 ℃ in September (Tables 4 and 5; Figures 10 and 11). Bottom water temperatures for this period remained nearly equal to (KS) or 2 ^{o}C above (RS) influent temperatures for this period. Surface temperatures, in contrast, remained, on average, 5 to 8 ^{o}C above influent temperatures, occasionally reaching a maximum difference of nearly 10 ℃ at

both sites. Depth-average mean temperatures tended to remain 5 ^{o}C greater than the influents of both wetlands.

Submersed macrophytes rapidly senesced in October, with almost no submersed cover remaining in either wetland by the middle of the month (Figures 6 and 7). Depth-average temperatures at KS in October were 13.7 ℃, while average temperatures at RS were 14.5 ℃. Average surface and bottom temperatures were 13.5 and 13.7 ℃ and 14.9 and 14.3 ℃ at the KS and RS wetlands, respectively (Tables 4 and 5; Figures 10 and 11). During this period, depth-average mean, surface, and bottom temperatures tended to be 2 to 5 ^{o}C warmer than ambient air temperatures, and approximately equal to influent temperatures.

Spatial Temperature Patterns

Prior to the establishment of vegetation, temperatures at the water surfaces of both wetlands exhibited little variability with water depth. Temperatures at the bottom of the water column at the sediment-water interface, in contrast, tended to decrease with increasing depth (Figures 12 and 13). These patterns are also evident during periods of high vegetative growth (Figures 14 and 15). However, during this period, surface and bottom temperatures tended to exhibit greater variability, particularly with respect to extreme temperatures values, and with respect to differences between top and bottom values.

During spring and summer months when average air temperatures tended to exceed influent temperatures, surface and bottom water temperatures generally increased with distance from inlet to outlet along the length of each system (Figures 16 through 19), with more rapid heating of surface layers, indicating a net gain of heat from atmospheric inputs during these periods. During the cooler fall months when ambient air temperatures were often lower than

influent temperatures, surface and bottom temperatures tended to decrease from inlet to outlet, with bottom temperatures often exceeding those at the surface (Figures 20 and 21); indicating a net heat loss from both wetlands and a generally unstably stratified water column along the lengths of both systems for this period. These patterns are common to shallow flow-through surface water bodies such as constructed treatment wetlands (Kadlec and Wallace, 2009), but to our knowledge have not previously been observed in flow-through wetlands in agricultural landscapes.

The distances along the lengths of both wetlands at which surface and depth-average temperatures plateau mark the locations within these systems where the upper portion of the water column has established an approximate heat exchange equilibrium with the atmosphere (Kadlec and Wallace, 2009). At these points, neglecting sediment losses and gains, net heat inputs to these wetlands from shortwave and longwave radiation and influent temperatures approximately equal net heat losses from evaporation, convective cooling, and advective exports through the outlets. As shown in Figures 16 and 18, in the KS wetland surface thermal equilibrium tended to become established for both spring and summer months at approximately 181 m from the inlet (~65% of the total length). In the RS wetland (Figures 17 and 19) surface thermal equilibrium tended to become established for these periods at approximately 318 m from the inlet (~52% of the total length). For the cooler fall months, thermal equilibrium on average tended to be reached at 132 m from the inlet for the KS wetland, and 465 m for the RS wetland. These results suggest that the KS wetland during fall months tended to lose heat more rapidly than the RS wetland.

In contrast to surface temperatures, bottom temperatures in both wetlands tended to exhibit more gradual changes with distance from inlet to outlet (Figures 16 through 19). During

spring and summer months bottom temperatures in both wetlands were, on average, approximately 5 to 8 ^{o}C less than surface temperatures, and tended to gradually increase with distance from the inlet, but generally remained close to influent temperatures (an average of approximately 8 ^{o}C) (Figure 16). During fall months, bottom temperatures were, on average, 1 to 2 ^{o}C higher than surface temperatures and generally declined with distance at a smaller rate than did surface temperatures (Figure 18). Of the two systems, the RS wetland exhibited significantly greater longitudinal variability in bottom temperatures than did the KS wetland. These patterns are consistent with other observations of shallow flow-through systems (Kadlec and Wallace, 2009).

Stratification Dynamics

As has also been observed for other shallow water bodies (e.g. Gu and Stefan, 1995; Herb and Stefan, 2005; Chimney *et al*., 2007, Andersen *et al*., 2017), diel thermal stratification was found to occur at nearly all temperature sensor arrays within each wetland throughout the study period, but tended to be most prevalent during late spring to early fall. During some periods of daytime stratification, particularly in the middle summer months when submersed macrophyte cover and distributions were greatest and solar radiation inputs highest, the difference between surface and bottom temperature at each monitoring location within each wetlands was observed to exceed 5 ℃ in less than a meter of water, with this difference increasing up to 10 ℃ with increasing depth and vegetative cover (Figures 22 through 25). Brief periods of successive daytime and nighttime stratification were also observed to occur throughout both systems, particularly during summer months when submersed macrophyte cover was greatest but tended to be most prevalent and persistent in shallow locations. Complete mixing of the water column at

all depths tended to occur most frequently during early spring and late fall months. Contour plots showing the vertical structure of daily average water column temperatures for all arrays are shown in Appendix A.

Gu and Stefan (1995) formally identified and defined three dominant thermal stratification regimes in shallow water bodies exposed to ambient atmospheric forcings: Type 1 stratification, defined by a completely mixed water column during contiguous daytime and nighttime hours; Type 2 stratification, defined by a stratified water column during the day and a mixed water column at night; and Type 3 stratification, defined by the water column remaining continuously stratified between successive daytime and nighttime hours. These stratification classifications were evaluated for our datasets for both wetlands by calculating the percent of time within contiguous sunrise-to-sunrise periods (defined from identification of daytime and nighttime hours from continuous 15-minute solar radiation time-series) that each monitoring array experienced a mean temperature gradient (estimated from the absolute value of the difference between the water surface and bottom temperatures, divided by the local water depth) greater than 4 °C m^{-1}. Each sunrise-to-sunrise period in the temperature time-series for each array was assigned to Type 1 stratification if the percent of observations spent above the gradient threshold was less than 2%. Type 3 was assigned if the gradient threshold was exceeded for 98% of a defined period. Type 2 was assigned to all other cases. The frequency of stratification types aggregated by month for all arrays at both KS and RS are shown in Figures 26 and 27 respectively. Examples of diurnal stratification patterns in both shallow and deep locations within both wetlands are given in Figures 28 and 29.

In the KS wetland, a large portion of the spring months consisted of types 1 and 2 stratification, while Type 3 was very rarely observed. Type 1 stratification became less common

throughout the end of spring into early summer, while both types 2 and 3 became more prevalent. By June, almost no Type 1 stratification was observed, and Type 2 was the most prevalent condition. At this time, Type 3 stratification was also becoming more common, particularly at arrays positioned in deeper water, with the two deepest arrays exhibiting this condition for between 38 and 50% of observations. By July, when vegetative growth had reached its peak, Type 3 stratification was observed to occur at all arrays for at least 10% of observations, and for up to 25% of observations at the shallowest array (0.2 m). Throughout the remainder of the growing season, Type 1 stratification was observed most commonly in arrays in deep water, while Type 3 stratification was consistently only observed in arrays positioned in shallow water. By October, during which submersed macrophyte senescence had begun in earnest, the two deepest arrays in the KS wetland almost always exhibited Type 1 stratification, while types 2 and 3 remained more common in shallower locations (Figure 26)

Similar patterns were observed at the RS wetland; however, this system tended to exhibit a greater percentage of Type 1 stratification than did the KS wetland, particularly during spring and fall months, and within deeper locations in the wetland pool (Figure 27). At the beginning and the end of the growing season, almost all arrays in this wetland had spent over 50% of observations in types 1 and 3 stratification. Type 2 stratification, in contrast, was less commonly observed in deeper locations in this system than in the KS wetland for this period but did exhibit the same tendency to occur more often in shallow locations.

Discussion

Both wetlands exhibited complex spatiotemporal temperature distributions and thermal stratification patterns over the course of the study period. These temperature dynamics result

from complex time-varying interactions between unregulated flow-through rates and inlet temperatures, solar radiation inputs, wind shear, and the regulating effects of vegetative cover on these processes.

In general, daytime stratification followed by nighttime mixing was the most dominant form of stratification within the wetlands studied. This observation is in accordance with the findings of Gu and Stefan (1995), Herb and Stefan (2005), and Andersen (2017) for similarly sized shallow water bodies. However, in contrast to common belief (e.g. Condie and Webster, 2002) our study reveals that persistent daytime-nighttime stratification is also possible, and indeed somewhat prevalent, in these systems, even within extremely shallow water.

Effects of Wind and Flow on Stratification Patterns

Wind and flow are factors that can, separately and together, impact the spatiotemporal distribution of temperatures as well as stratification regimes in shallow water systems. Dale and Gillespie (1978) showed that higher wind speeds tend to increase vertical mixing of the water column, and increase evaporation, resulting in a more isothermal water column. Additionally, submersed macrophytes were found to have reduced the impact of wind mixing, but only at low wind speeds, a finding also supported by Herb and Stefan (2005). Dale and Gillespie (1978) suggest a wind speed threshold of 4 m s^{-1}, above which wind mixing tends to no longer be affected by submersed macrophyte density.

At our study sites, wind speed rarely exceeded 4 m s^{-1}, occurring only during a brief period at the KS study site very late in the fall when isothermal conditions tended to dominate in both wetlands and vegetation had generally senesced. However, while wind shear tended to have a lesser effect on stratification dynamics than flow-through rates (data not shown), there are a

few brief periods within our dataset that seem to suggest that wind may play a role in vertical mixing in our study wetlands under certain conditions, particularly during low-flow periods and for locations with relatively sparse vegetative cover. For instance, as shown in Figures 22 through 25 (and in similar figures in Appendix A) isothermal or near-isothermal conditions for both deep and shallow locations in both wetlands tended to occur during brief periods of relatively high wind speeds (> 2 m s^{-1}), low flow rates (0 - 2500 m^3 d^{-1}), and low to moderate vegetative cover (approximately 5 to 10%) on days 160 (early June), 180 (late June), and 190 (early July). Cloud cover during these periods was relatively low and solar radiation relatively high, indicating that wind-driven vertical mixing was sufficient, and submersed aquatic vegetation sparse enough, to overcome the natural tendency for the water column to stratify under such conditions, at least in deeper locations within each wetland. This is particularly notable given the tendency at both wetlands, as discussed previously, for cooler inlet waters to be transported within lower layers of the water column nearer the sediment. In general, our results are in agreement with the findings of Herb and Stefan (2005) that wind shear can reduce stratification in shallow systems, but tends to be less important than other factors such as through-flow rates and vegetative cover.

The few brief periods of storm-induced high flow rates encountered during this study similarly tended to coincide with vertical isothermal conditions, under both sparsely and densely vegetated conditions; however, this tendency appears to be strongly influenced by the magnitude of flow. For example, storms occurring during the 3-day period surrounding day 200 (corresponding to late July) resulted in flows of up to 1000 and 3000 m^3 d^{-1} at the KS and RS wetlands, respectively. During this brief period nearly all arrays within the RS wetland exhibited nearly uniform vertical temperature profiles. In contrast, only the more shallow arrays within the

KS wetland tended to exhibit isothermal profiles during this period, and, while reduced with respect to the period before this flow event, deeper arrays tended to show diminished, but not absent, stratification. The difference in the stratification behavior of these two systems during this event is likely attributable to the nearly 3-fold higher flow rates seen at the RS site. Similar dynamics are also observed for the flow events occurring around days 230 and 240. While anecdotal, these examples support the general conclusions of Condie and Webster (2001) that through-flow can strongly impact vertical temperature distributions, regardless of local water depth, and that this effect can sometimes greatly exceed the effects of wind-driven mixing.

Effects of Vegetation on Stratification and Temperature Patterns

Figure 30 shows that higher submersed macrophyte percent cover tended to coincide with an increase in Type 2 stratification, and a decrease in Type 1. In contrast, the likelihood of Type 3 stratification is shown to be only slightly affected by vegetative cover. These observations support the conclusions of other research into the effects of submersed macrophytes on the stratification dynamics of shallow water bodies. For instance, Dale and Gillespie (1977) observed that submersed macrophyte biomass near the top of the water column tends to trap heat from solar radiation, with the amount trapped being a positive function of plant biomass (Dale and Gillespie, 1978; Herb and Stefan, 2005).

This is particularly the case for *S. pectinata*, which has been shown to intercept higher amount of radiation than other species (Dibble, 1996), and is highly prevalent in our study wetlands. In the absence of advective stirring, such as through wind shear at the water surface or strong flow-through currents, heat trapped in vegetation near the water surface is likely only able to be transported to lower shaded layers of the water column through thermal diffusion or

convective nighttime mixing. These processes result in the development of persistent daytime stratification proceeded by nighttime mixing (Type 2 stratification), which becomes more likely with increases in submersed macrophyte biomass and relatively cool bottom waters (Herb and Stefan, 2005). This seems to be particularly common in the areas of the KS and RS wetlands comprised primarily of *S. pectinata* and *C. demersum*, as a large percentage of the biomass of these species at the peak of their growth cycles is concentrated at the water surface (Dibble et al., 1996).

The trapping of heat by the vegetation canopy nearest the water surface may also explain the increased occurrence of Type 3 stratification observed at both wetlands during the months of June and July; the period during which vegetative cover tended to be highest. These months, with the exception of brief episodic flow events, also corresponds to the period of lowest flows and wind speeds and highest rates of solar radiation, suggesting that the likelihood that persistent daytime-nighttime stratification will develop at a given location is also strongly dependent on these factors.

Conclusions

Temperature and stratification dynamics of these shallow flow-through wetlands showed complex spatiotemporal patterns over the course of the study. In general, for most of the study period prior to mid to late fall, water temperatures tended to be cooler at the bottoms of both wetlands than at the surface, particularly within deeper sections. During mid to late fall this pattern was inverted, indicating heating of the water column from heat stored in the wetland sediments. Likewise, bottom, surface, and depth-averaged temperatures tended to increase with distance from the wetland inlets during spring and summer months and decreased with distance

during fall months. The former case suggests a net heating of the water column during spring and summer months, while the latter indicates a net loss of heat during fall months. In both cases each wetland tended to approach thermal equilibrium with the atmosphere between 50 and 60% of the distance into each system.

Type 2 stratification, defined by strong vertical daytime temperature gradients followed by nighttime mixing, was the most common stratification regime observed in both systems. Types 1 and 3 stratification, defined by a completely mixed water column of the successive daytime and nighttime periods, and contiguous periods of complete daytime and nighttime stratification respectively, were therefore less common, with Type 1 stratification being primarily observed during colder, sparsely vegetated conditions while Type 3 stratification was primarily observed during warmer, densely vegetation conditions. Stratification appears to be enhanced with the presence of submersed macrophytes both by permitting the formation of higher temperatures at the surface of the wetland and shading lower portions of the water column. Additionally, submersed macrophytes inhibit some of the environmental factors that are associated with creating a more isothermal water column. However, submersed macrophytes appear to have little effect on nocturnal mixing patterns. As a result, the most common temperature regime is a diel pattern of stratification during the day and mixing during the night.

While this study provides empirical evidence that complex stratification and temperature behavior can occur in these shallow flow-through wetlands, a more detailed understanding of the effects of submersed macrophytes on these dynamics and their physical causes will require future research. A more detailed analysis of submersed macrophyte cover and structure could yield more information about relationships between temperature, stratification, and submersed macrophyte cover, and help to identify conditions during which individual stratification types are

likely to develop, and whether the effects of vegetation can be distilled to include individual species effects. For example, a more detailed, species-specific, morphometric analysis of the submersed macrophyte leaves, stems, and canopy structure could provide additional evidence about the effects individual species have on temperature and stratification.

Acknowledgements

This work was supported by funding from the Iowa Department of Agriculture and Land Stewardship. We thank Blake Sunkle and Alex Andera for assistance with vegetation surveys and temperature monitoring. Additionally, we would like to thank the landowners of the wetland study sites for granting us access and permission to conduct this research.

References

Andersen, M. R., Sand-Jensen, K., Woolway, R. I., & Jones, I. D. (2017). Profound daily vertical stratification and mixing in a small, shallow, wind-exposed lake with submerged macrophytes. *Aquatic Sciences*, *79*(2), 395-406.

Chimney, M. J., Wenkert, L., & Pietro, K. C. (2006). Patterns of vertical stratification in a subtropical constructed wetland in south Florida (USA). *Ecological engineering*, *27*(4), 322-330.

Condie, S. A., & Webster, I. T. (2001). Estimating stratification in shallow water bodies from mean meteorological conditions. *Journal of Hydraulic Engineering*, *127*(4), 286-292.

Condie, S. A., & Webster, I. T. (2002). Stratification and circulation in a shallow turbid waterbody. *Environmental Fluid Mechanics*, *2*(3), 177-196.

Crumpton, W. G., Helmers, M. J., Stenback, G. A., Lemke, D. W., & Richmond, S. (2012). Integrated Drainage-Wetland Systems for Reducing Nitrate Loads from Des Moines Lobe Watersheds.

Crumpton, W. G. and G.A. Stenback. (2016). 2016 Annual Report on Performance of Iowa CREP Wetlands: Monitoring and Evaluation of Wetland Performance. https://www.iowacrep.org/files/page/files/crep_wetland_monitoring_and_evaluation_2016_final_report.pdf

Dale, H. M., & Gillespie, T. (1976). The influence of floating vascular plants on the diurnal fluctuations of temperature near the water surface in early spring. *Hydrobiologia*, *49*(3), 245-256.

Dale, H. M., & Gillespie, T. J. (1977). The influence of submersed aquatic plants on temperature gradients in shallow water bodies. *Canadian Journal of Botany*, *55*(16), 2216-2225.

Dale, H. M., & Gillespie, T. J. (1978). Diurnal temperature gradients in shallow water produced by populations of artificial aquatic macrophytes. *Canadian Journal of Botany*, *56*(9), 1099-1106.

Daubenmire, R. (1959). A canopy-coverage method of vegetational analysis. *Northwest Science*, *33*(1), 43-64.

Dibble, E. D., Killgore, K. J., & Dick, G. O. (1996). Measurement of plant architecture in seven aquatic plants. *Journal of Freshwater Ecology*, *11*(3), 311-318.

Green, David Immanuel, "Environmental factors affecting the residence time distribution dynamics of constructed agricultural wetlands" (2016). *Graduate Theses and Dissertations*. 15920. https://lib.dr.iastate.edu/etd/15920

Gu, R., & Stefan, H. G. (1995). Stratification dynamics in wastewater stabilization ponds. *Water Research*, *29*(8), 1909-1923.

Herb, W. R., & Stefan, H. G. (2005). Model for wind-driven vertical mixing in a shallow lake with submersed macrophytes. *Journal of hydraulic engineering*, *131*(6), 488-496.

Iowa State University Department of Agronomy. (n.d.) *Iowa Environmental Mesonet.* Retrieved from https://mesonet.agron.iastate.edu/agweather/

Kadlec, R. H., & Reddy, K. R. (2001). Temperature effects in treatment wetlands. *Water Environment Research*, *73*(5), 543-557.

Kadlec, R. H., & Wallace, S. (2009). *Treatment wetlands*. CRC press.

Natural Resources Conservation Service. (n.d.). *Climate Data*. Retrieved from https://www.wcc.nrcs.usda.gov/climate/

R Core Team (2015). R: A language and environment for statistical computing. R Foundation for Statistical Computing, Vienna, Austria. URL http://www.R-project.org/.

Rose, C. 1996. Effects of emergent vegetation on wetland microbial processes. Ph.D. Thesis. Iowa State University, Ames, IA, USA.

Rose, C. and W. G. Crumpton. 1996. Effects of emergent macrophytes on dissolved oxygen dynamics in a prairie pothole wetland. Wetlands 16:495–502.

Titus, J. E., Grisé, D., Sullivan, G., & Stephens, M. D. (2004). Monitoring submersed vegetation in a mesotrophic lake: correlation of two spatio-temporal scales of change. *Aquatic Botany*, *79*(1), 33-50.

TABLES

Table 1. Temperature Array Attributes by Wetland. [1]Horizontal datum: UTM NAD 83. Measured parameters represent the temperature measured of various components of a given array: water (W), sediment (S), and atmospheric (A).

Wetland	Array	Location Type	Water Column Depth (m)	Number of Sensors	Measured Parameters	Latitude (m)[1]	Longitude (m)[1]
KS	1	Shallow	0.58	5	W, S	442780.59	4666751.25
KS	2	Shallow	0.64	6	W, S, A	442701.42	4666789.14
KS	3	Inlet	0.2	1	W	442848.36	4666666.53
KS	5	Outlet	0.2	1	W	442631.18	4666819.63
KS	6	Shallow	0.44	4	W, S	442726.37	4666840.27
KS	7	Shallow	0.49	6	W, S, A	442670.31	4666849.51
KS	8	Shallow	0.46	5	W, S	442654.90	4666788.52
KS	9	Deep	1.46	7	W, S	442712.20	4666811.93
KS	10	Deep	1.34	7	W, S, A	442663.53	4666822.10
KS	11	Shallow	0.24	4	W, S	442779.66	4666801.46
KS	12	Shallow	0.46	5	W, S	442750.09	4666782.36
RS	1	Deep	2.7	11	W, S, A	457004.42	4662738.80
RS	2	Shallow	0.33	3	W, S, A	457135.39	4662634.73
RS	3	Shallow	0.40	4	W, S	456986.78	4662696.02
RS	4	Deep	1.75	9	W, S, A	457250.43	4662757.56
RS	5	Shallow	0.30	4	W, S	457223.66	4662682.51
RS	6	Shallow	0.33	4	W, S	457045.88	4662657.66
RS	7	Shallow	0.50	4	W, S	457163.11	4662704.39
RS	8	Shallow	0.45	5	W, S	457053.77	4662708.40
RS	9	Deep	1.80	8	W, S	457173.75	4662687.59
RS	10	Deep	2.15	1	W, S	457069.65	4662663.63
RS	11	Inlet	1.60	8	W, S	457283.26	4662872.70
RS	12	Outlet	0.05	9	W	456988.55	4662759.08

Table 2. Percent vegetative cover for each sensor array for each vegetation survey date at study site KS.

Wetland	Array	5/19	6/6	6/22	7/5	8/5	8/16	9/1	9/15	10/6	10/20
KS	1	0	0	0	13	14	2	5	5	6	5
KS	2	8	26	59	93	96	87	91	101	95	37
KS	3	0	0	0	0	0	0	0	0	0	0
KS	4	0	0	0	0	0	0	0	0	0	0
KS	5	0	0	0	0	0	0	0	0	0	0
KS	6	6	30	13	56	23	31	64	45	52	30
KS	7	23	7	10	15	19	32	27	56	36	16
KS	8	1	13	40	76	66	94	78	60	69	26
KS	9	0	4	30	17	56	18	26	0	71	49
KS	10	2	8	56	76	33	13	10	3	0	14
KS	11	0	8	8	13	13	4	7	0	3	6
KS	12	0	43	61	93	33	87	65	93	57	34

Table 3. Percent vegetative cover for each sensor array for each vegetation survey date at study site RS.

Wetland	Array	5/17	6/7	6/23	7/15	8/5	8/18	8/28	9/22	10/22
RS	1	2	16	0	12	7	18	10	17	1
RS	2	21	15	24	27	26	43	9	3	0
RS	3	59	62	18	51	120	39	15	5	0
RS	4	3	10	28	13	6	0	0	0	1
RS	5	37	57	63	70	14	63	11	0	0
RS	6	18	29	29	31	79	24	12	13	0
RS	7	4	24	51	38	13	17	6	15	0
RS	8	39	94	39	44	63	81	56	24	0
RS	9	24	55	50	76	31	69	12	11	0
RS	10	0	24	3	27	75	5	65	8	0
RS	11	0	1	87	1	0	0	2	1	0
RS	12	0	2	2	2	1	2	3	3	0

Table 4. Average monthly temperatures, average surface temperatures, and average bottom temperatures (°C) of all arrays (not including inlet/outlet) at study site KS.

Month	KS	Surface	Bottom
April	11.1	11.8	10.4
May	13.2	14.5	12.3
June	21.0	23.6	18.7
July	22.5	25.1	20.7
August	19.4	21.2	18.3
September	17.2	17.5	16.9
October	13.7	13.5	13.7

Table 5. Average monthly temperatures, average surface temperatures, and average bottom temperatures (°C) of all arrays (not including inlet/outlet) at study site RS.

Month	Overall	Surface	Bottom
May	15.1	17.6	12.3
June	21.4	26.1	14.5
July	22.7	26.8	17.0
August	20.6	23.3	18.0
September	18.8	20.0	17.7
October	14.5	14.9	14.3

Table 6. Percentage of depth distributions in study sites

Depth (m)	KS	RS
0 – 0.5	37.25%	31.73%
0.5 – 1	42.87 %	42.30%
1 – sediment	19.88%	25.97%

FIGURES

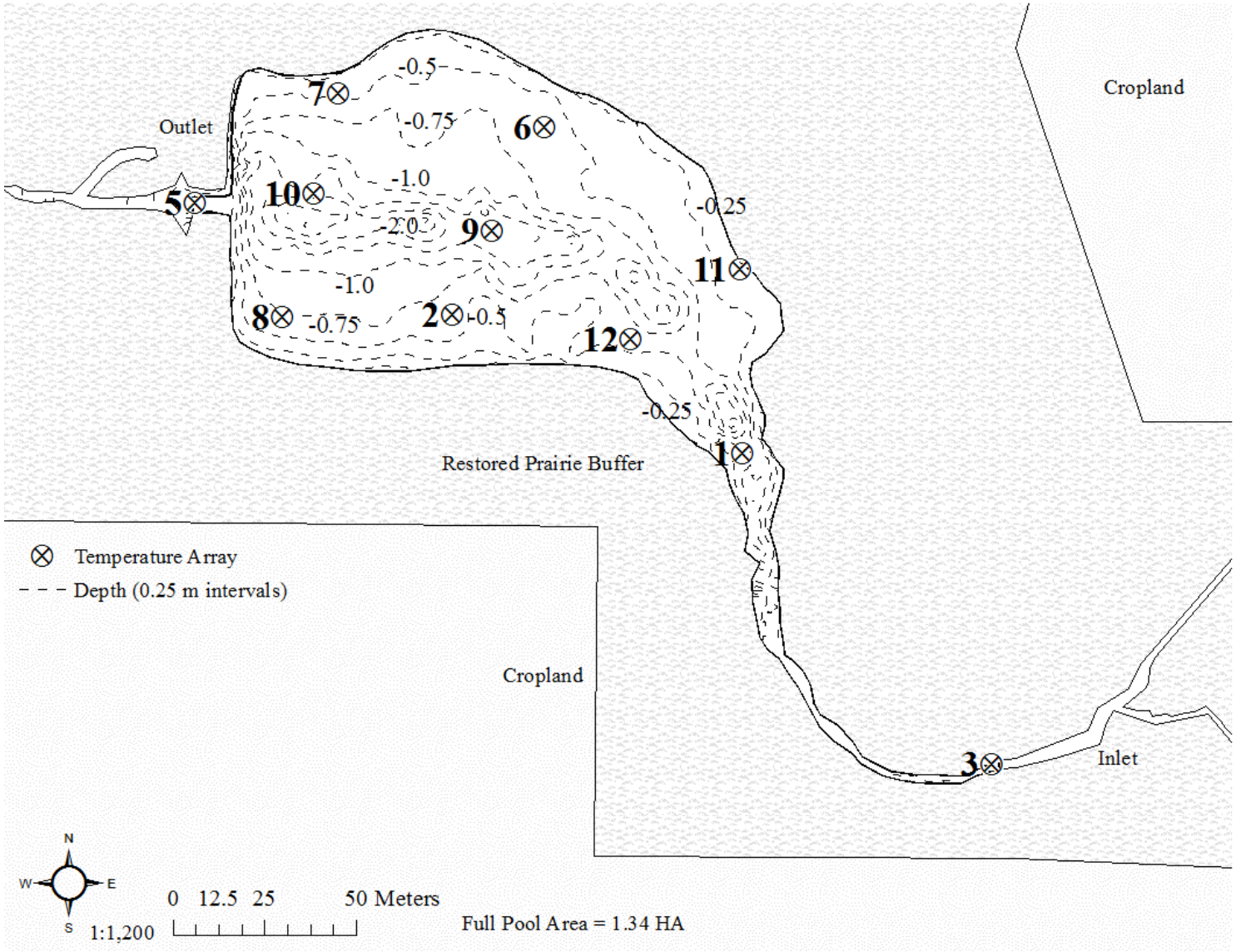

Figure 1. Map of study site KS showing temperature array locations and water depth in 0.25 meter intervals.

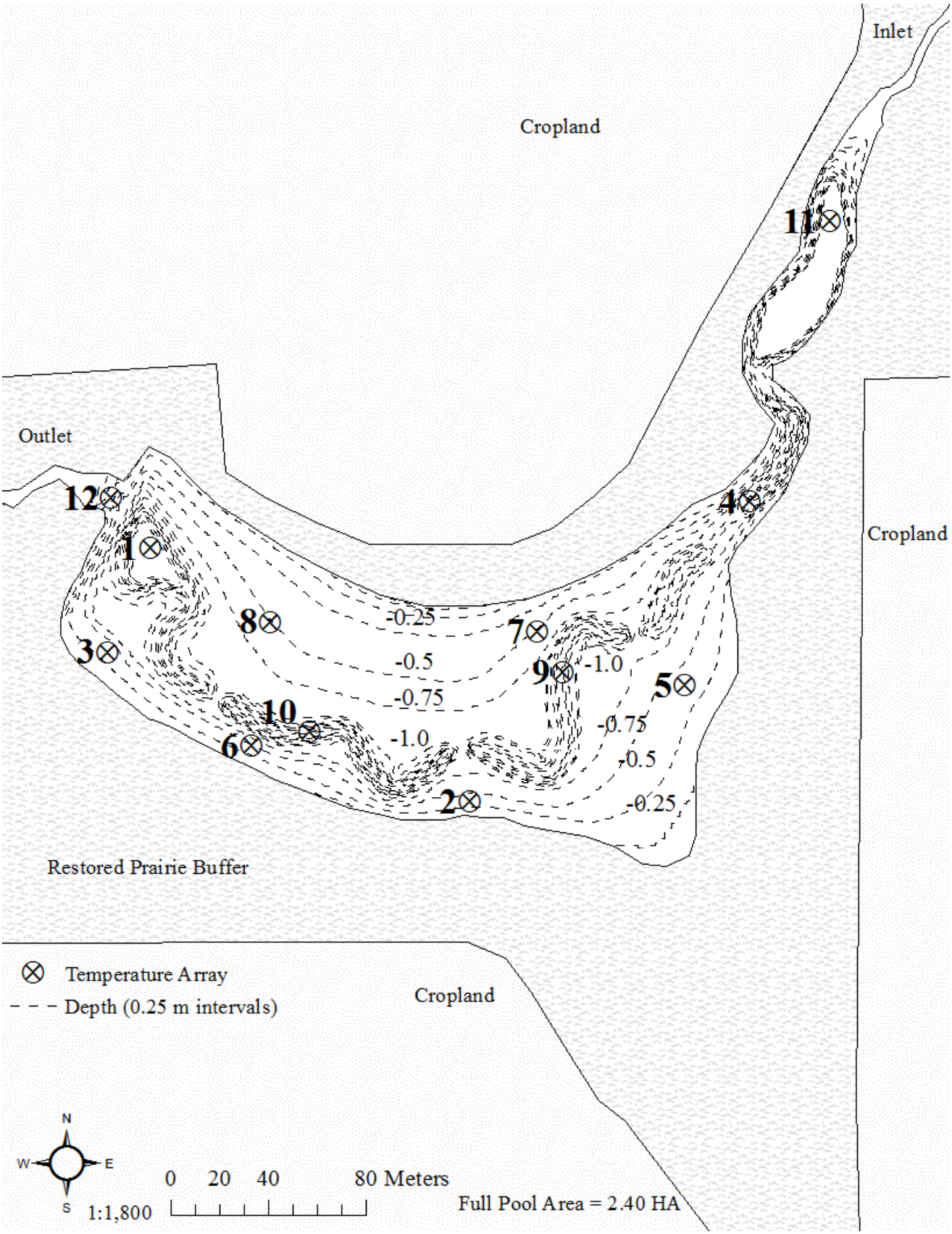

Figure 2. Map of study site RS showing temperature array locations and water depth in 0.25 meter intervals.

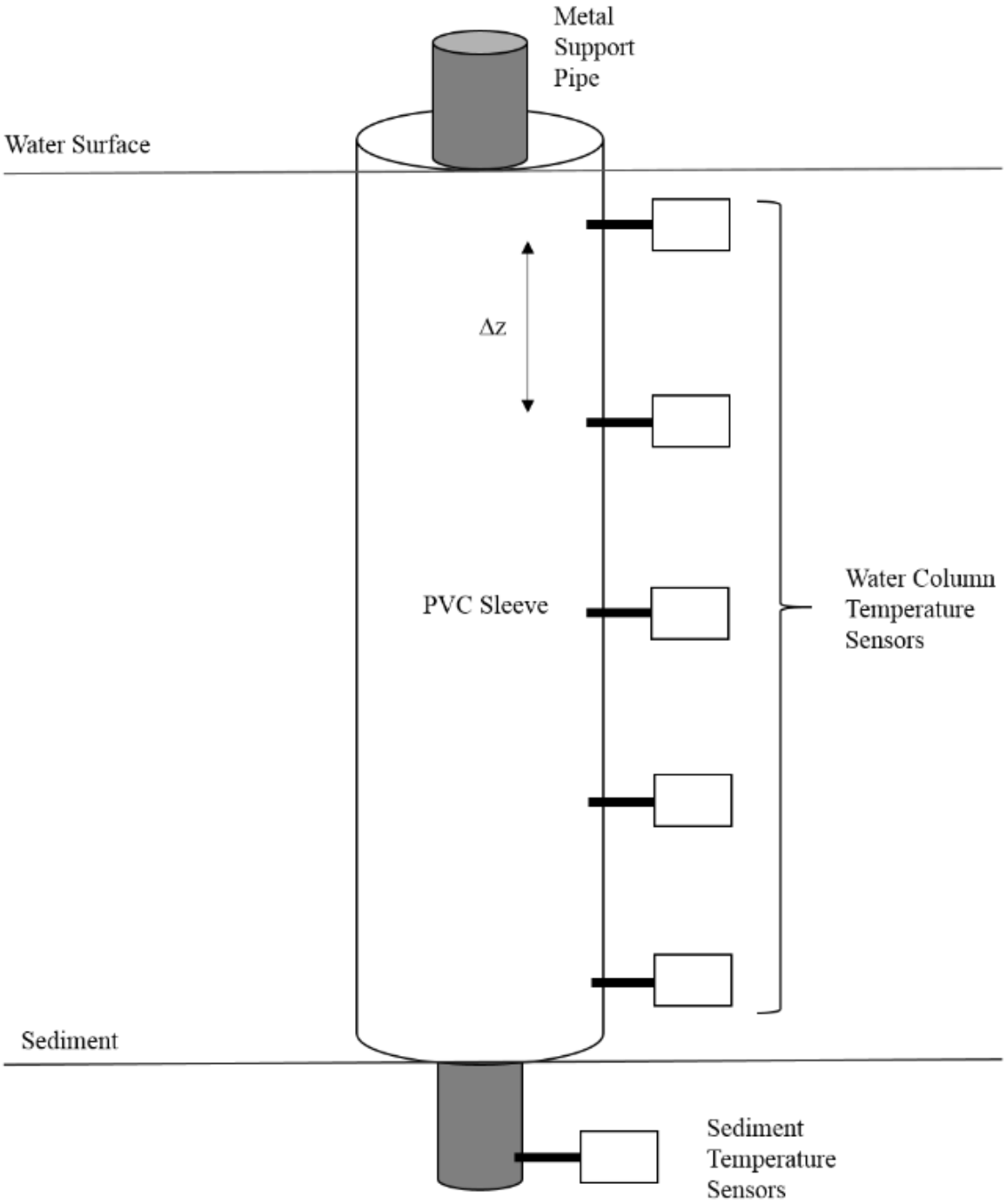

Figure 3. Illustration of temperature sensor array. Each array consisted of several sensors within the water column. A few arrays also possessed a single temperature sensor placed approximately 2 cm below the sediment-water interface.

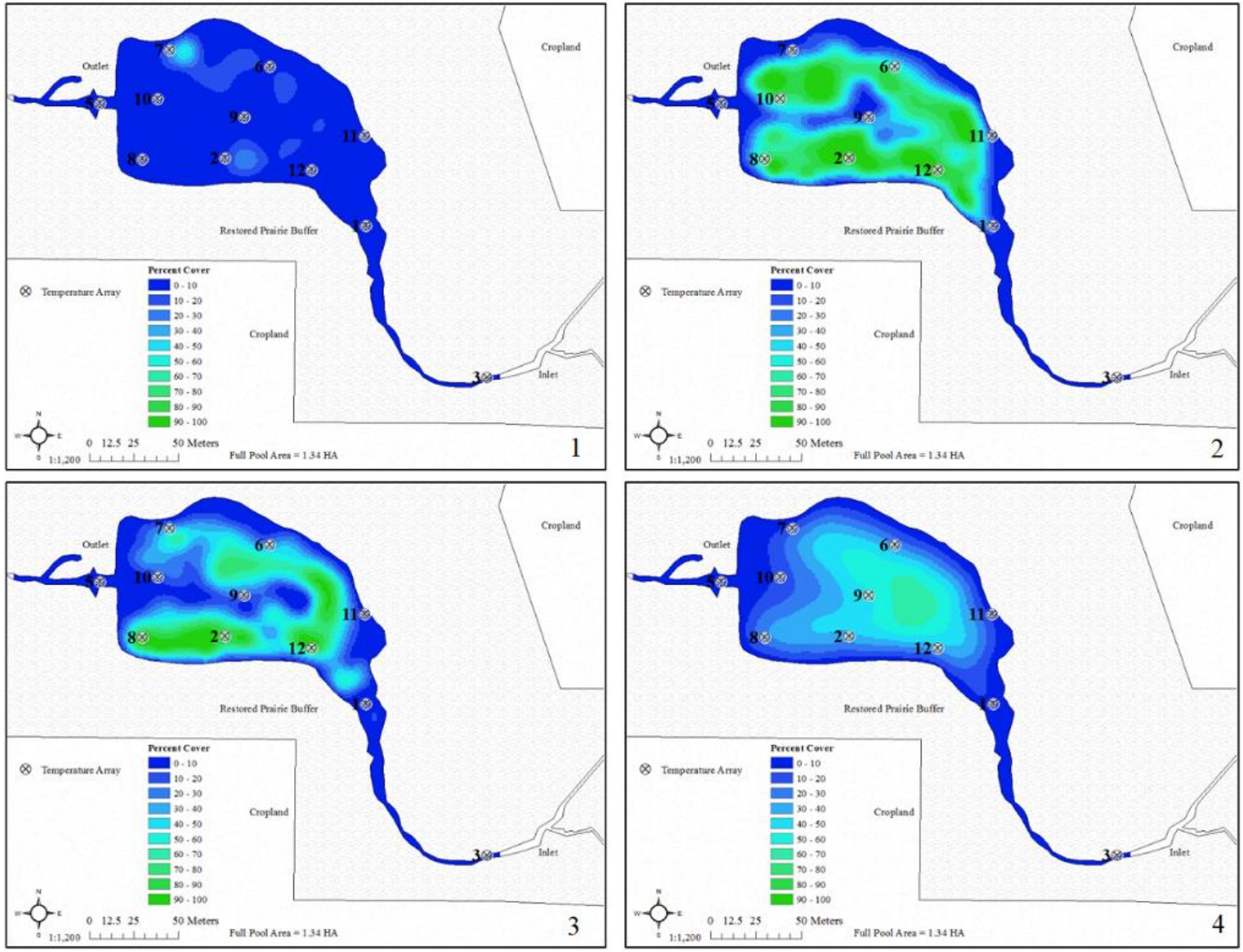

Figure 4. Series of vegetative surveys showing progression of submersed macrophyte cover at study site KS with surveys on May 19 (1), July 5 (2), August 16 (3), and October 20 (4).

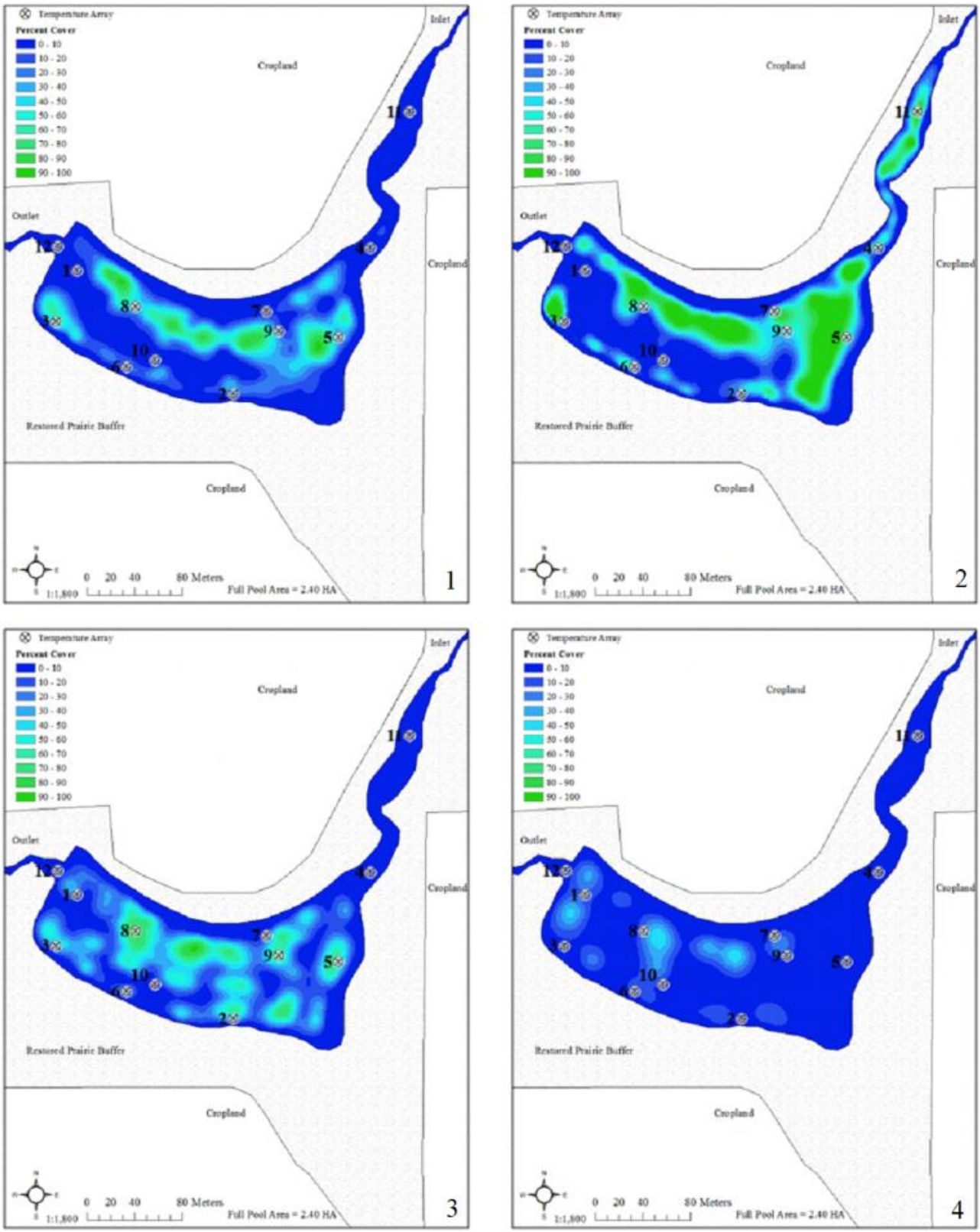

Figure 5. Series of vegetation surveys showing progression of submersed macrophyte cover at study site RS with surveys on May 17 (1), June 23 (2), August 18 (3), and September 22 (4).

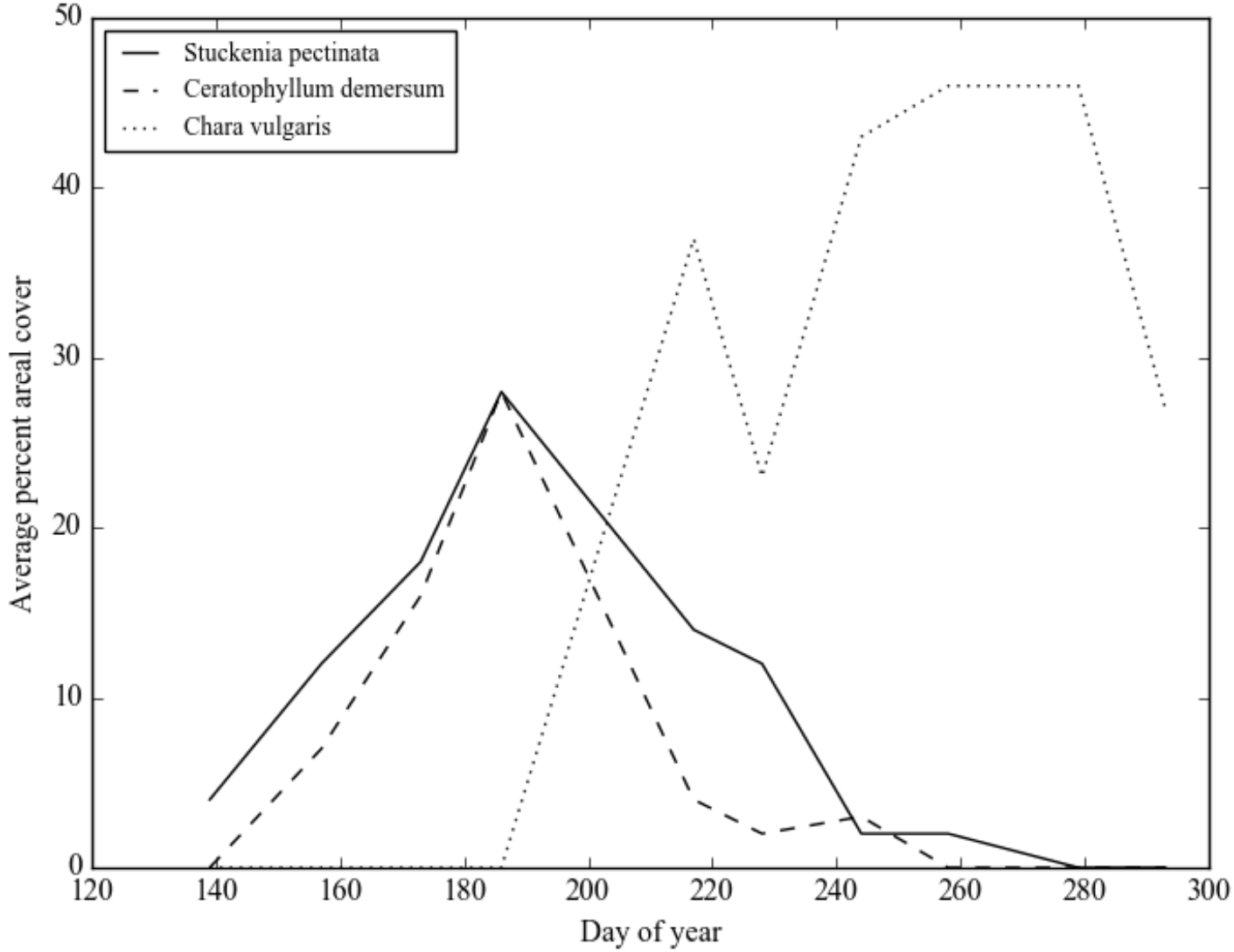

Figure 6. Time-series of submersed macrophyte succession at study site KS in 2016.

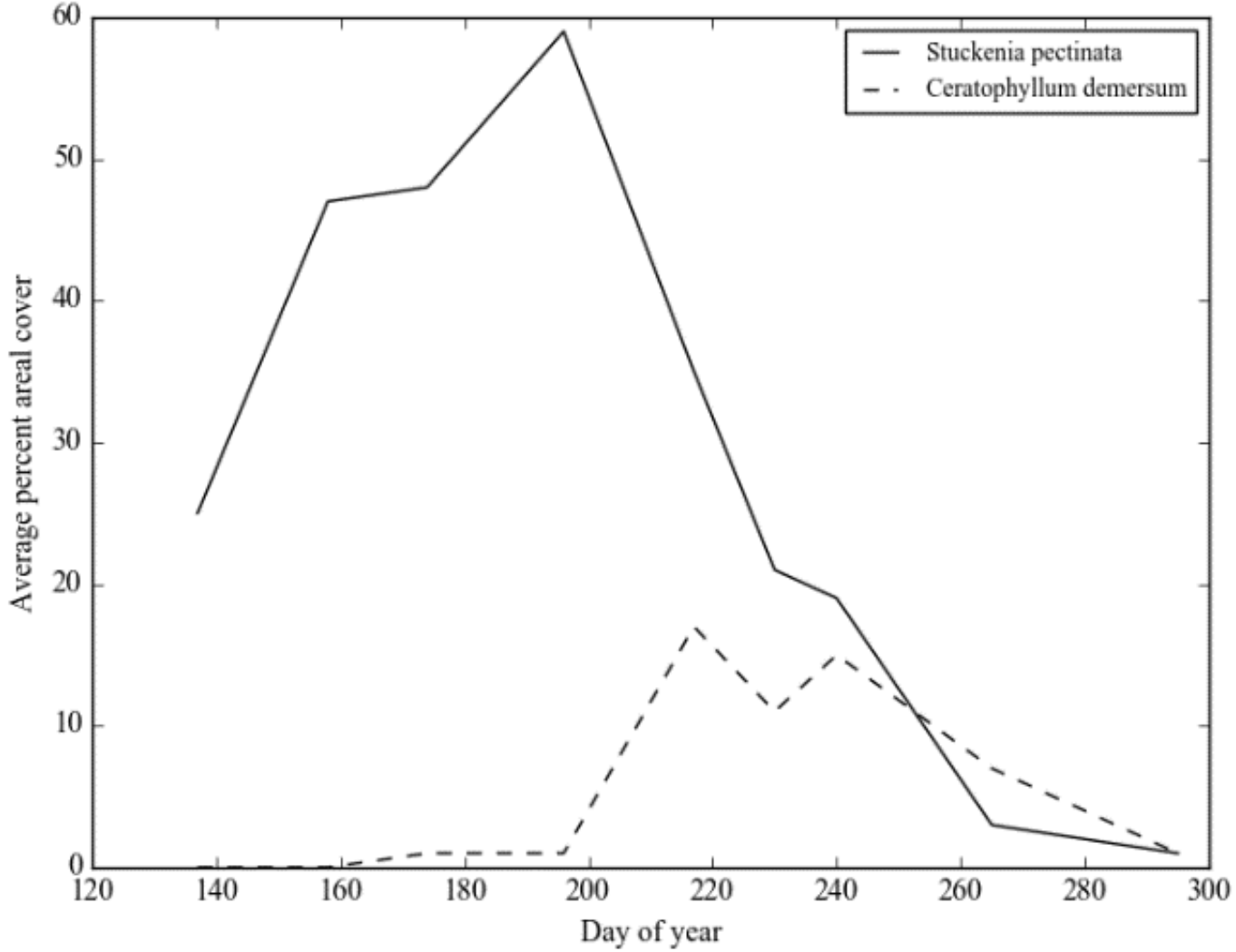

Figure 7. Time-series of submersed macrophyte succession at study site RS in 2016.

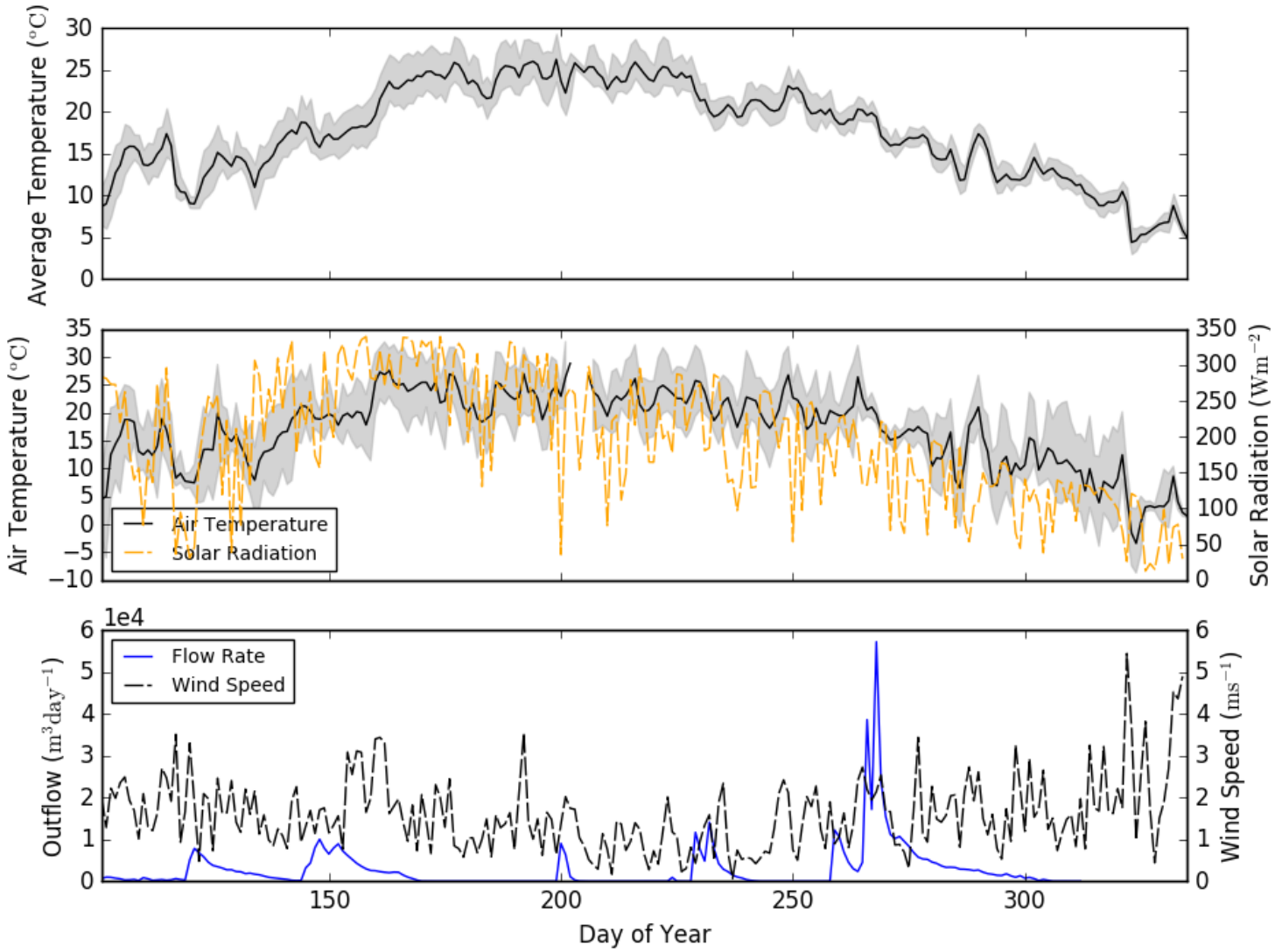

Figure 8. Time-series of water temperatures, air temperatures, solar radiation, wind speed, and flow rate at study site KS.

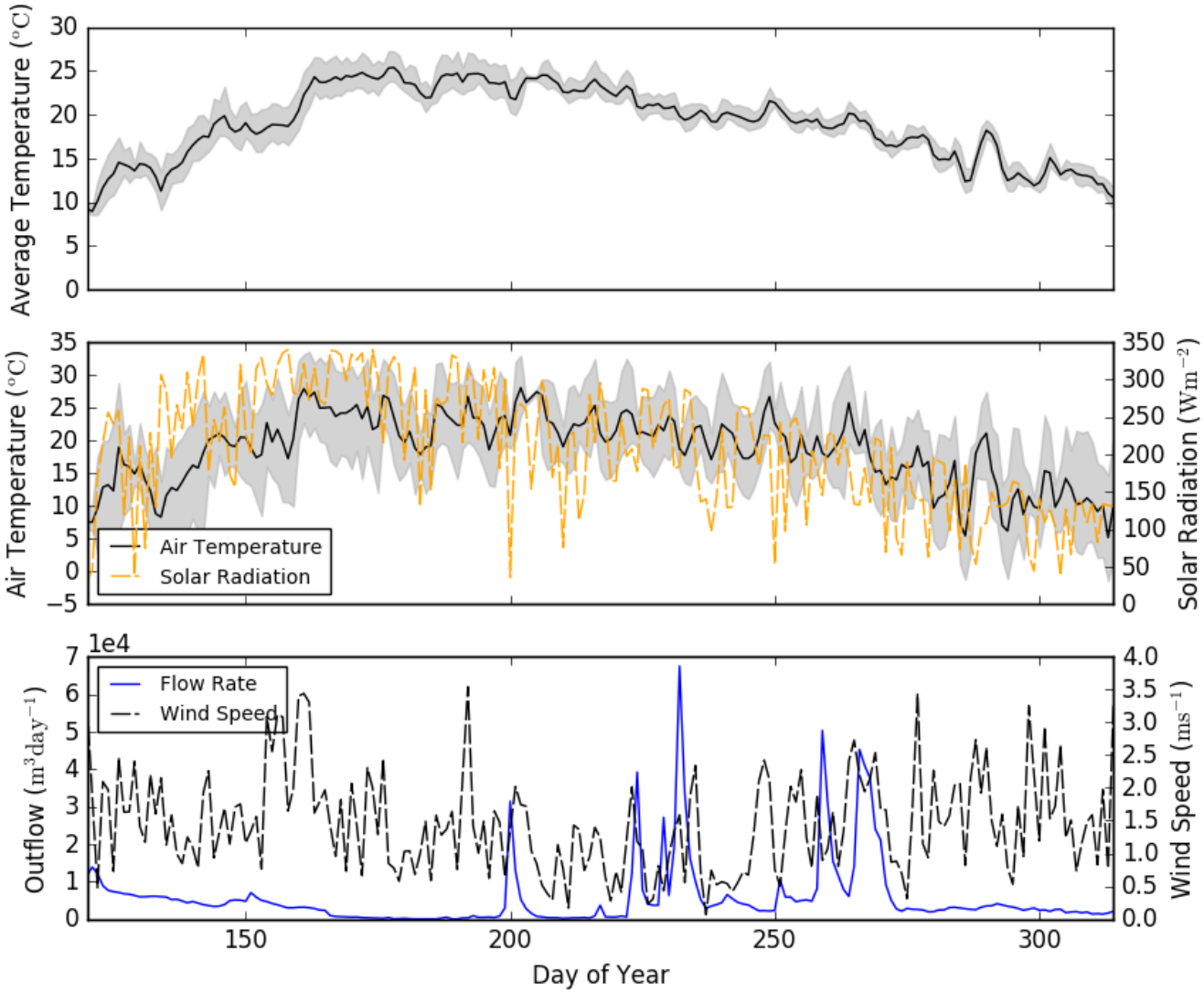

Figure 9. Time-series of water temperatures, air temperatures, solar radiation, wind speed, and flow rate at study site RS.

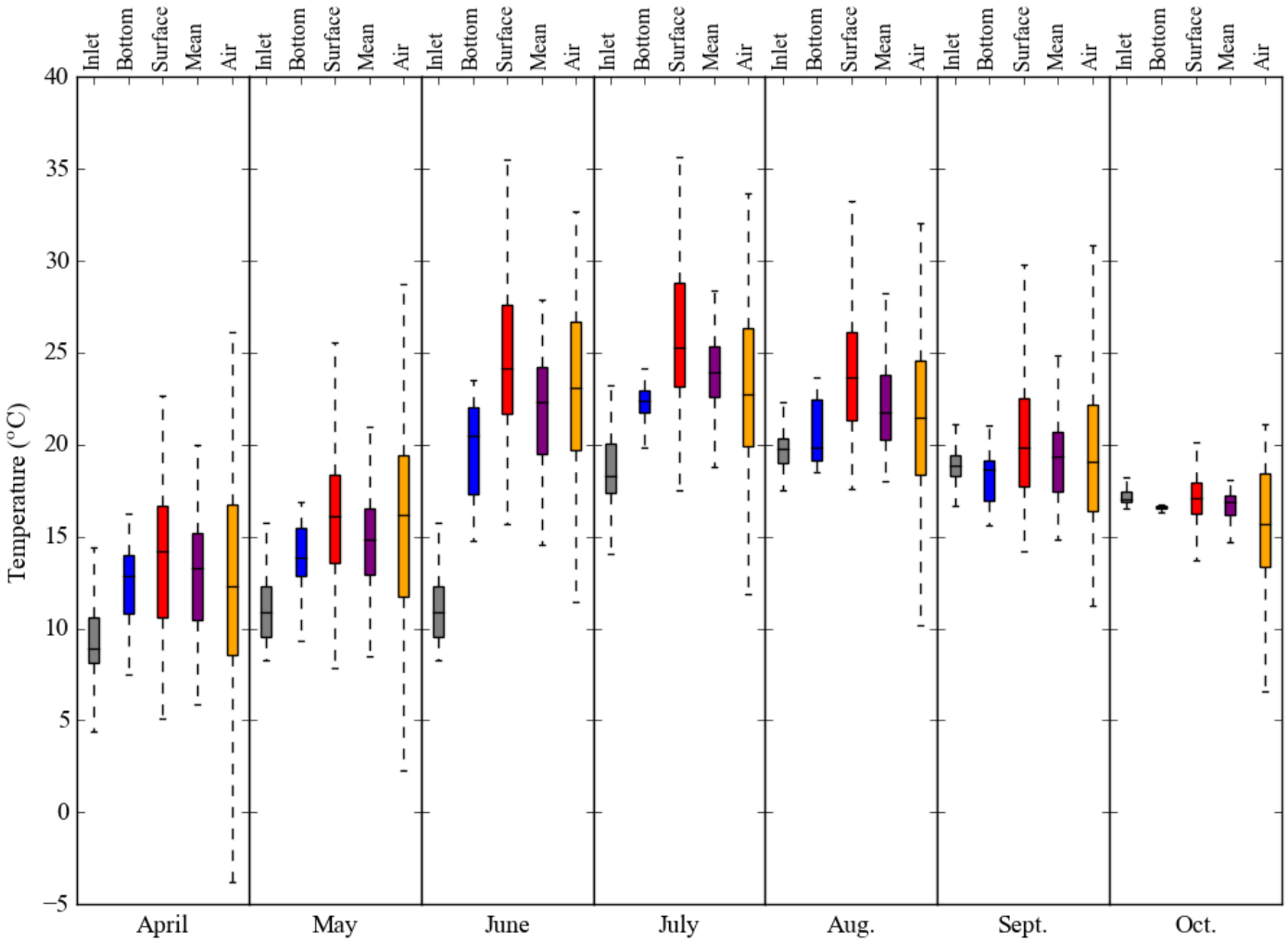

Figure 10. Box and whisker plots of temperatures at study site KS for each month of observation for the inlet of the wetland, bottom of the water column, surface of the water column, mean of the water column, and air temperatures. The line is the median, boxes are the 25th and 75th quartiles, and whiskers represent the maximum and minimum.

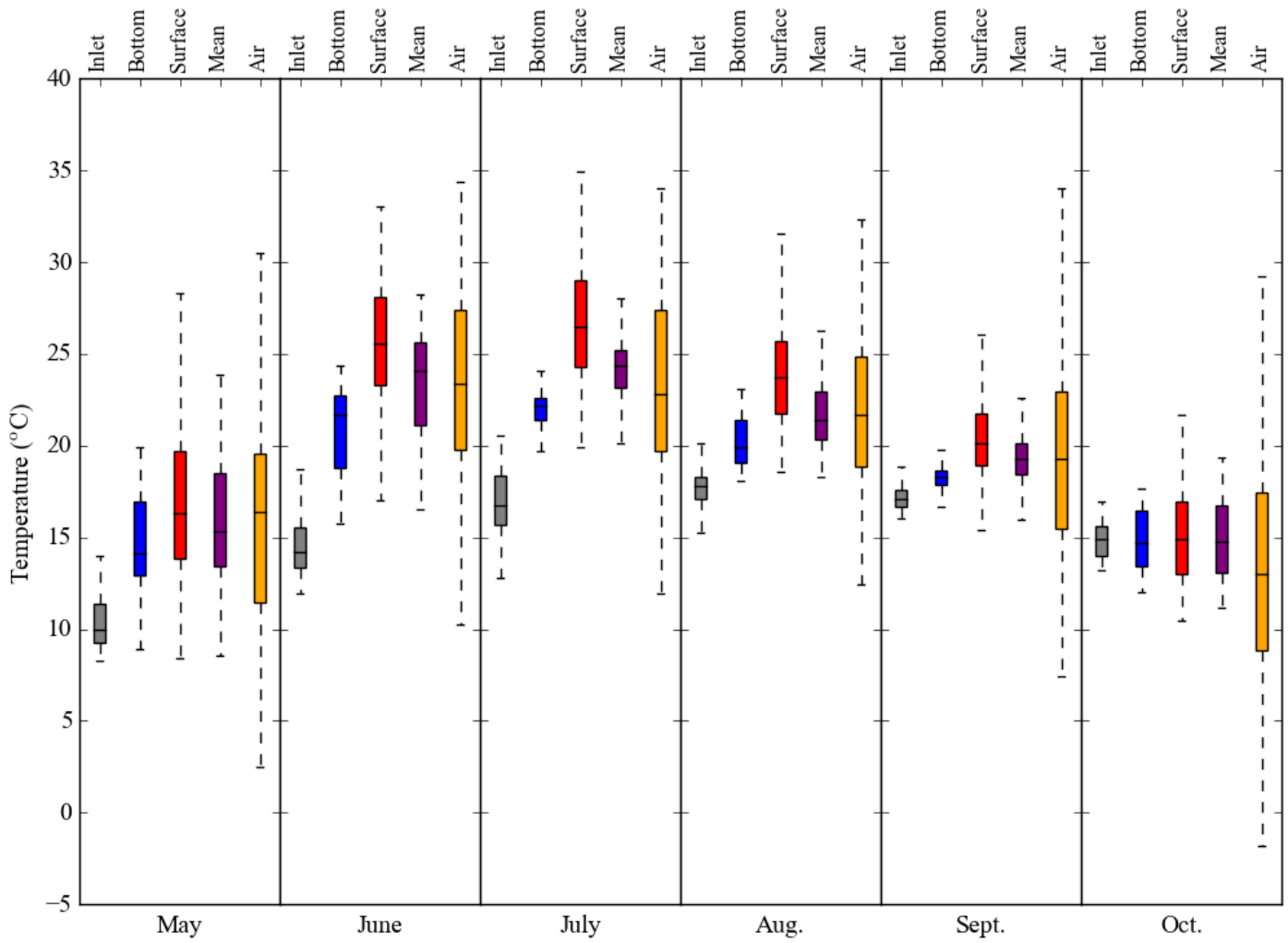

Figure 11. Box and whisker plots of temperatures at study site RS for each month of observation for the inlet of the wetland, bottom of the water column, surface of the water column, mean of the water column, and air temperatures. The line is the median, boxes are the 25th and 75th quartiles, and whiskers represent the maximum and minimum.

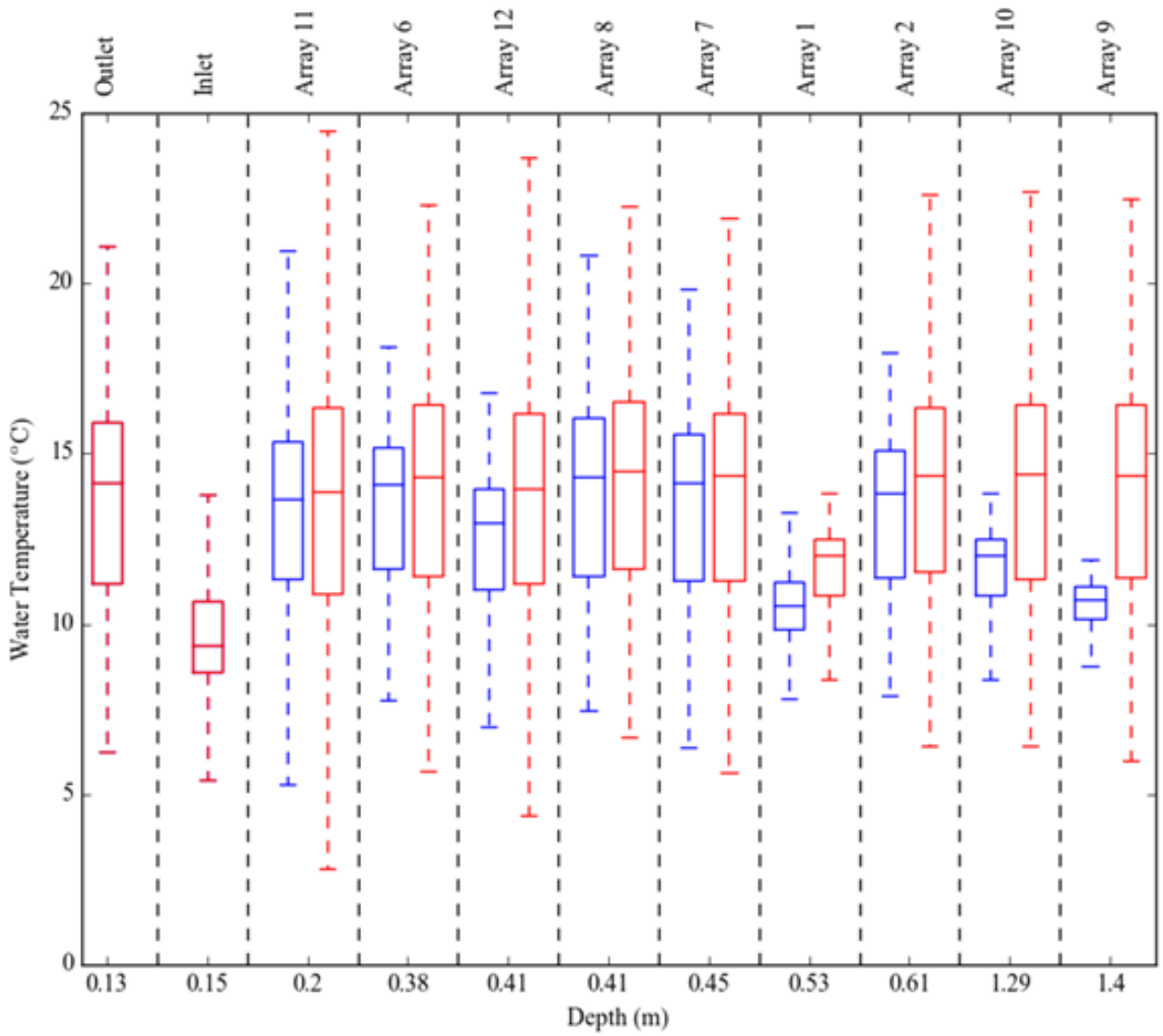

Figure 12. Box and whisker plots of temperatures for each array at study site KS before submersed macrophytes had become established. The line is the median, boxes are the 25th and 75th quartiles, and whiskers represent the maximum and minimum.

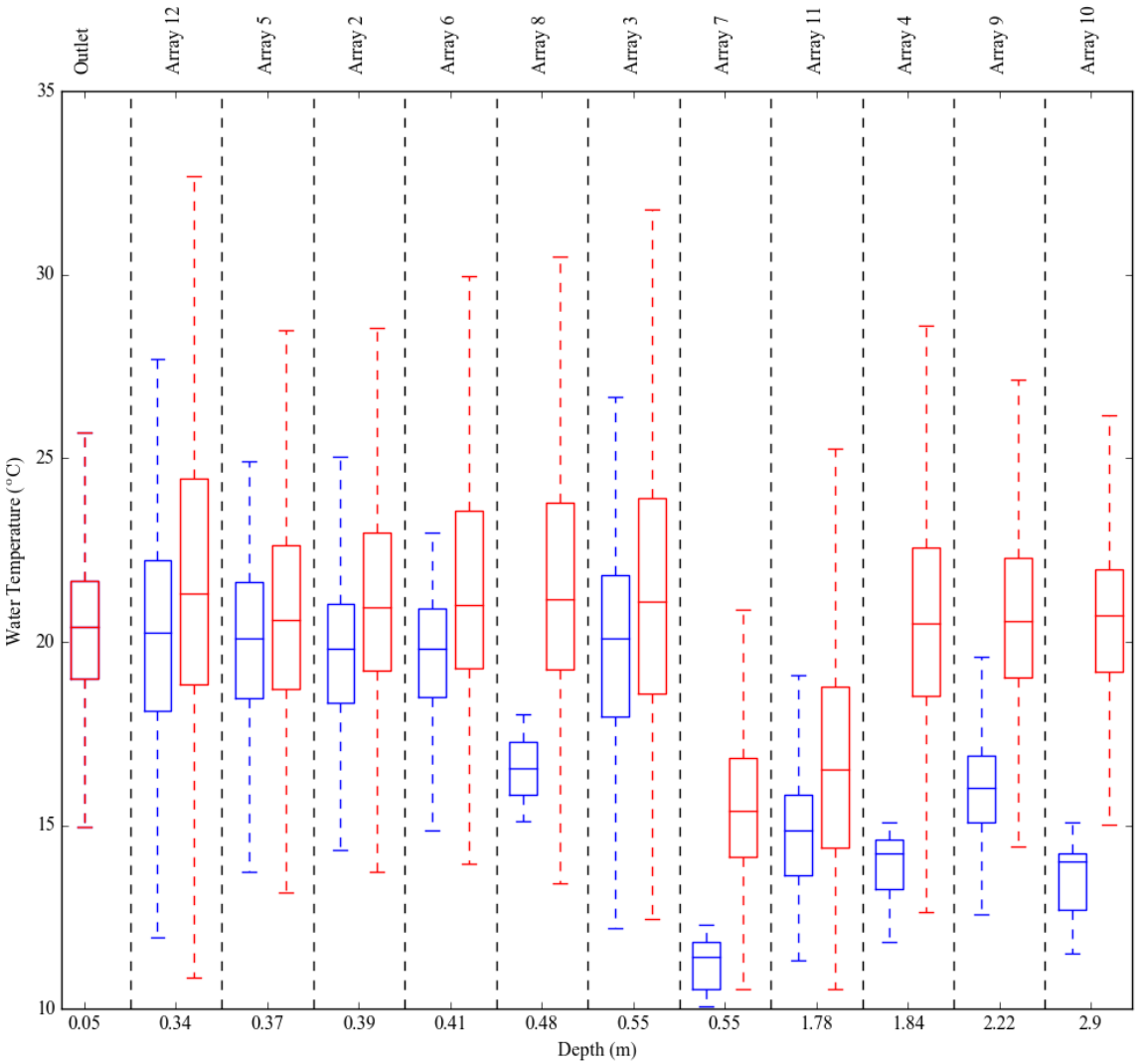

Figure 13. Box and whisker plots of temperatures for each array at study site RS before submersed macrophytes had become established. The line is the median, boxes are the 25th and 75th quartiles, and whiskers represent the maximum and minimum.

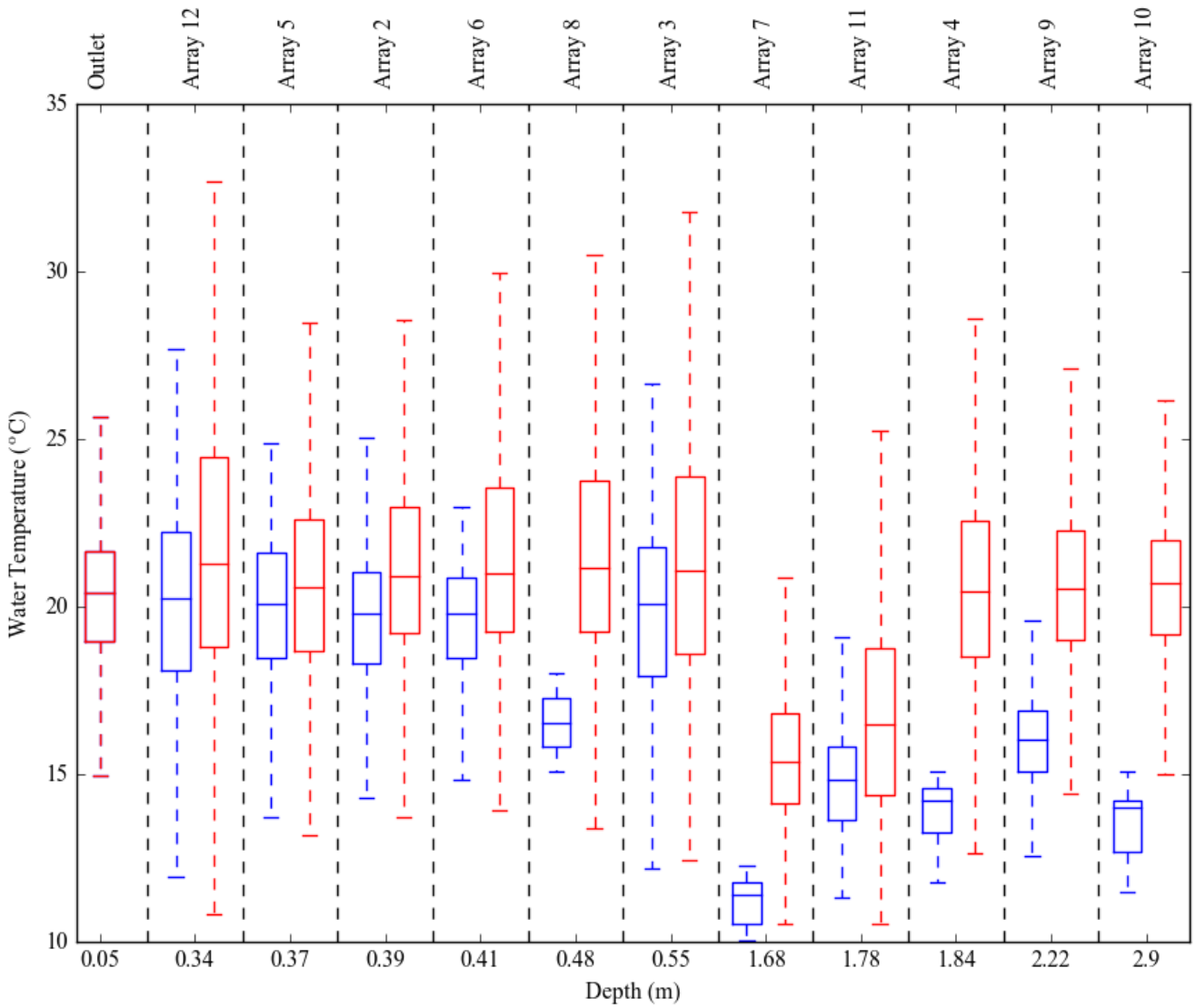

Figure 14. Box and whisker plots of temperatures for each array at study site KS after submersed macrophytes had become established. The line is the median, boxes are the 25th and 75th quartiles, and whiskers represent the maximum and minimum.

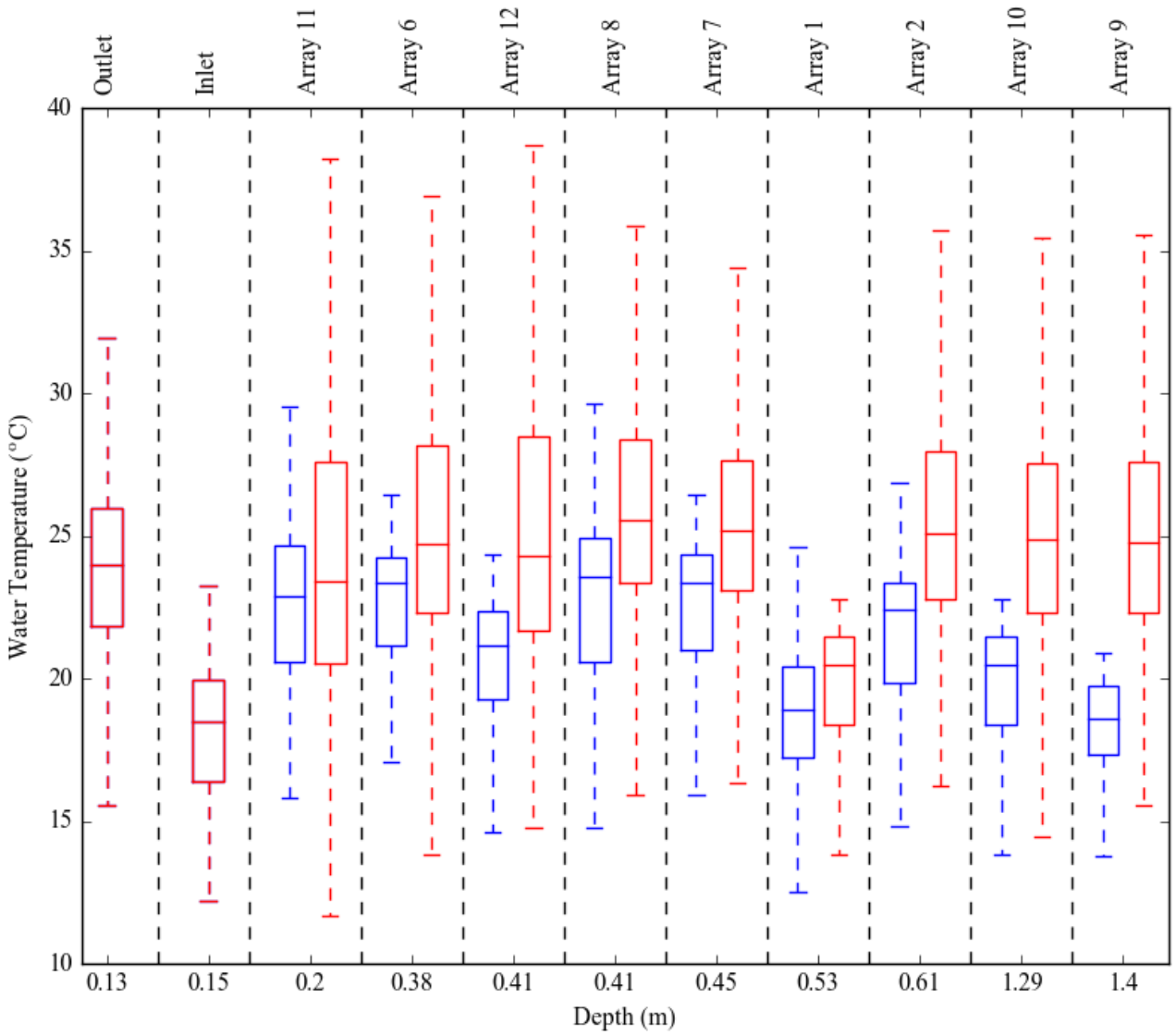

Figure 15. Box and whisker plots of temperatures for each array at study site RS after submersed macrophytes had become established. The line is the median, boxes are the 25th and 75th quartiles, and whiskers represent the maximum and minimum.

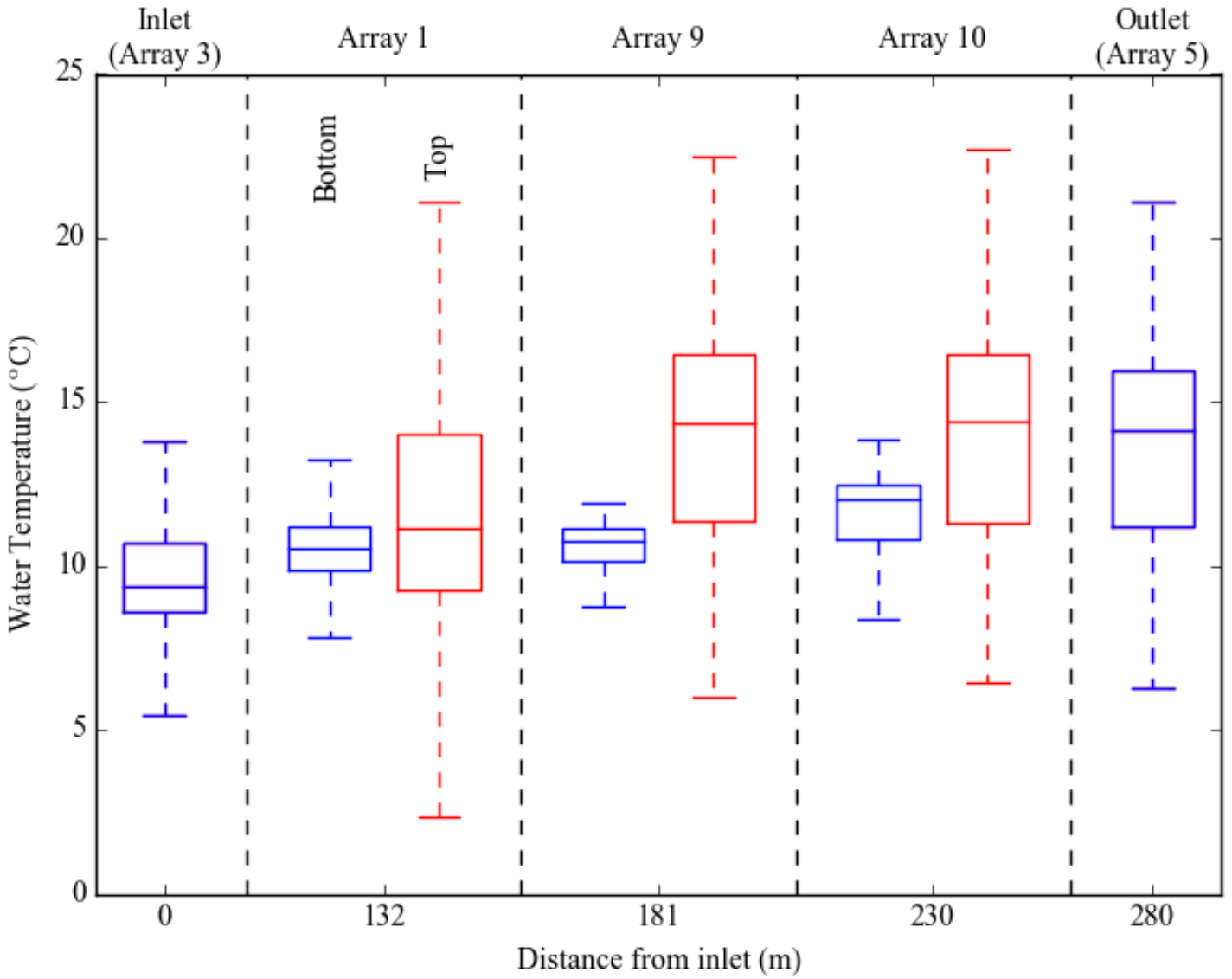

Figure 16. Box and whisker plots of temperatures at the surface and the bottom the arrays along the deep, central channel at study site KS on May 19. The line is the median, boxes are the 25th and 75th quartiles, and whiskers represent the maximum and minimum.

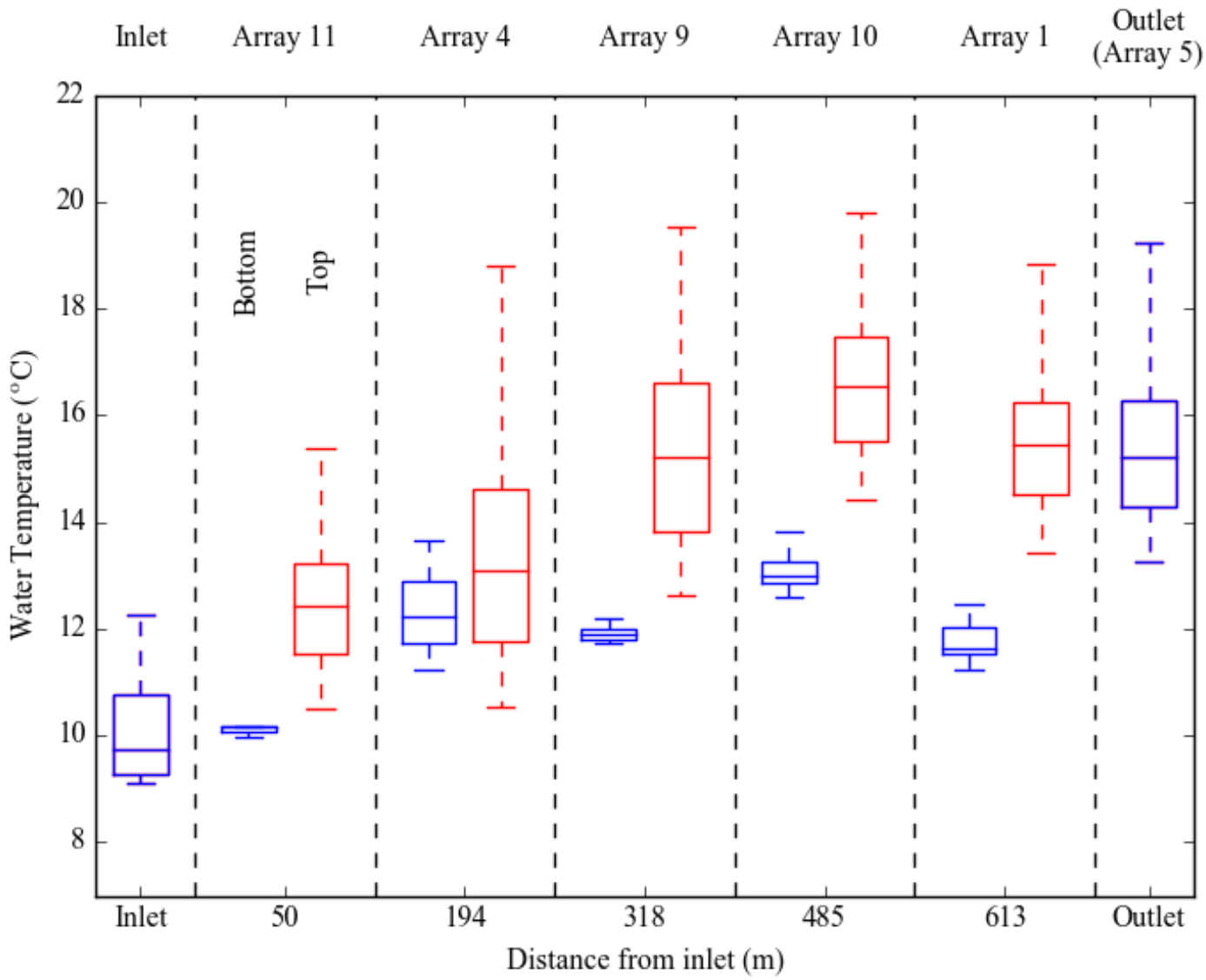

Figure 17. Box and whisker plots of temperatures at the surface and the bottom the arrays along the deep, central channel at study site RS on May 17. The line is the median, boxes are the 25th and 75th quartiles, and whiskers represent the maximum and minimum .

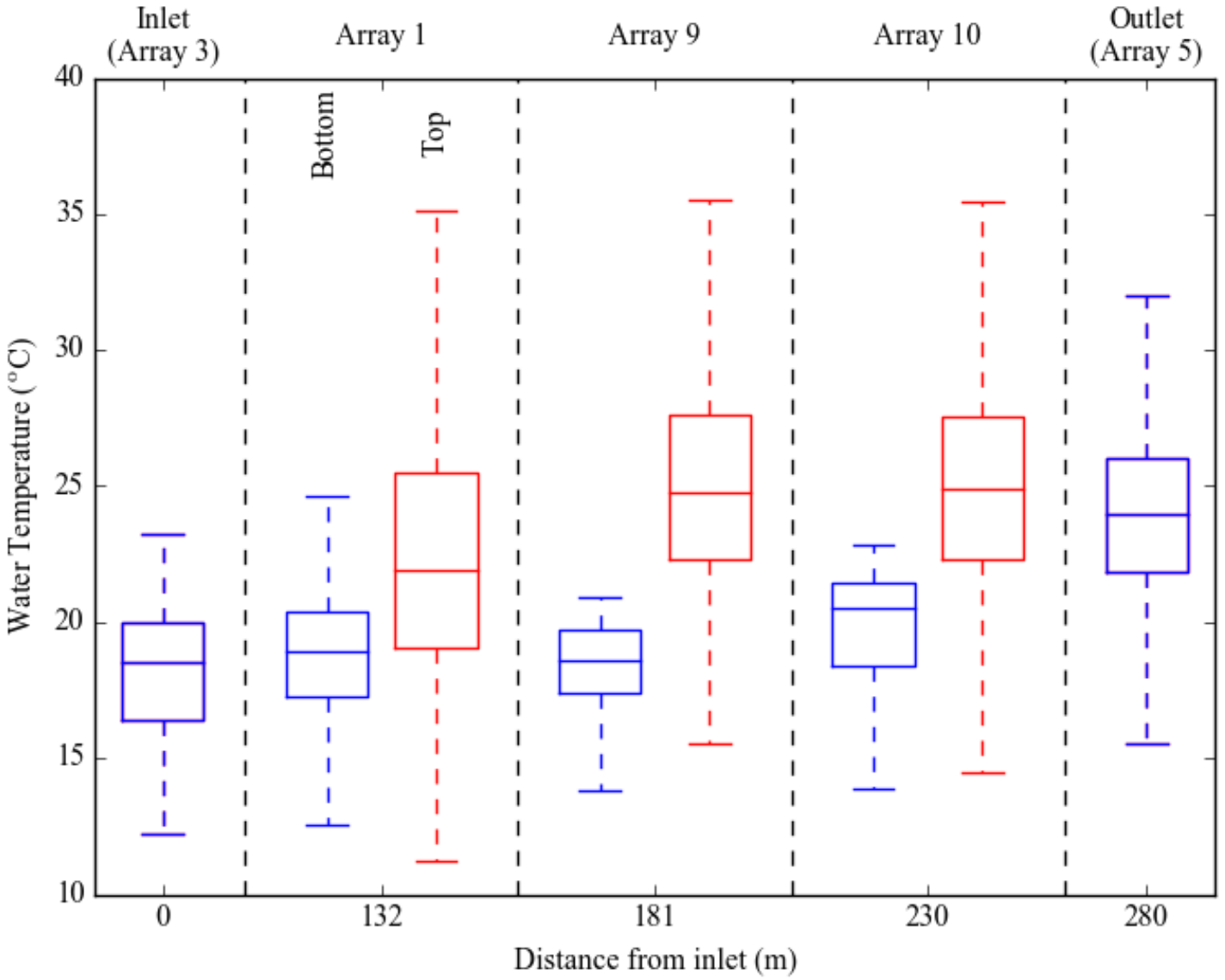

Figure 18. Box and whisker plots of temperatures at the surface and the bottom the arrays along the deep, central channel at study site KS on July 5. The line is the median, boxes are the 25th and 75th quartiles, and whiskers represent the maximum and minimum .

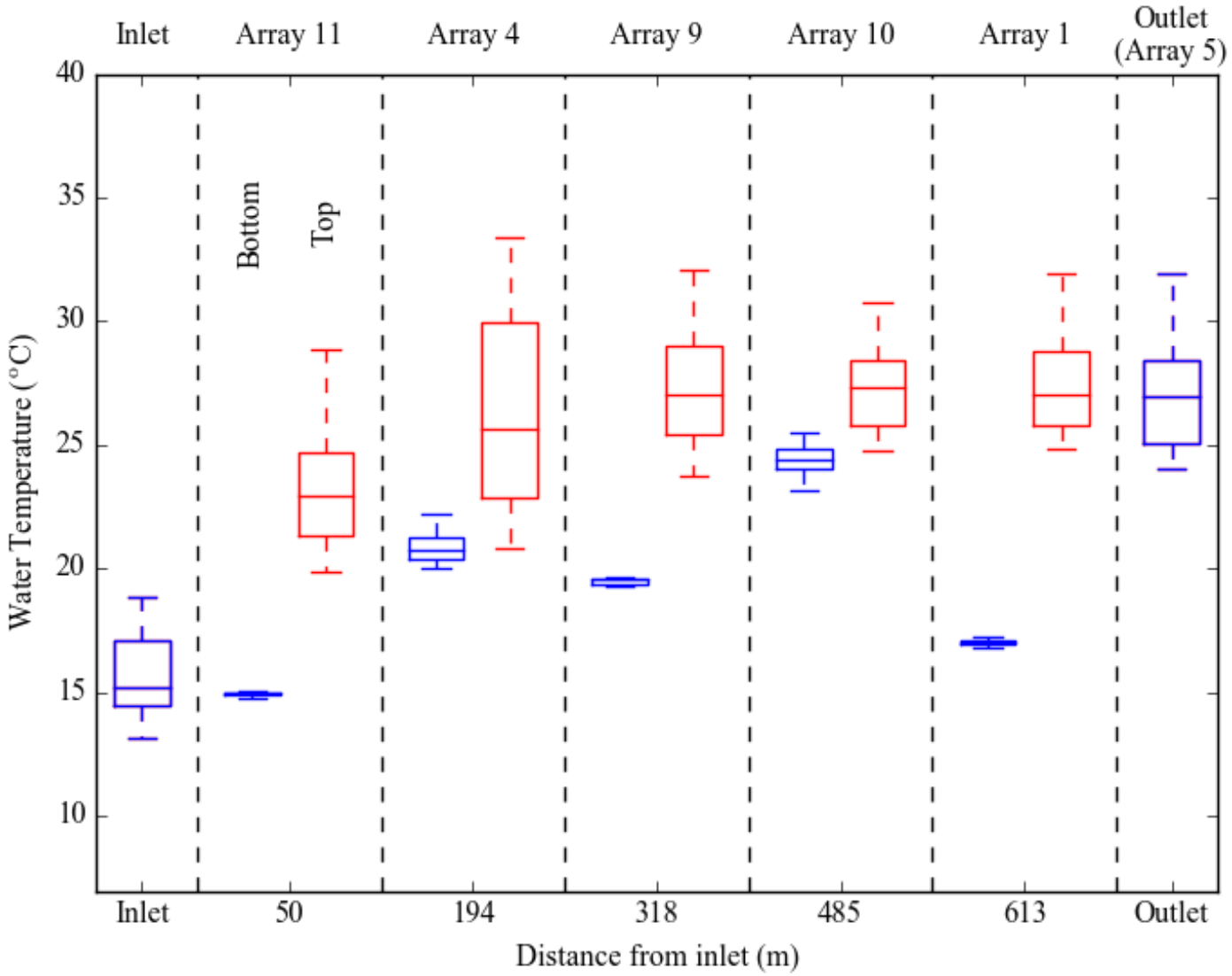

Figure 19. Box and whisker plots of temperatures at the surface and the bottom the arrays along the deep, central channel at study site RS on June 23. The line is the median, boxes are the 25th and 75th quartiles, and whiskers represent the maximum and minimum .

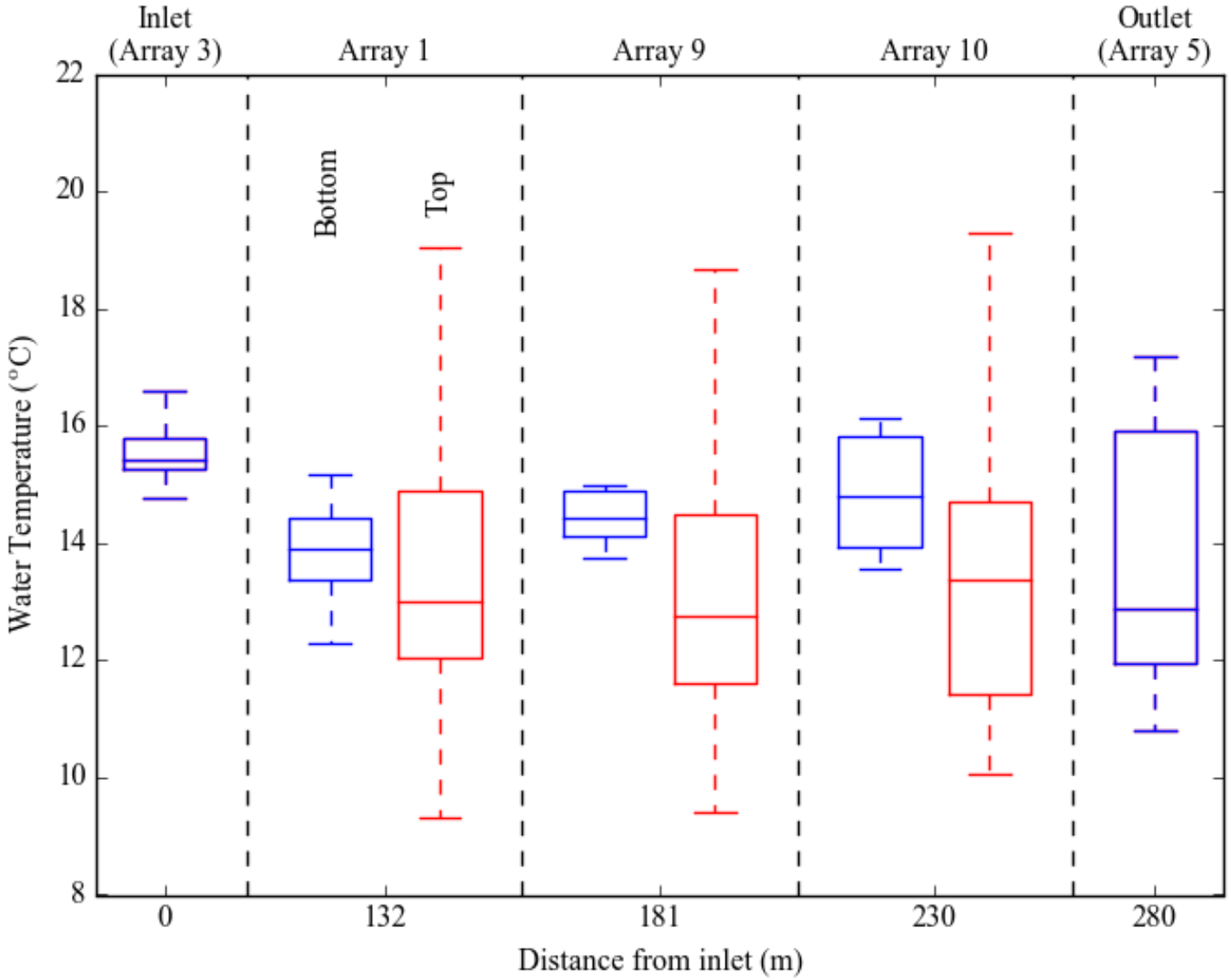

Figure 20. Box and whisker plots of temperatures at the surface and the bottom the arrays along the deep, central channel at study site KS on October 20. The line is the median, boxes are the 25th and 75th quartiles, and whiskers represent the maximum and minimum .

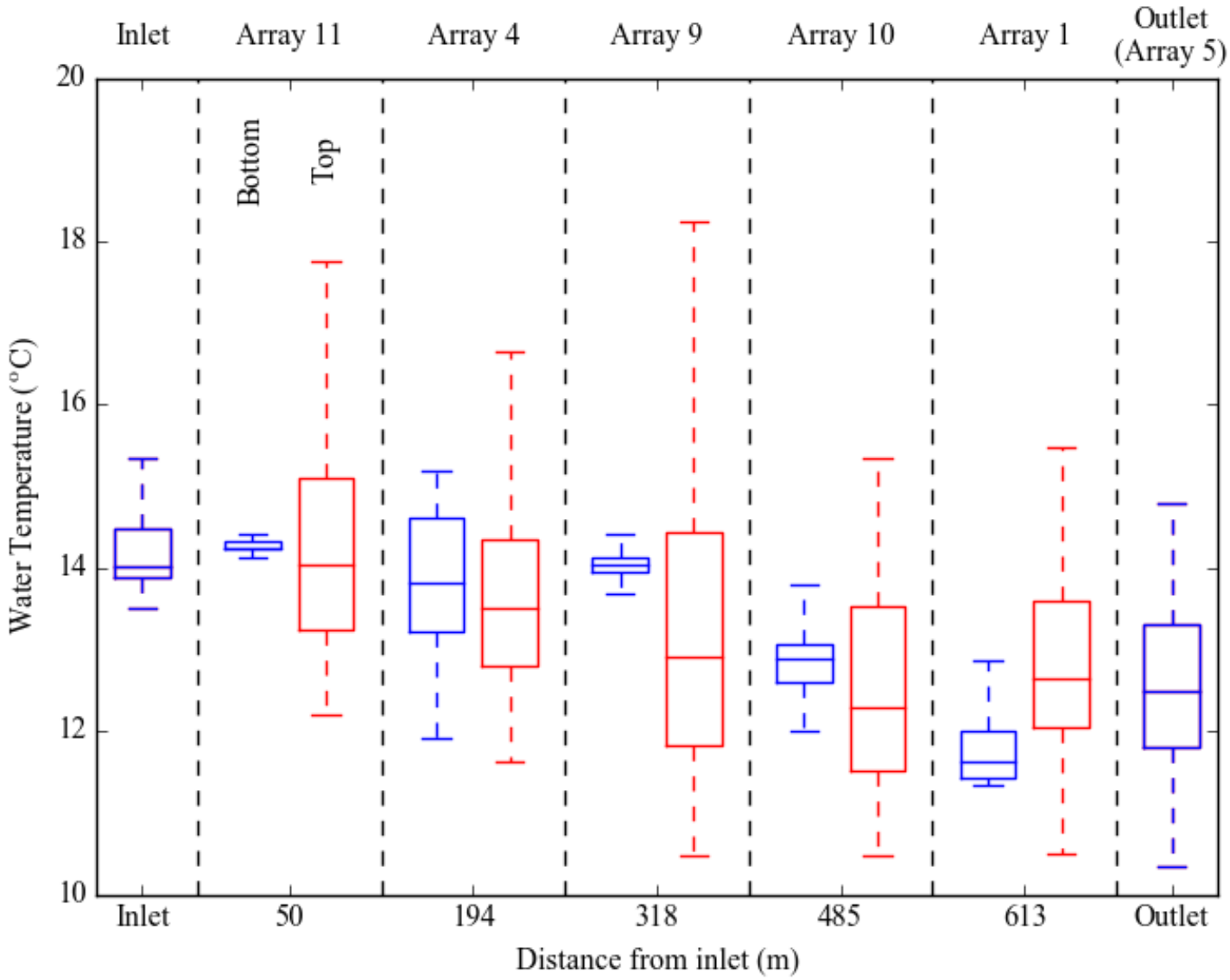

Figure 21. Box and whisker plots of temperatures at the surface and the bottom the arrays along the deep, central channel at study site RS on September 22. The line is the median, boxes are the 25th and 75th quartiles, and whiskers represent the maximum and minimum .

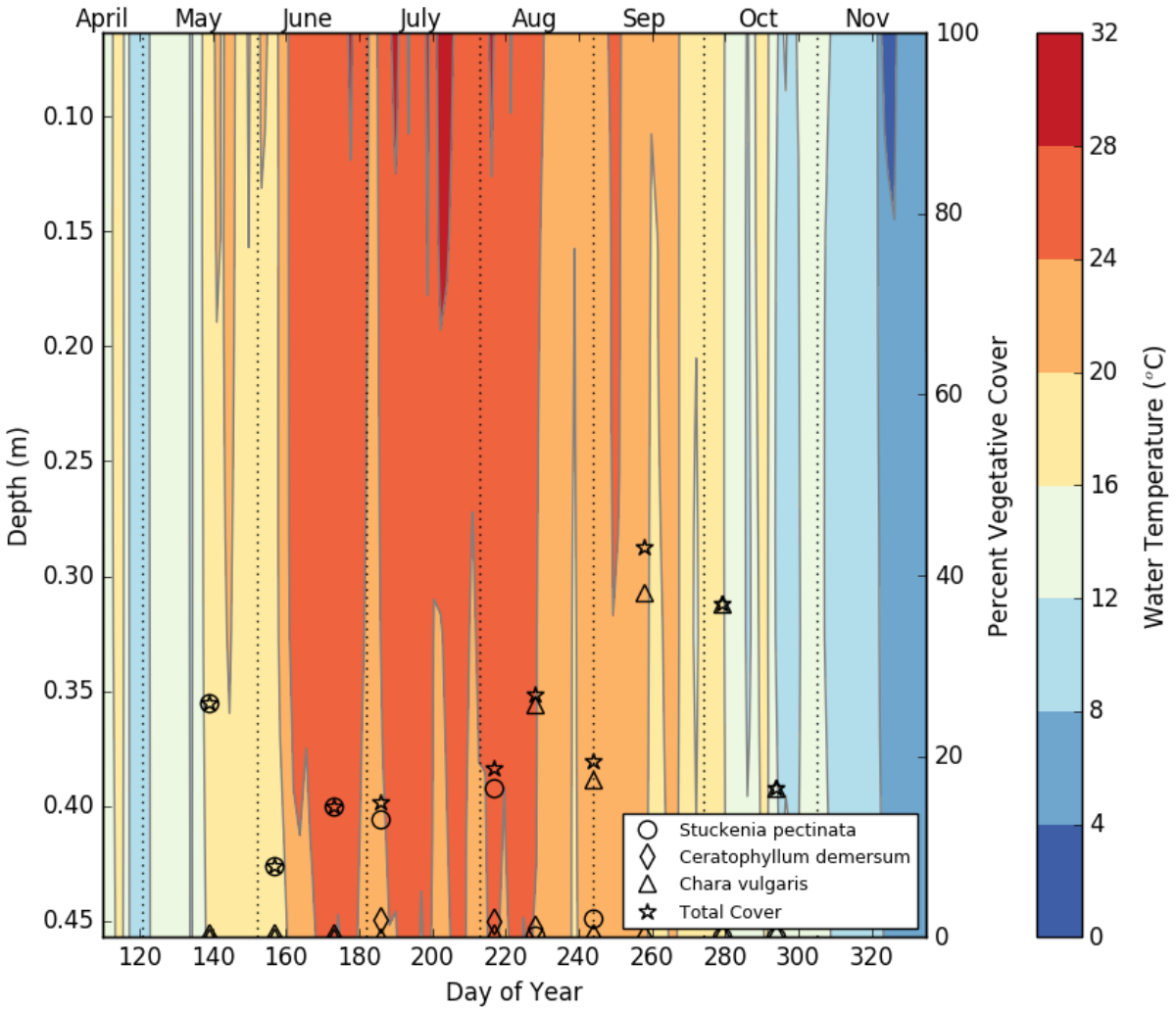

Figure 22. Temperature contour plot showing daily average temperature as a function of water depth and submersed macrophyte cover throughout the observation period at the KS7 array.

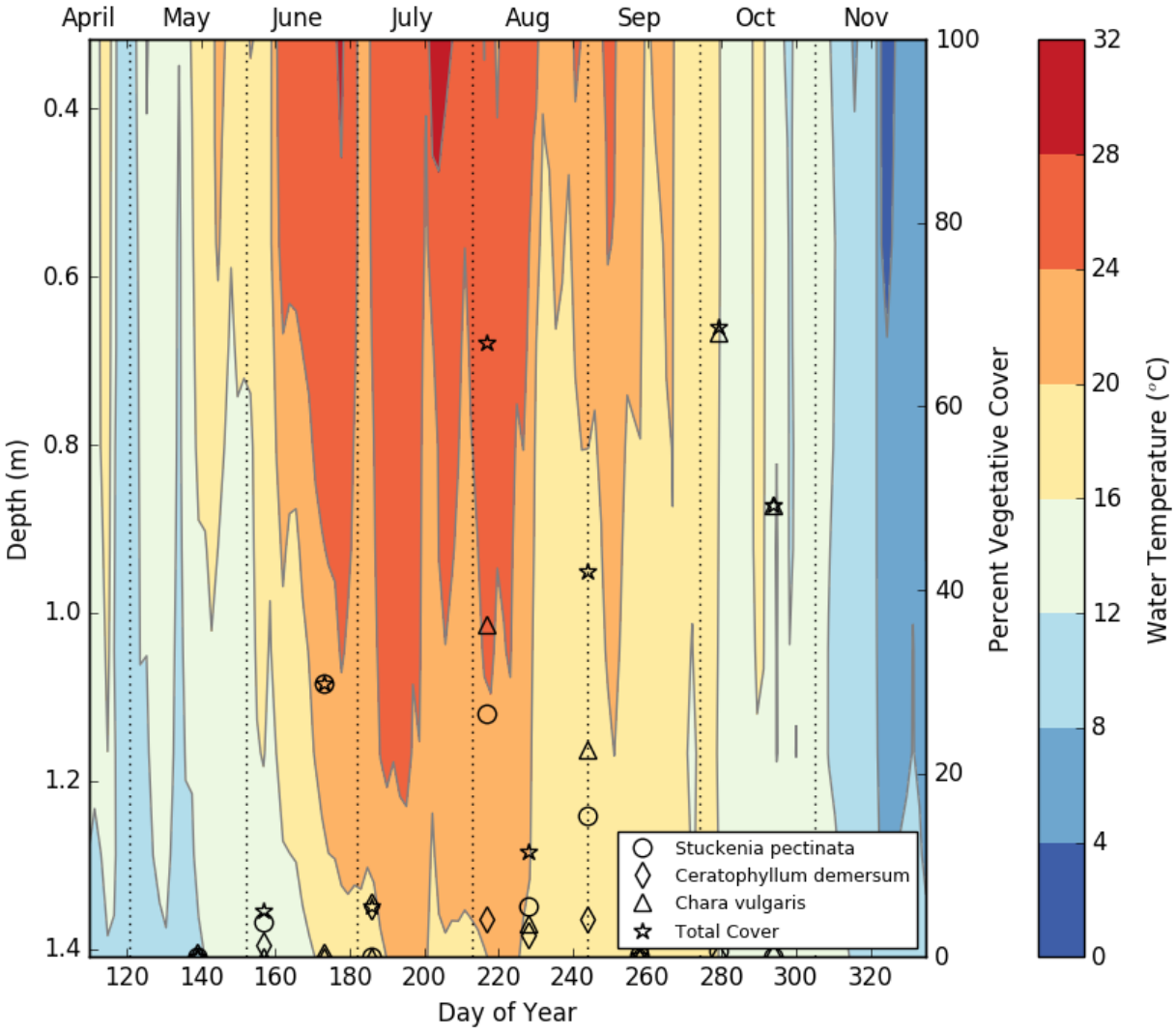

Figure 23. Temperature contour plot showing daily average temperature as a function of water depth and submersed macrophyte percent cover throughout the observation period at the KS9 array.

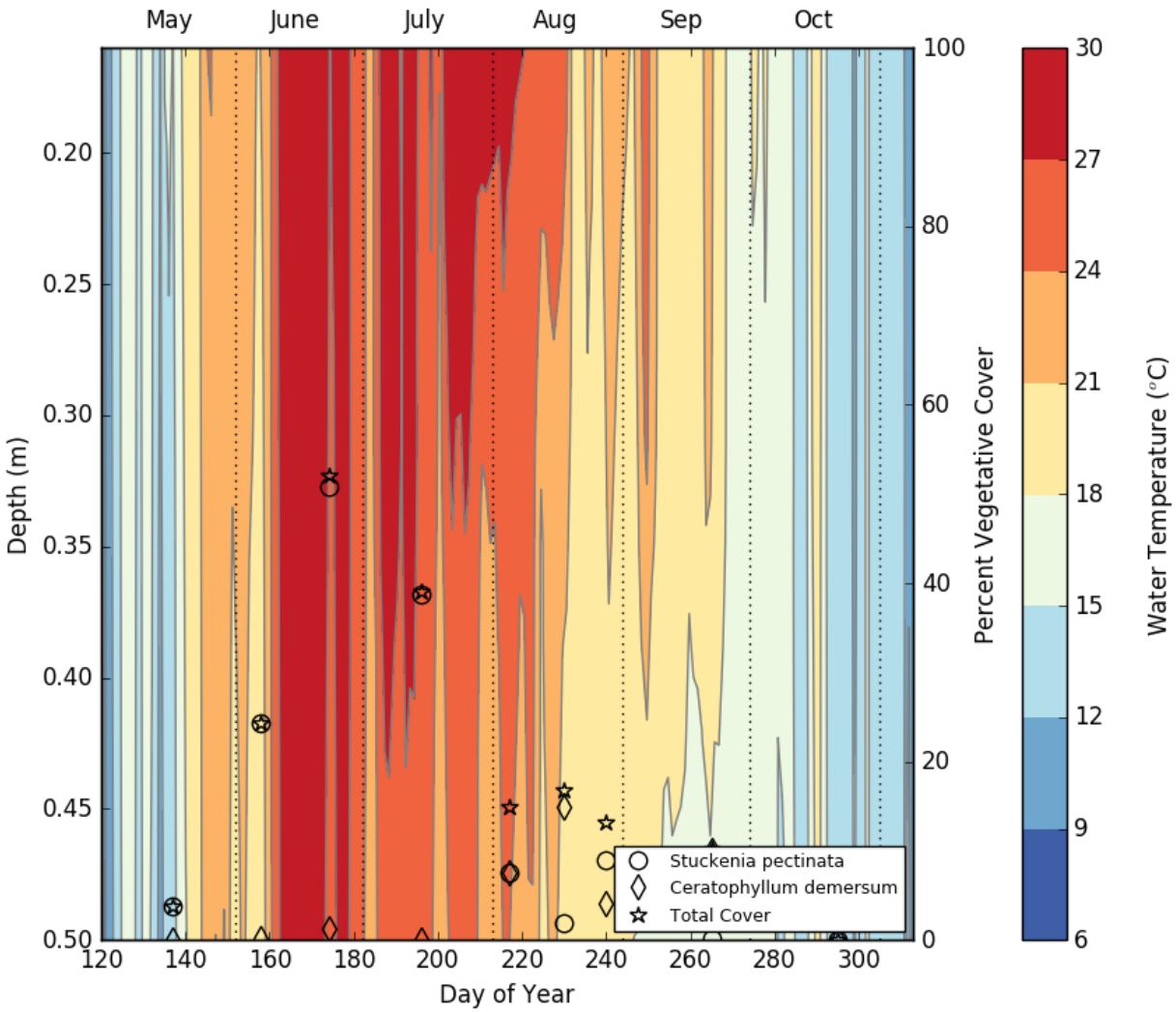

Figure 24. Temperature contour plot showing daily average temperature as a function of water depth and submersed macrophyte percent cover throughout the observation period at the RS7 array.

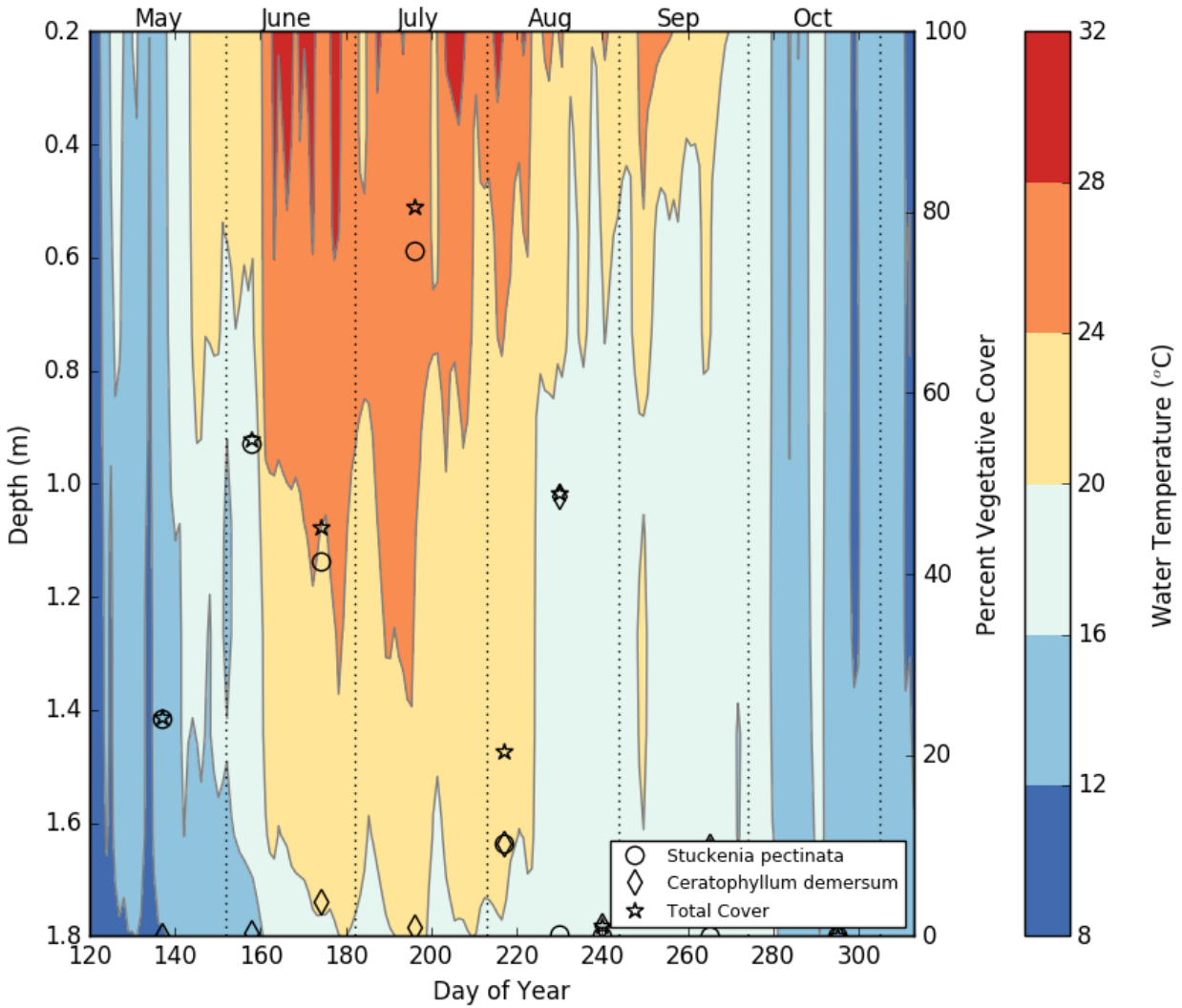

Figure 25. Temperature contour plot showing daily average temperature as a function of water depth submersed macrophyte percent cover throughout the observation period at the RS9 array.

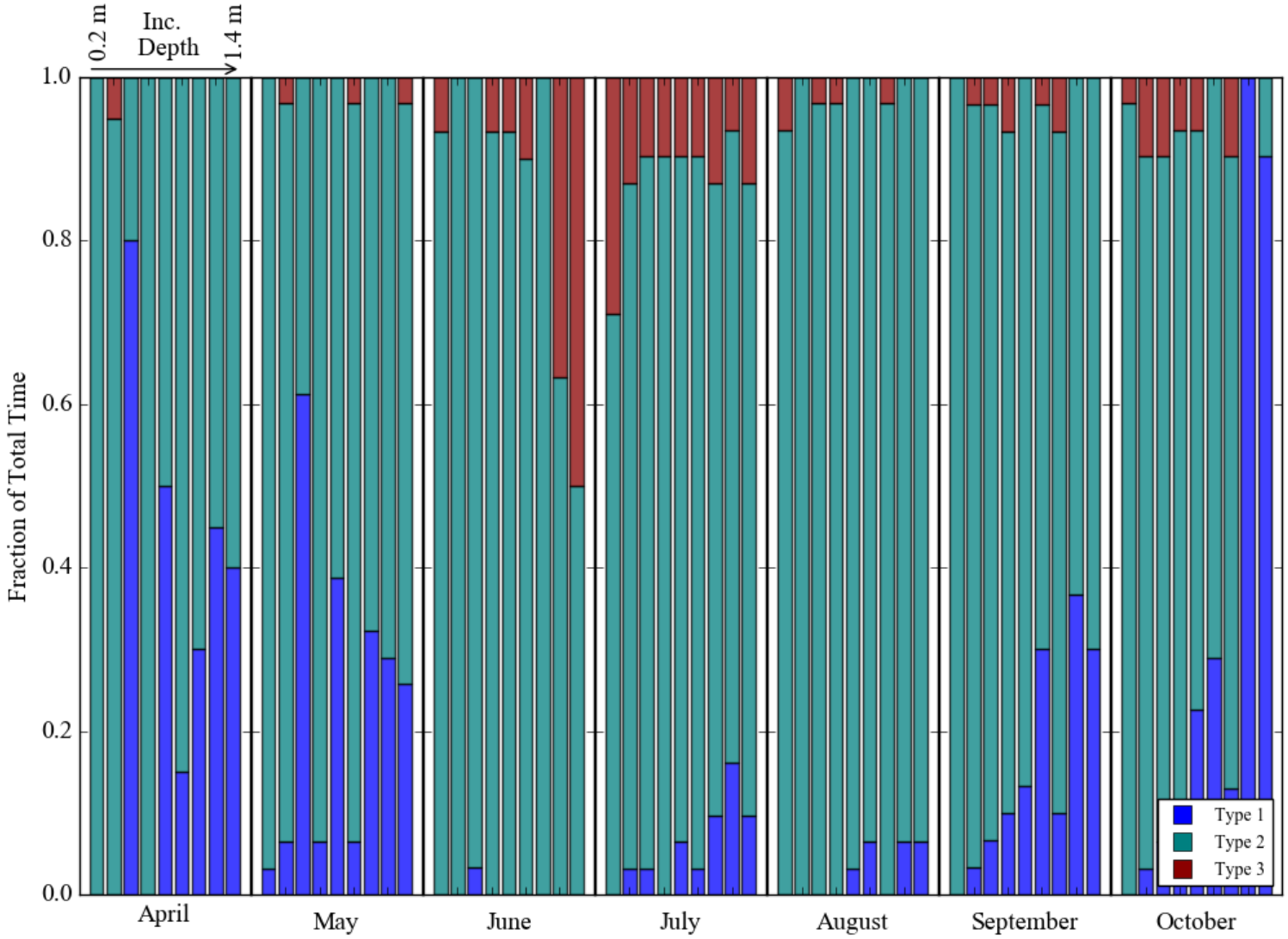

Figure 26. The total fraction of time that each stratification type was observed for each array for each month, ordered by water depth, at the KS wetland.

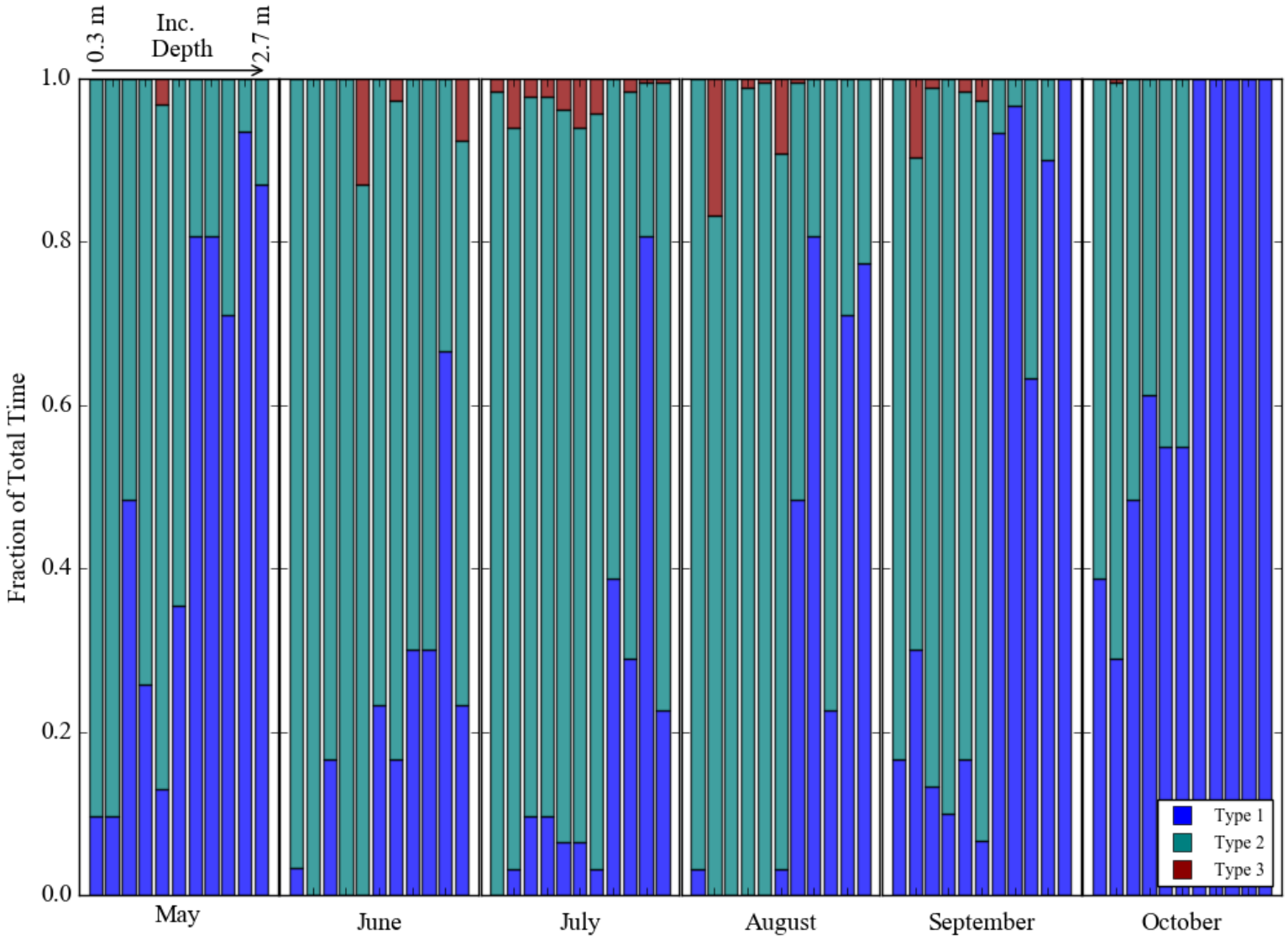

Figure 27. The total fraction of time that each stratification type was observed for each array for each month, ordered by water depth, at the RS wetland.

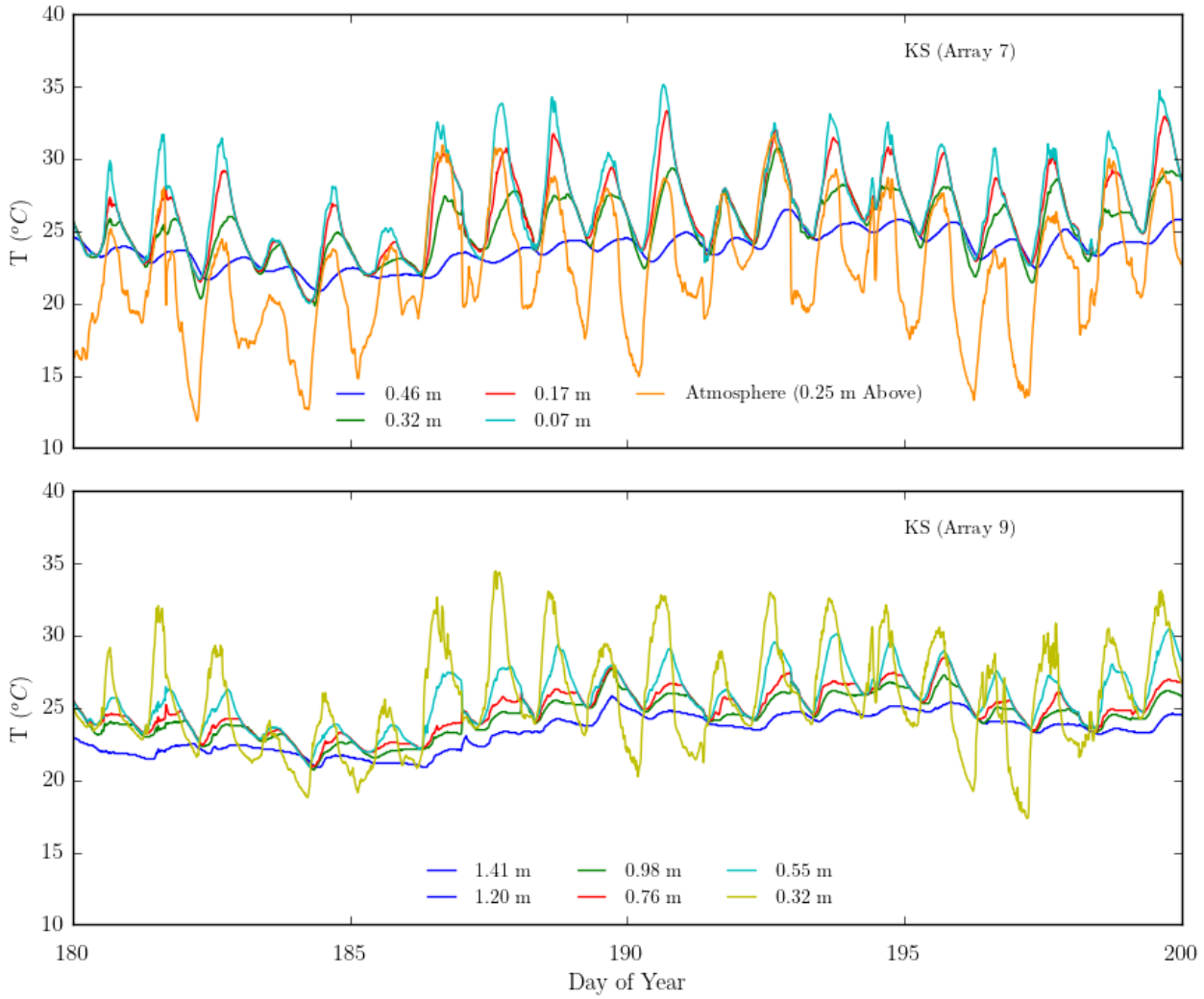

Figure 28. Raw temperatures for the period spanning the end of June to the middle of July (day of year 180 to 200) for the KS7 and KS9 arrays.

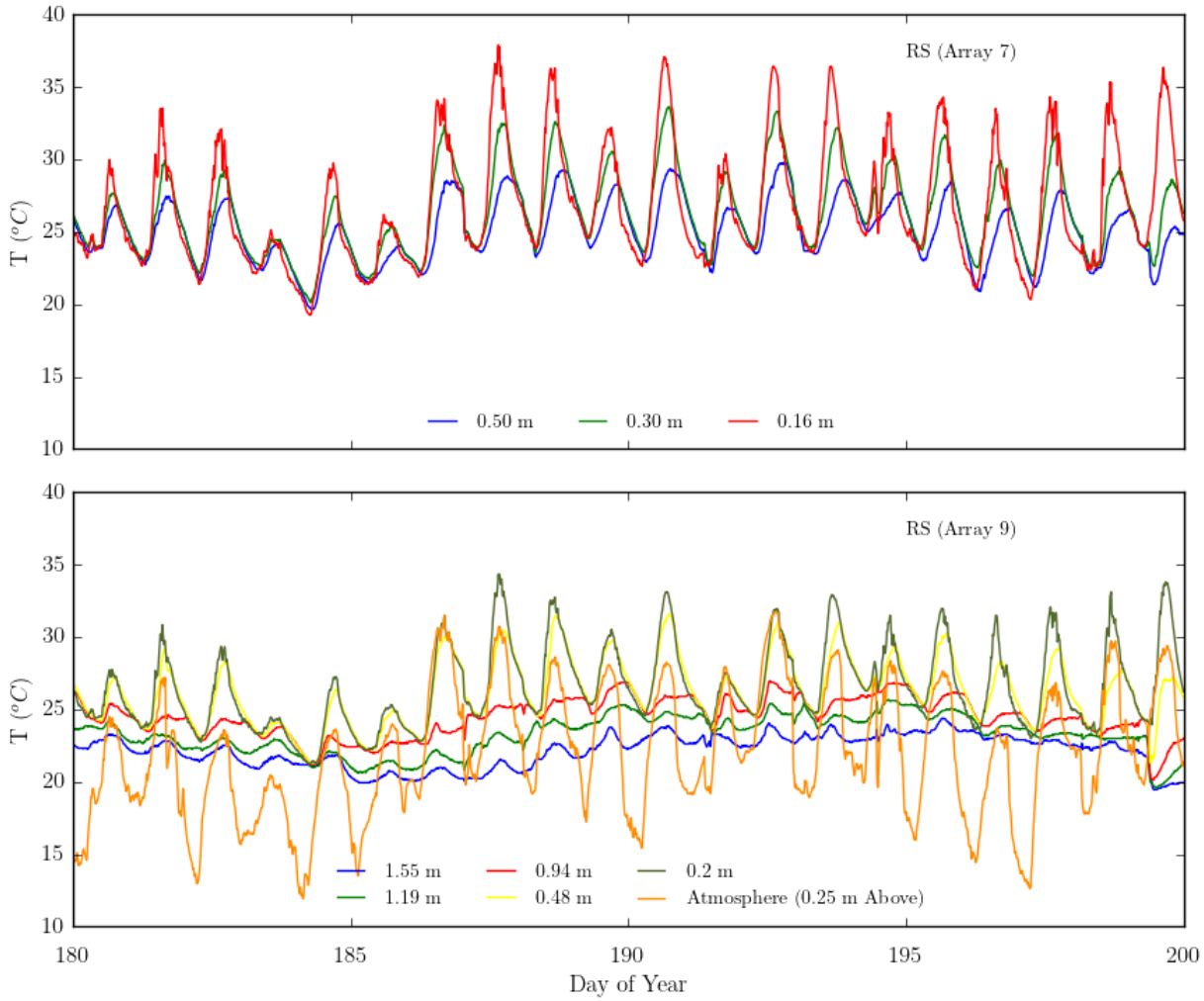

Figure 29. Raw temperatures for the period spanning the end of June to the middle of July (day of year 180 to 200) for the RS7 and RS9 arrays.

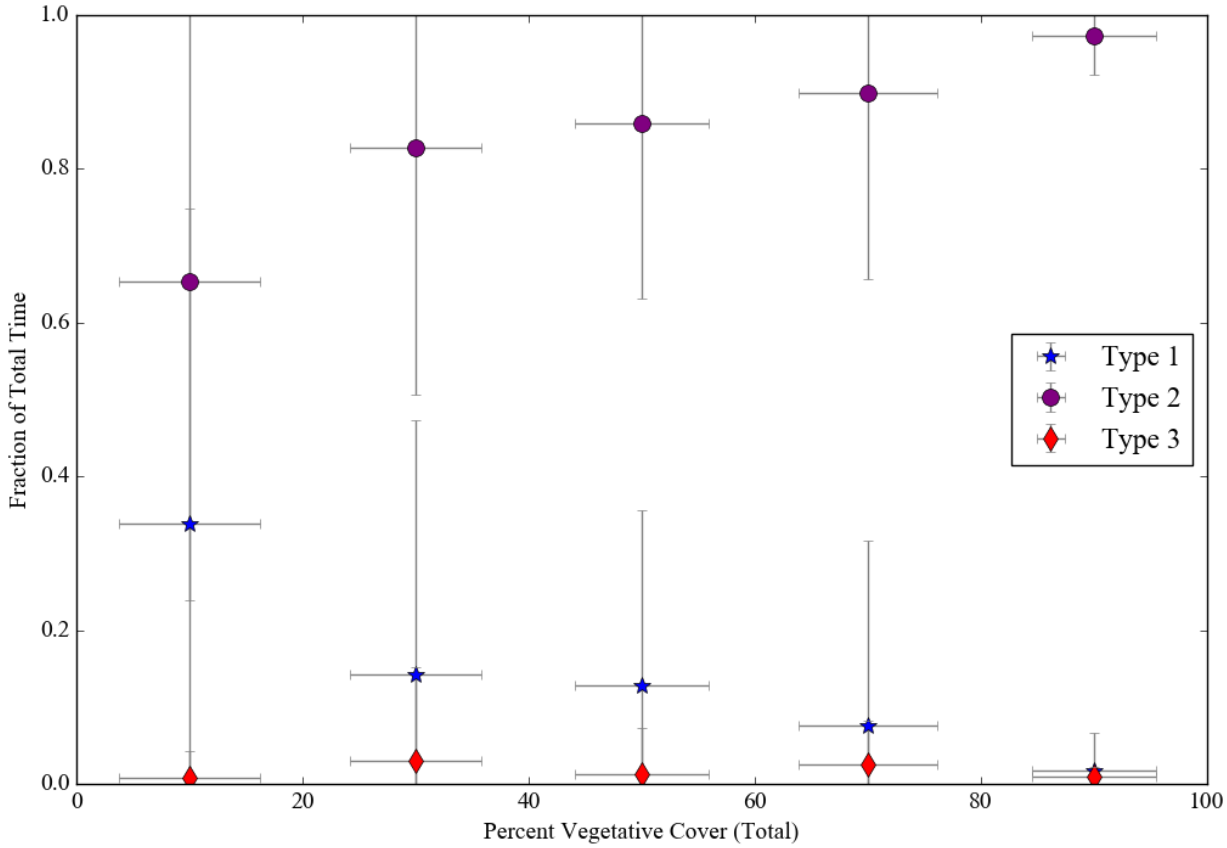

Figure 30. The likelihood of the occurrence of each stratification types as a function of percent submersed macrophyte cover. Horizontal and vertical lines represent the standard error for vegetative cover and the fraction of observed time spent in each stratification type, respectively. Data points and standard error lines were determined from an aggregation of observations from both wetlands.

CHAPTER 3. GENERAL CONCLUSIONS

This research studied the temperature dynamics and stratification and the relationship of these temperature patterns to submersed vegetation and other environmental factors in two shallow flow-through wetlands. Complex spatiotemporal temperature dynamics are present in shallow flow-through constructed wetlands. This supports research that shallow waterbodies, both natural and artificial, are subject to complex temperature dynamics and stratification. Water temperatures at the surface of the water were generally higher in the spring and summer while bottom temperatures were higher in mid to late fall. During the vast majority of the observation period, study sites exhibited diurnal stratification followed by nocturnal mixing. Some periods were observed where stratification would persist throughout the nighttime hours into the next day, particularly during warmer, densely vegetated conditions. Periods of contiguous mixing were also observed, primarily during colder, sparsely vegetated conditions.

This research has substantiated that the effects of submersed macrophytes on stratification and spatiotemporal temperature dynamics are a significant factor in the structure of thermal regimes in shallow flow-through constructed wetlands. The increase of submersed macrophyte cover coincided with an increase of diurnal stratification followed by nocturnal mixing. This supports previous research that has shown that submersed macrophytes are capable of increasing temperatures at the surface of the water while simultaneously inhibiting heating in the lower portions of the water column and limiting the effects of other environmental factors that promote a more isothermal water column (Condie and Webster, 2001; Herb and Stefan, 2005; Chimney *et al*., 2007 Andersen, 2017). However, submersed macrophytes appear to have little effect in inhibiting the nocturnal mixing.

This research provides greater understanding of temperature dynamics in shallow waterbodies, specifically in regard to shallow flow-through wetlands. However, further research is required to more fully investigate the effects of submersed macrophytes on temperature dynamics and stratification. A more detailed analysis of submersed macrophyte cover and structure could yield more information about relationships between temperature, stratification, and submersed macrophyte cover. This could provide information about what stratification regimes are more or less likely to develop and when, and any effects that the structure of individual species of submersed macrophyte can be extracted from this more detailed analysis.

References

Andersen, M. R., Sand-Jensen, K., Woolway, R. I., & Jones, I. D. (2017). Profound daily vertical stratification and mixing in a small, shallow, wind-exposed lake with submerged macrophytes. *Aquatic Sciences*, *79*(2), 395-406.

Chimney, M. J., Wenkert, L., & Pietro, K. C. (2006). Patterns of vertical stratification in a subtropical constructed wetland in south Florida (USA). *Ecological engineering*, *27*(4), 322-330.

Condie, S. A., & Webster, I. T. (2001). Estimating stratification in shallow water bodies from mean meteorological conditions. *Journal of Hydraulic Engineering*, *127*(4), 286-292.

Herb, W. R., & Stefan, H. G. (2005). Model for wind-driven vertical mixing in a shallow lake with submersed macrophytes. *Journal of hydraulic engineering*, *131*(6), 488-496.

APPENDIX A

COUNTOUR TEMPERATURE PLOTS

This appendix contains a contour plot for each temperature sensor array at KS an RS throughout the monitoring period. These figures show how temperatures change throughout the year in respect to the depth of the water column at each array.

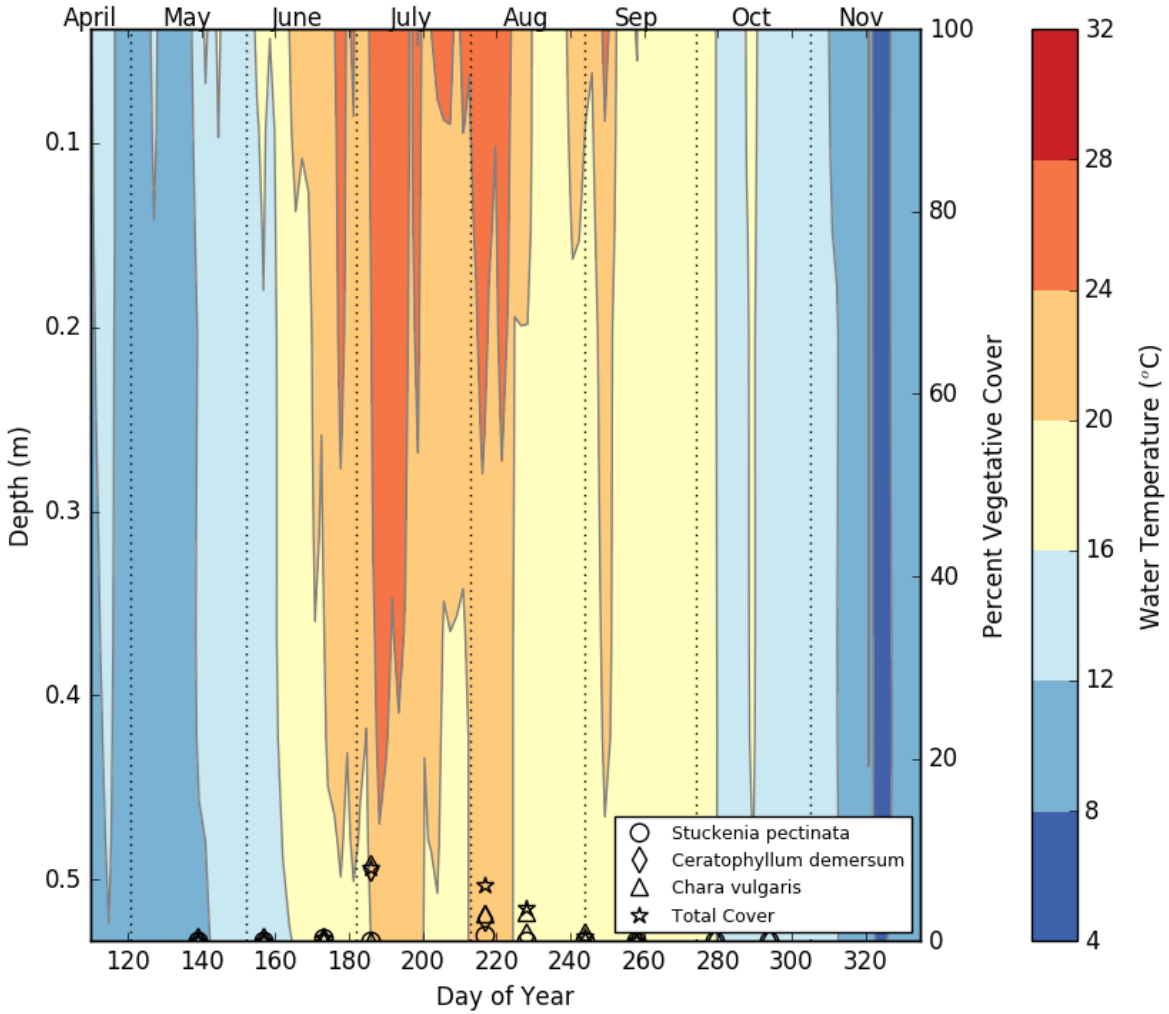

Figure 1A: Temperature contour plot showing daily average temperature as a function of water depth and submersed macrophyte percent cover throughout the observation period at the KS1 array.

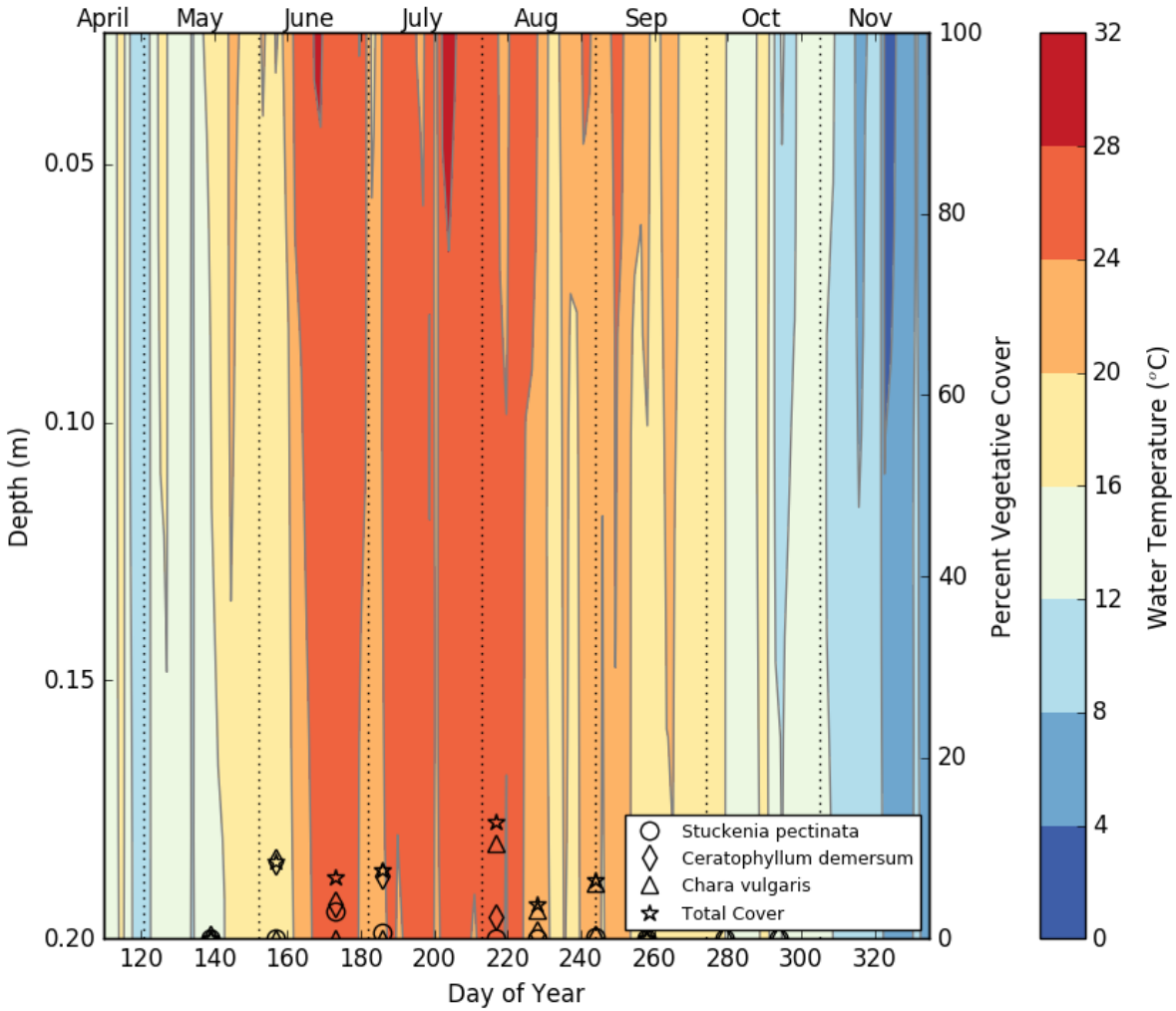

Figure 2A: Temperature contour plot showing daily average temperature as a function of water depth and submersed macrophyte percent cover throughout the observation period at the KS2 array.

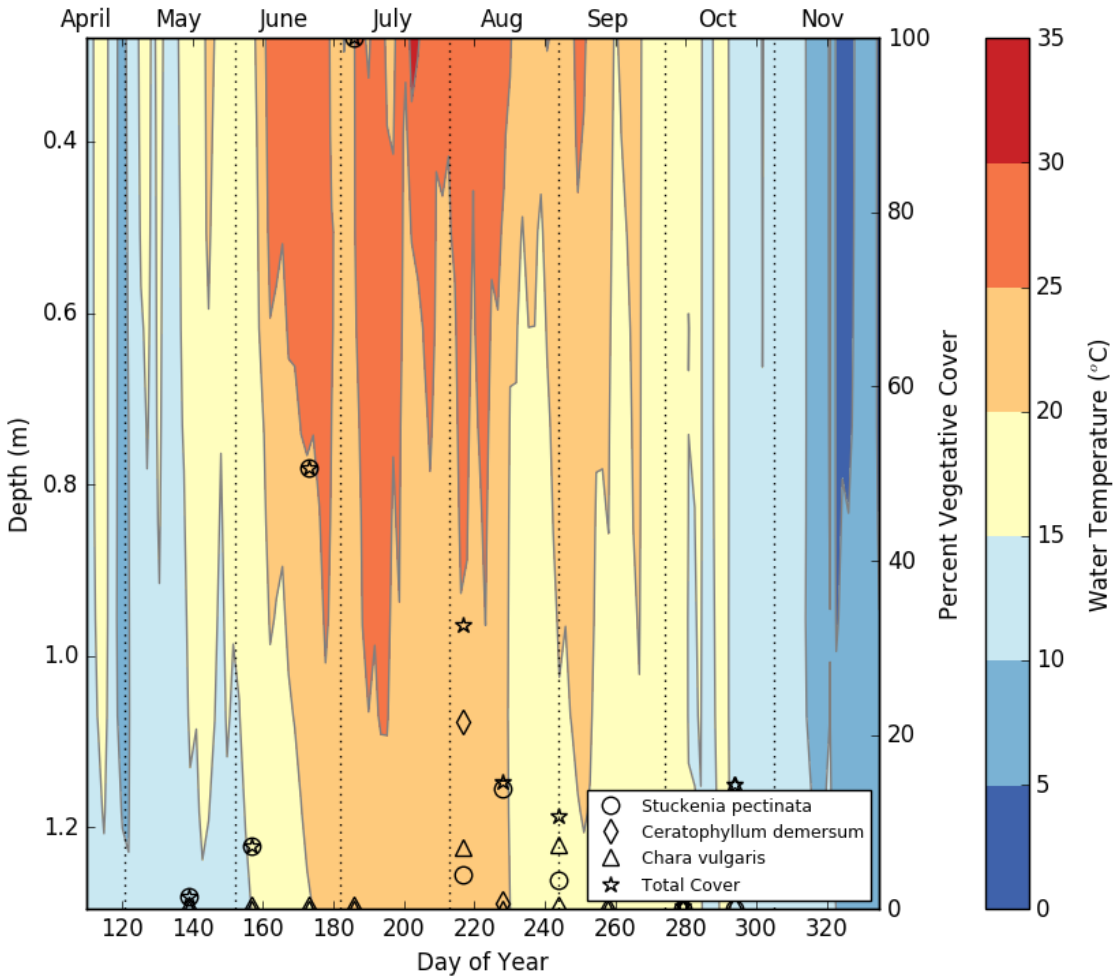

Figure 3A: Temperature contour plot showing daily average temperature as a function of water depth and submersed macrophyte percent cover throughout the observation period at the KS6 array.

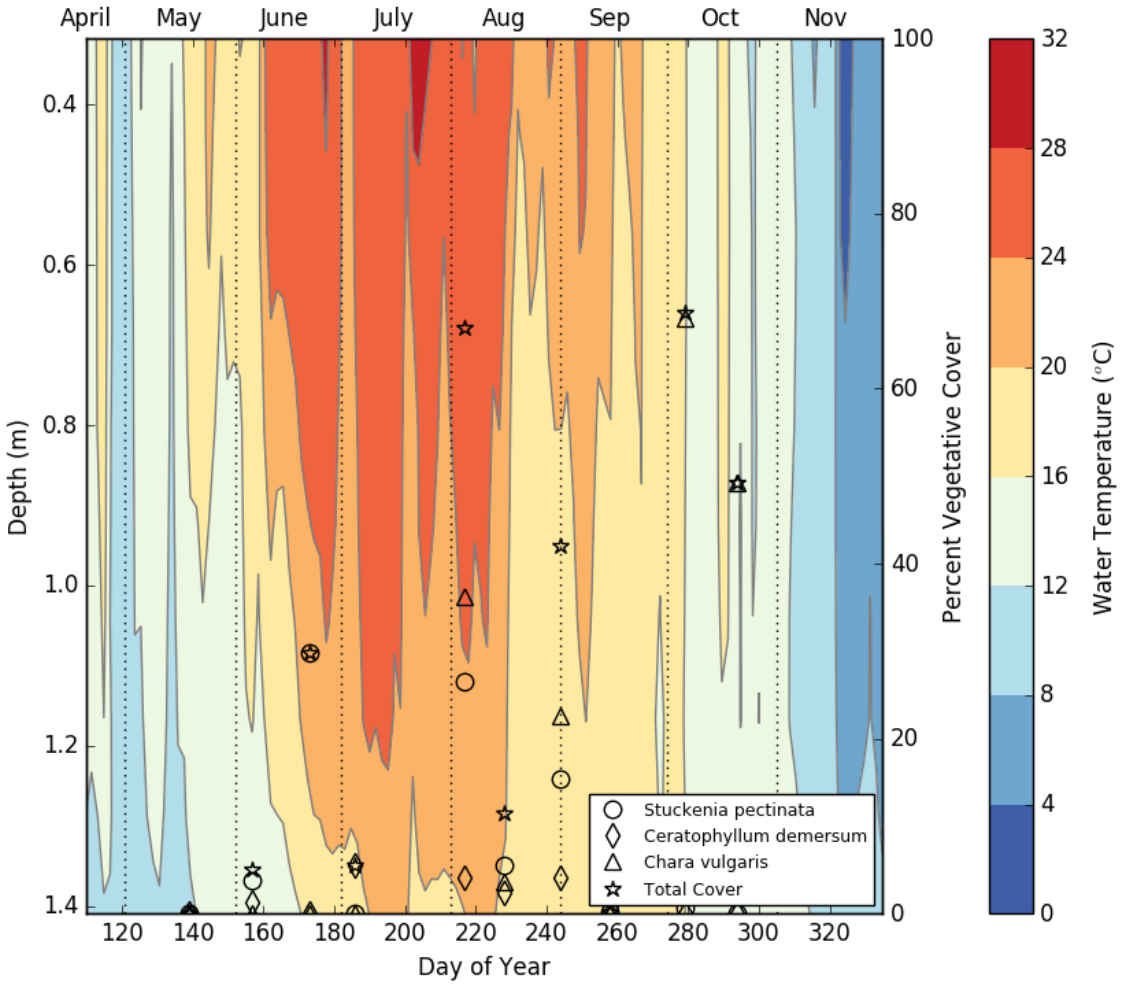

Figure 4A: Temperature contour plot showing daily average temperature as a function of water depth and submersed macrophyte percent cover throughout the observation period at the KS7 array.

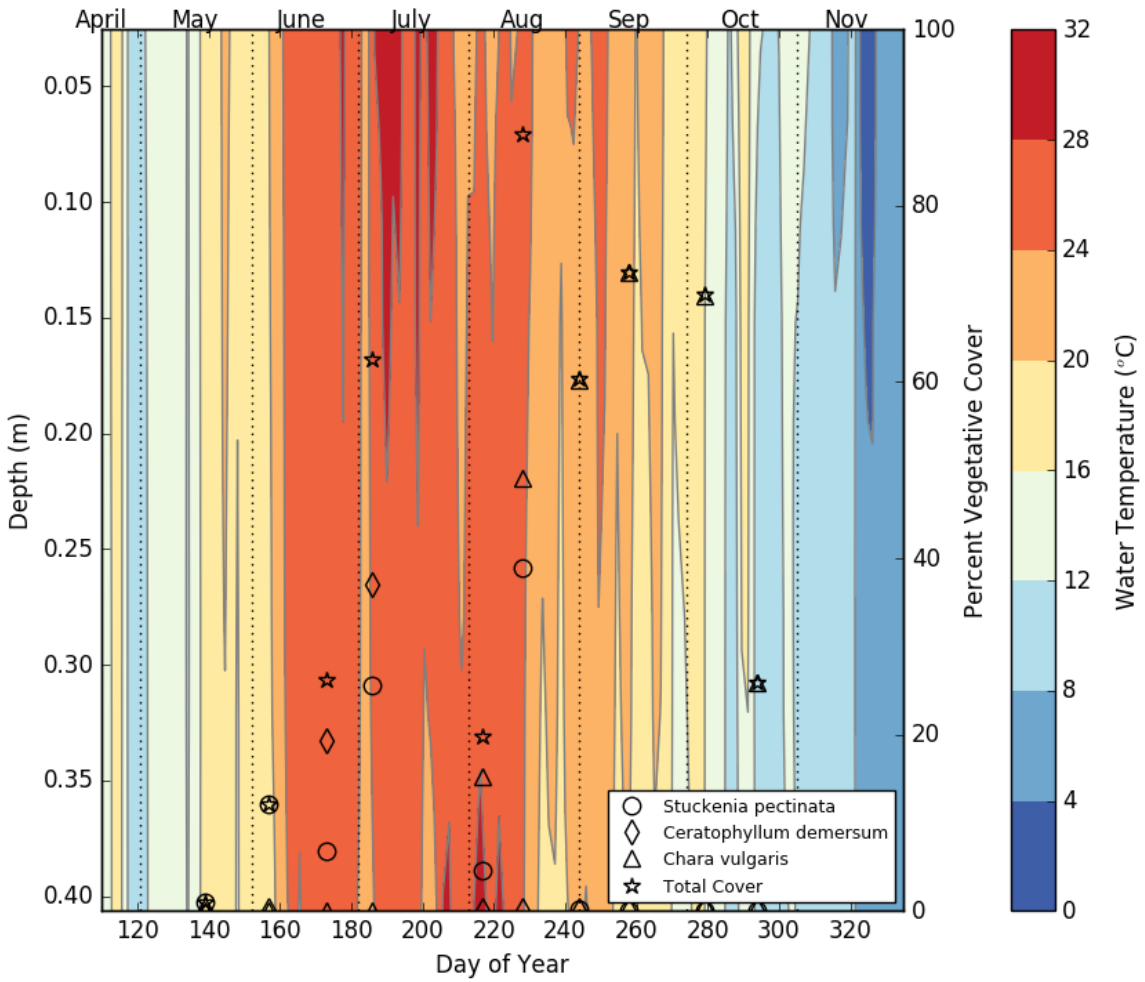

Figure 5A: Temperature contour plot showing daily average temperature as a function of water depth and submersed macrophyte percent cover throughout the observation period at the KS8 array.

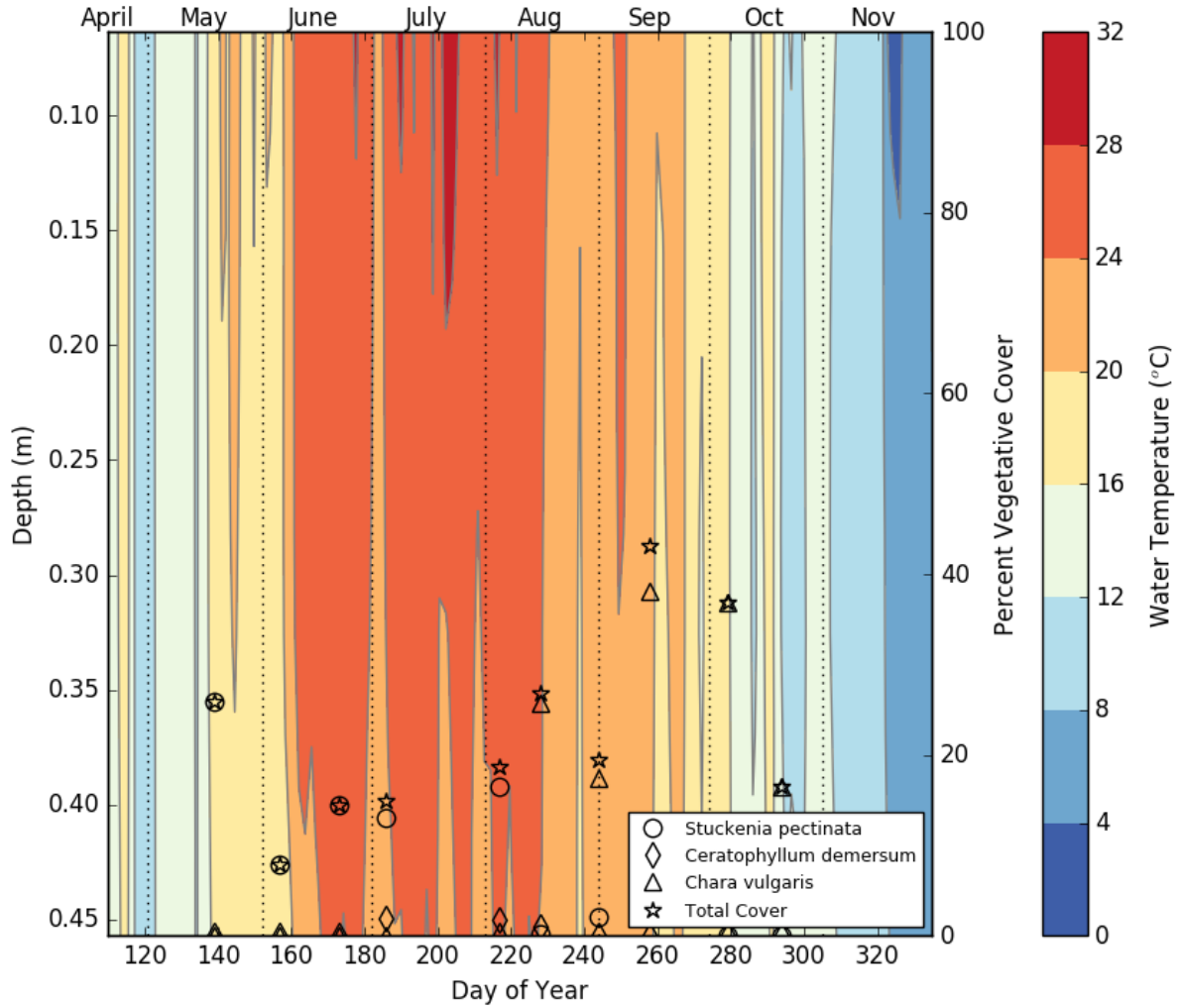

Figure 6A: Temperature contour plot showing daily average temperature as a function of water depth and submersed macrophyte percent cover throughout the observation period at the KS9 array.

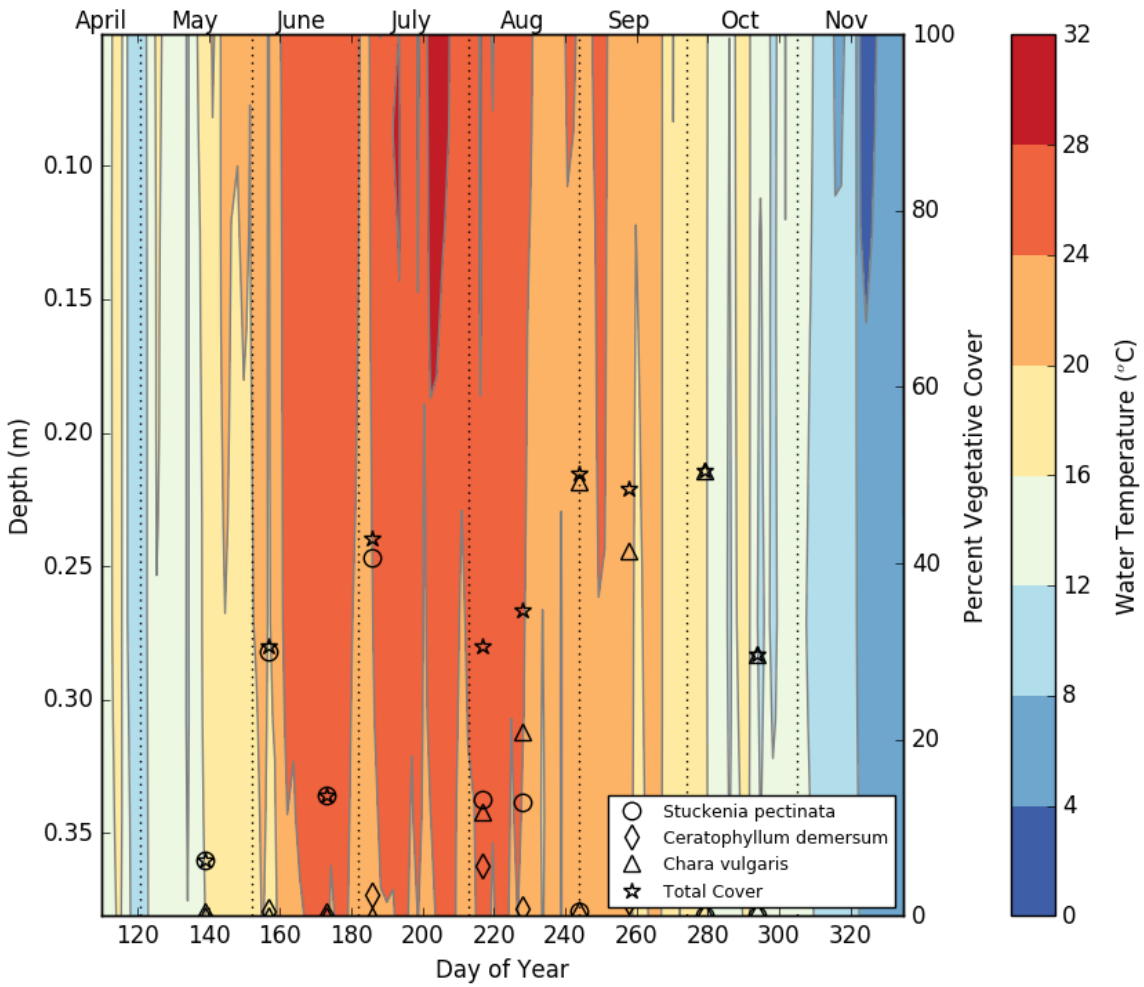

Figure 7A: Temperature contour plot showing daily average temperature as a function of water depth and submersed macrophyte percent cover throughout the observation period at the KS10 array.

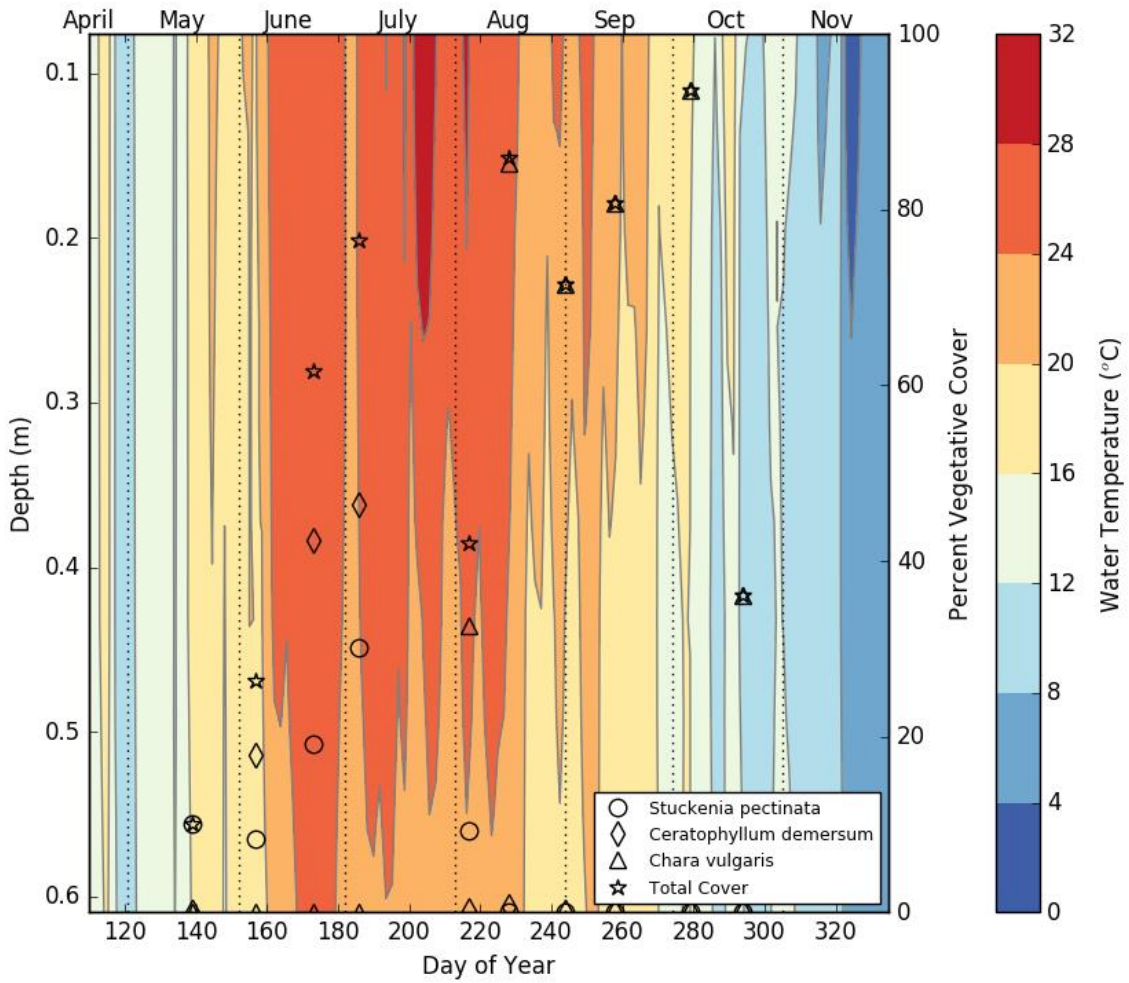

Figure 8A: Temperature contour plot showing daily average temperature as a function of water depth and submersed macrophyte percent cover throughout the observation period at the KS11 array.

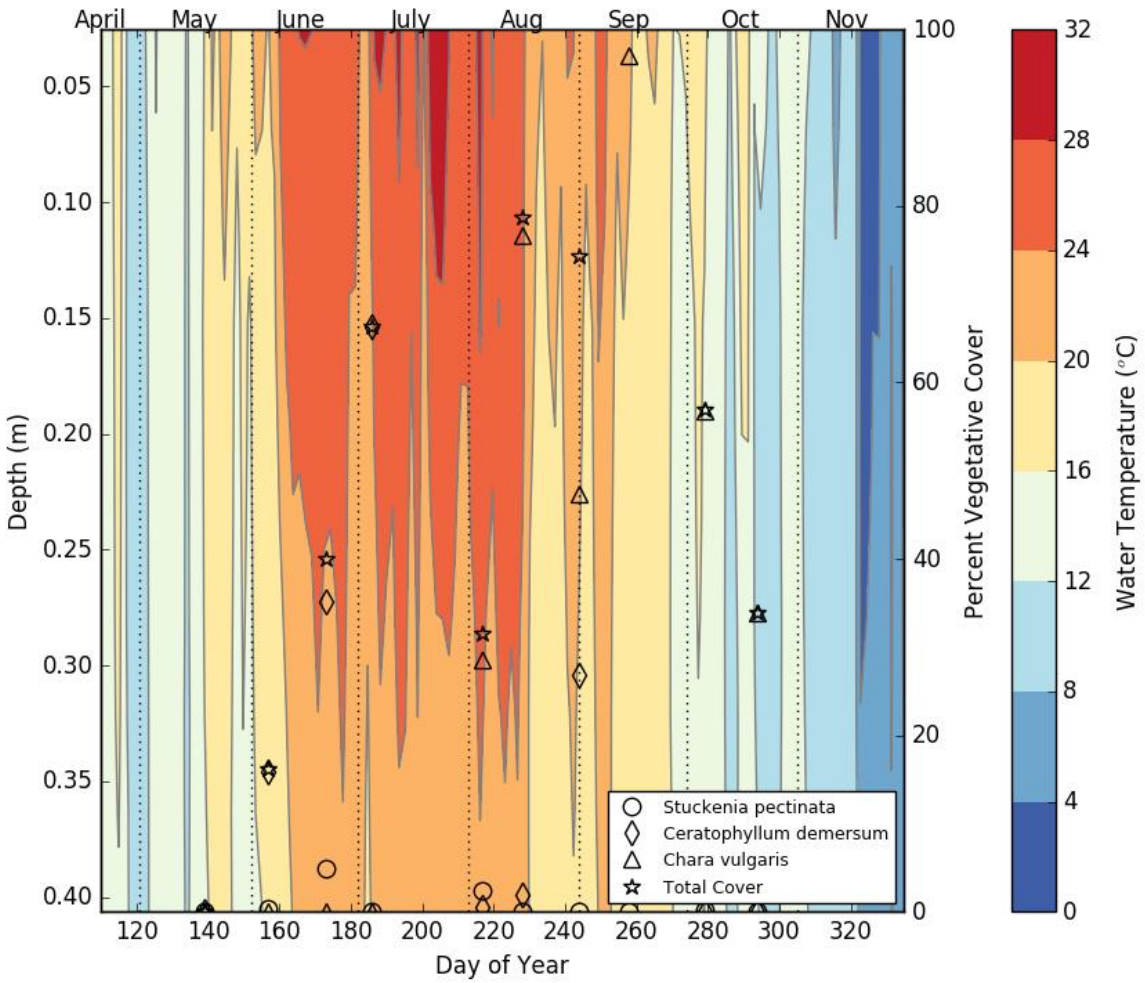

Figure 9A: Temperature contour plot showing daily average temperature as a function of water depth and submersed macrophyte percent cover throughout the observation period at the KS12 array.

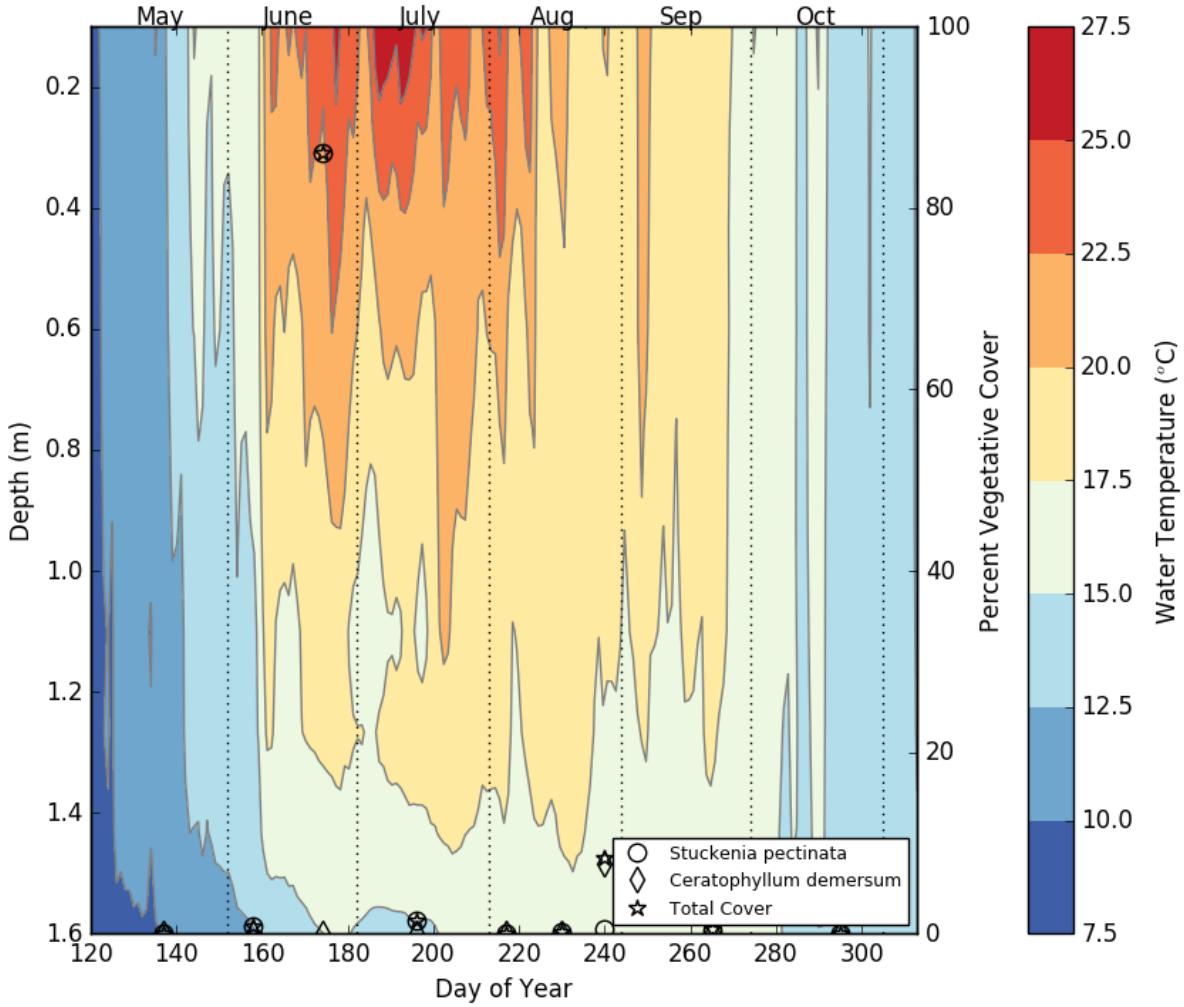

Figure 10A: Temperature contour plot showing daily average temperature as a function of water depth and submersed macrophyte percent cover throughout the observation period at the RS1 array.

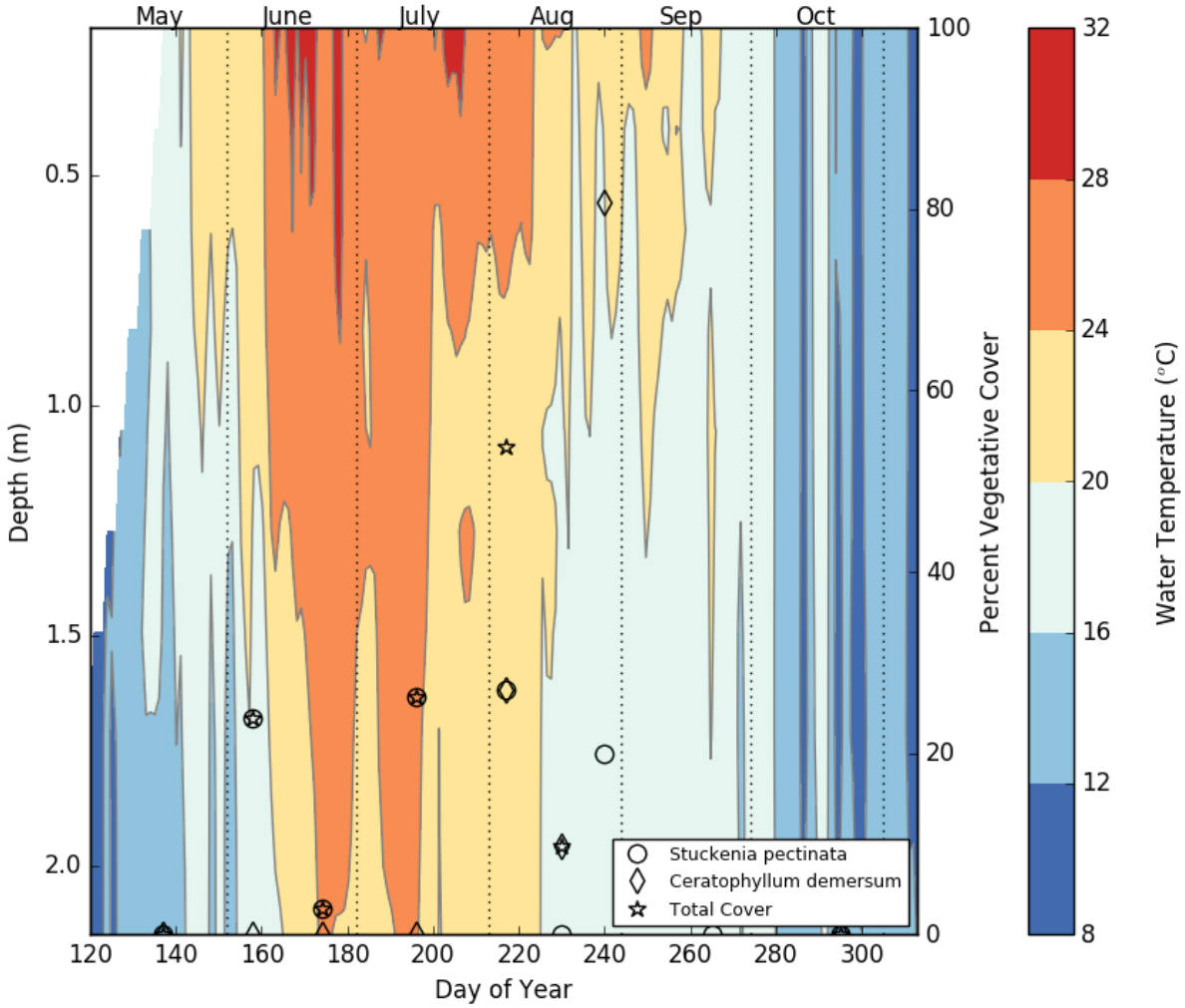

Figure 11A: Temperature contour plot showing daily average temperature as a function of water depth and submersed macrophyte percent cover throughout the observation period at the RS2 array.

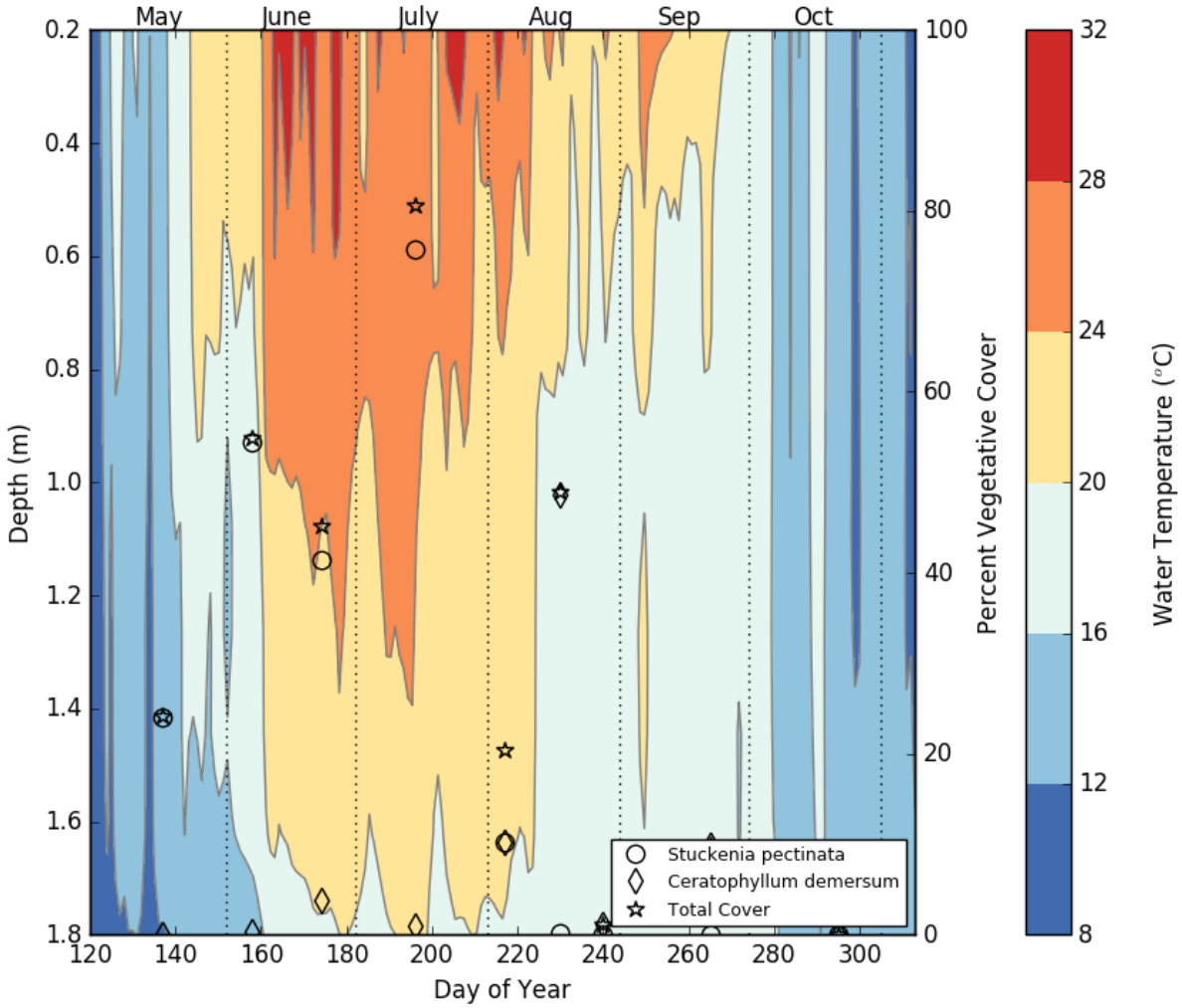

Figure 12A: Temperature contour plot showing daily average temperature as a function of water depth and submersed macrophyte percent cover throughout the observation period at the RS4 array.

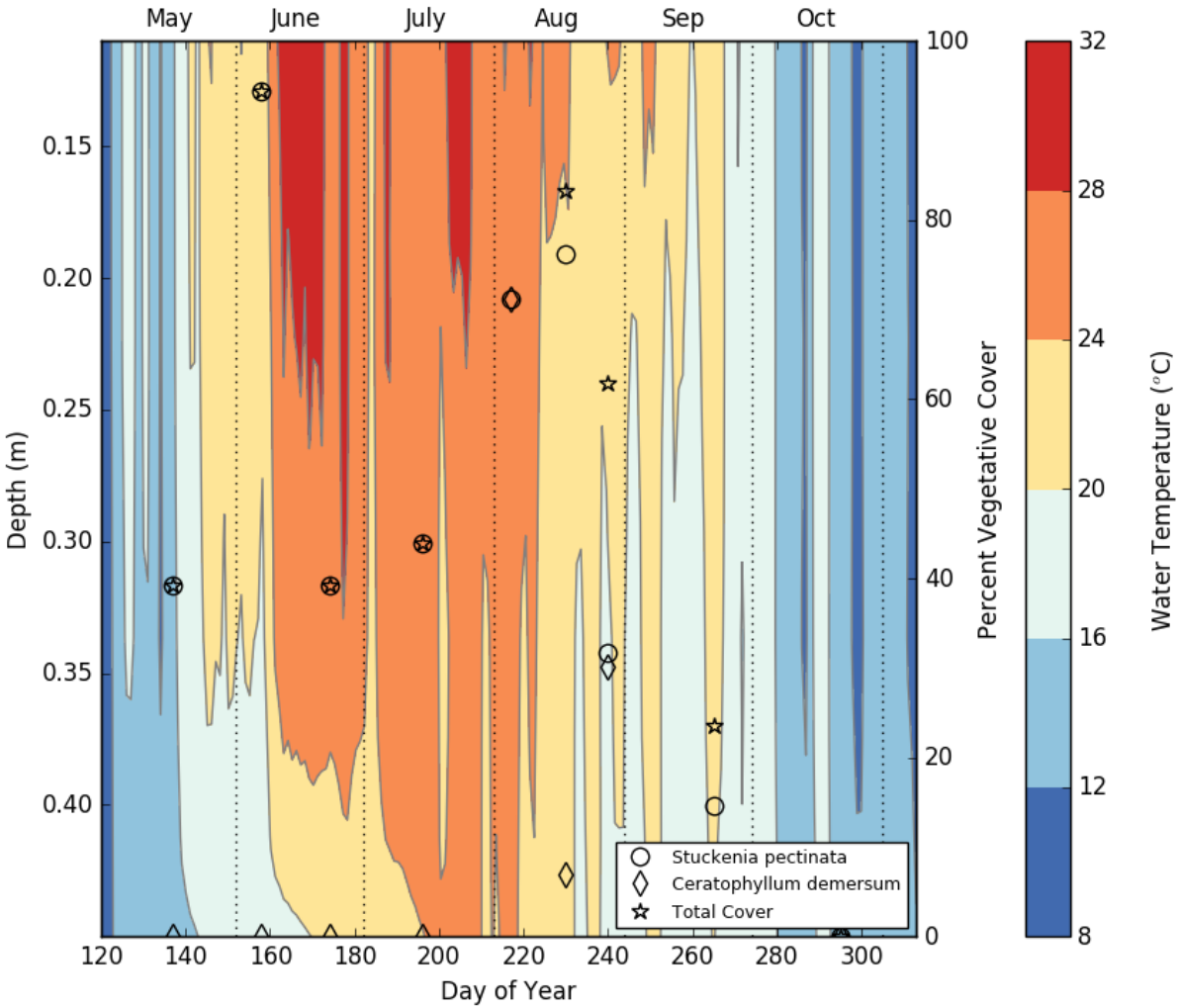

Figure 13A: Temperature contour plot showing daily average temperature as a function of water depth and submersed macrophyte percent cover throughout the observation period at the RS5 array.

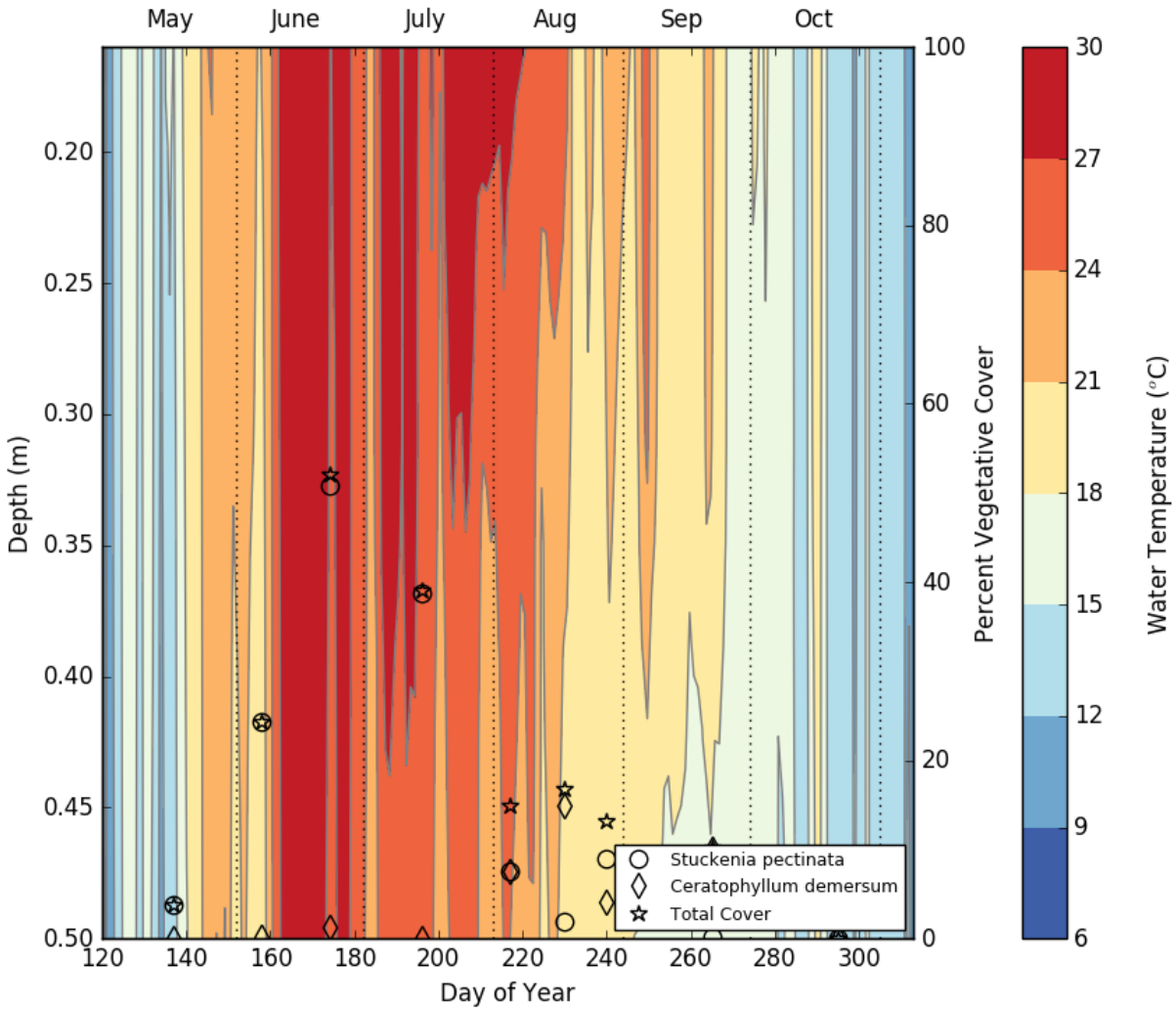

Figure 14A: Temperature contour plot showing daily average temperature as a function of water depth and submersed macrophyte percent cover throughout the observation period at the RS6 array.

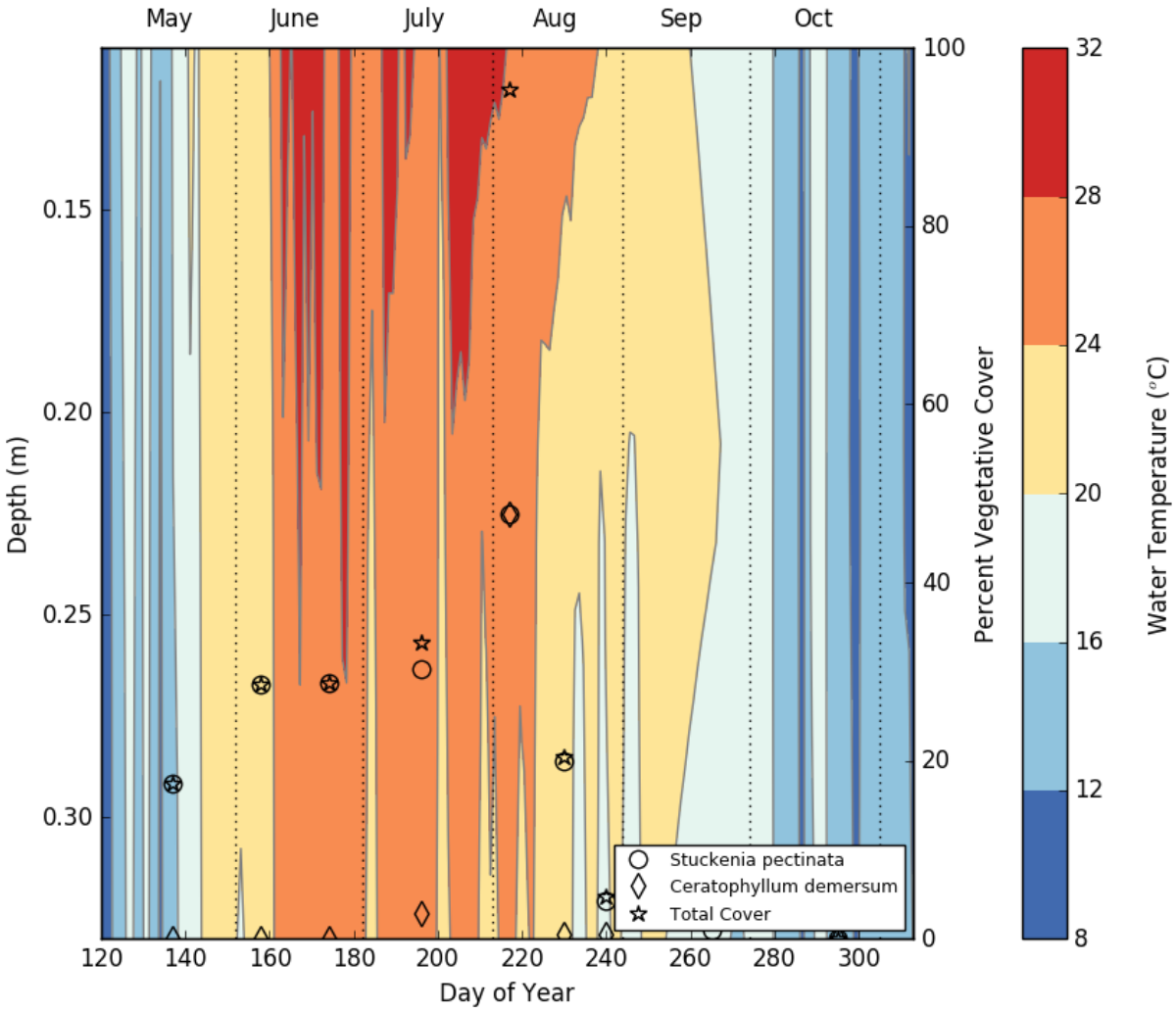

Figure 15A: Temperature contour plot showing daily average temperature as a function of water depth and submersed macrophyte percent cover throughout the observation period at the RS7 array.

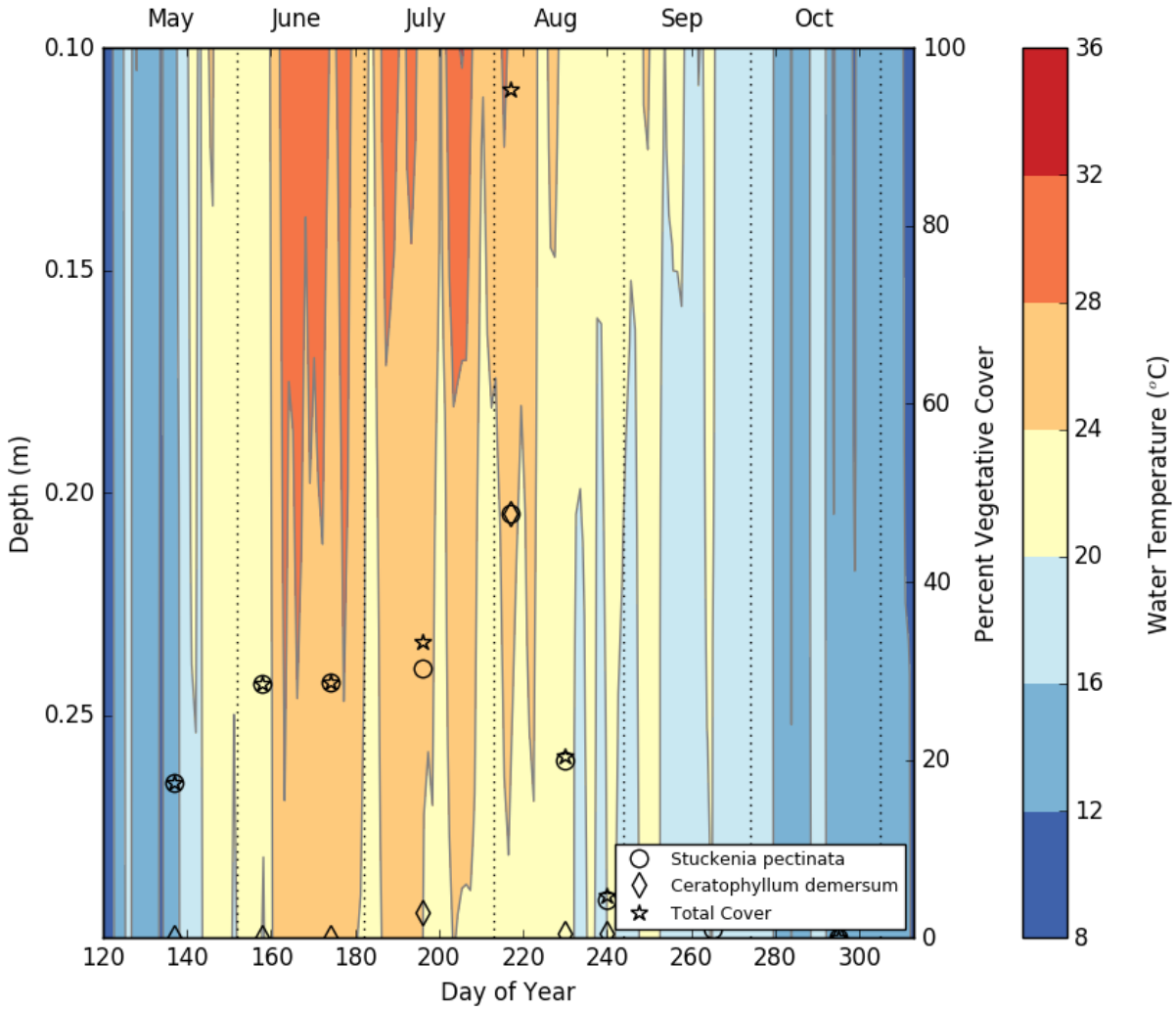

Figure 16A: Temperature contour plot showing daily average temperature as a function of water depth and submersed macrophyte percent cover throughout the observation period at the RS8 array.

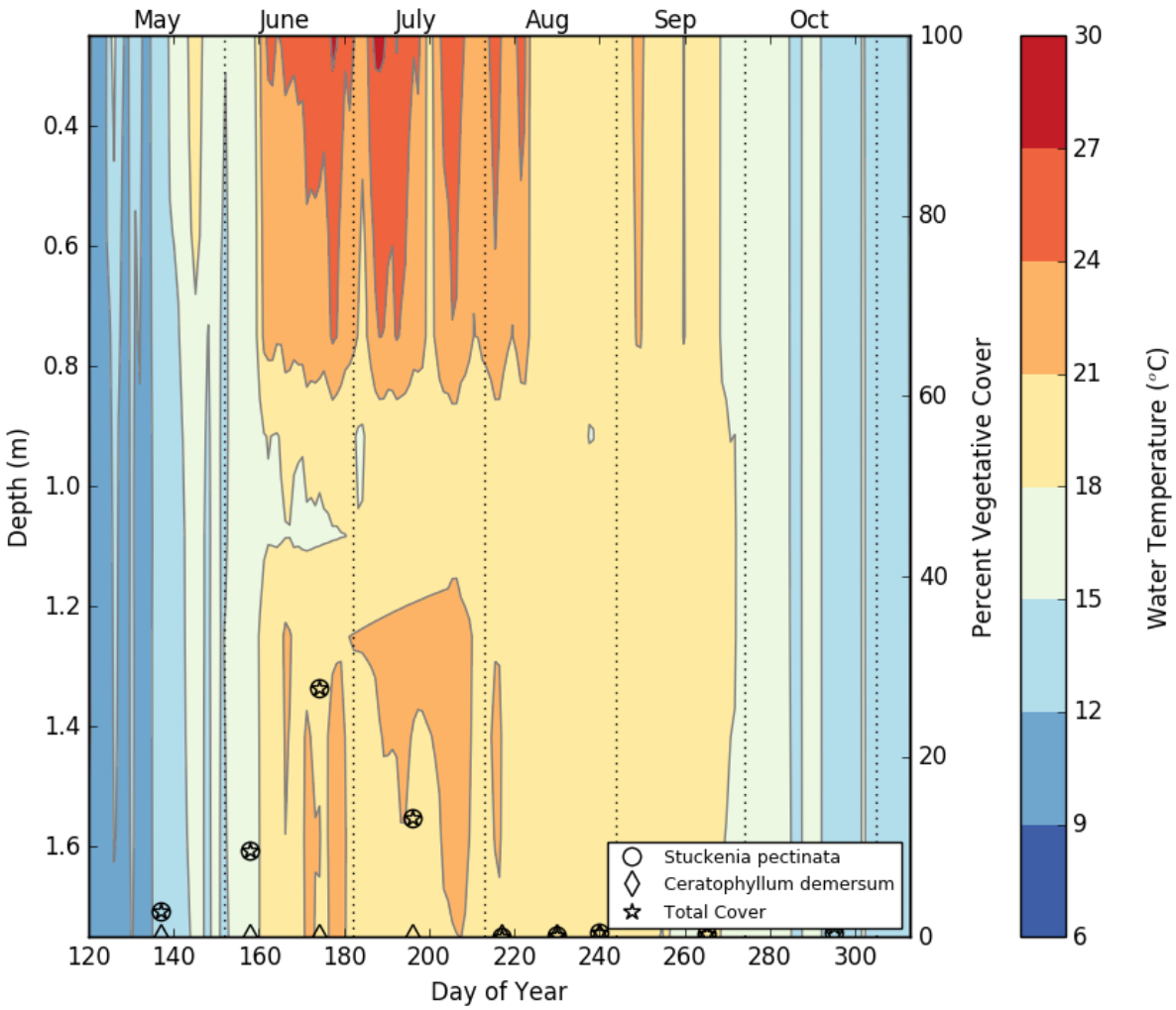

Figure 17A: Temperature contour plot showing daily average temperature as a function of water depth and submersed macrophyte percent cover throughout the observation period at the RS9 array.

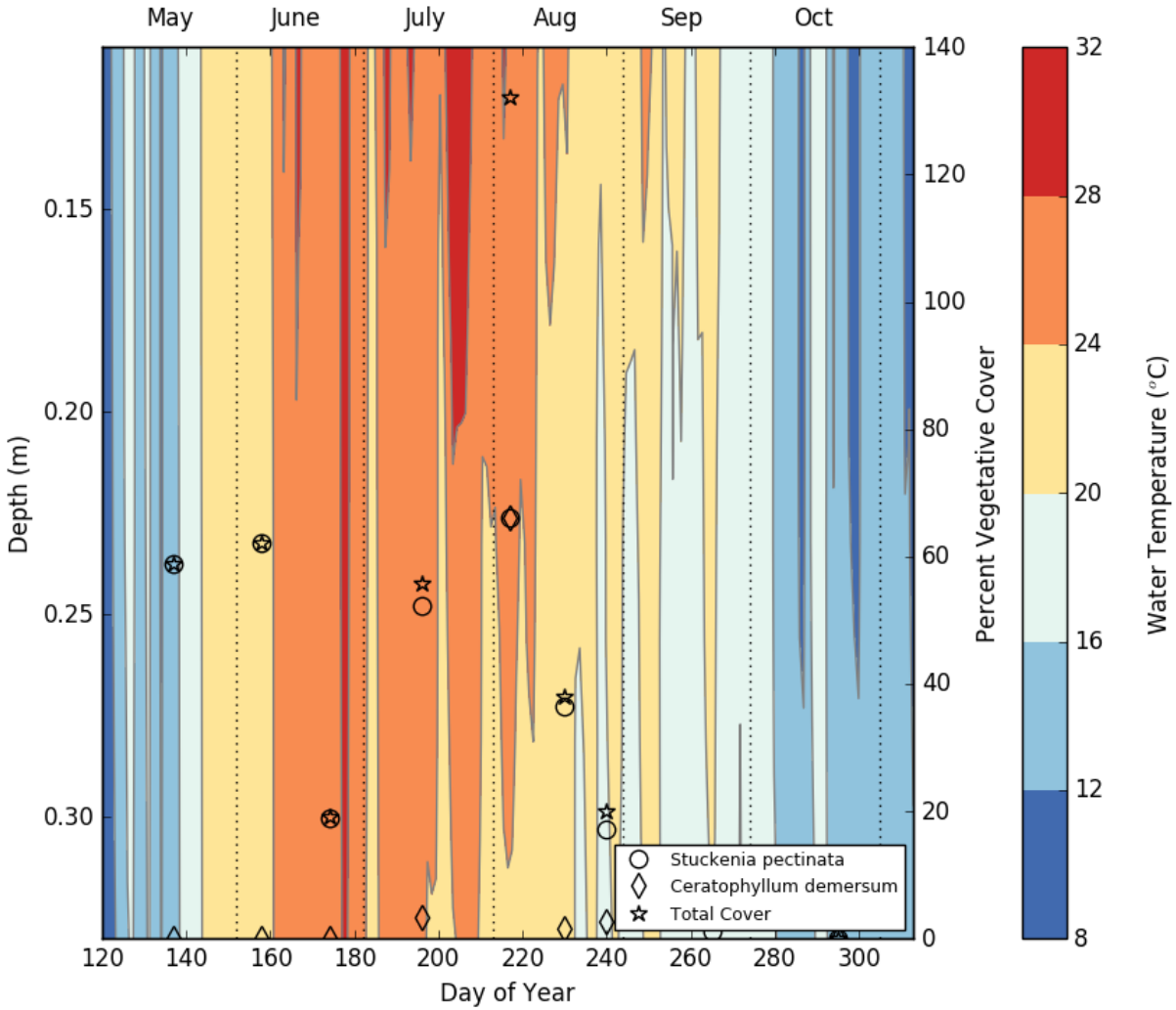

Figure 18A: Temperature contour plot showing daily average temperature as a function of water depth and submersed macrophyte percent cover throughout the observation period at the RS10 array.

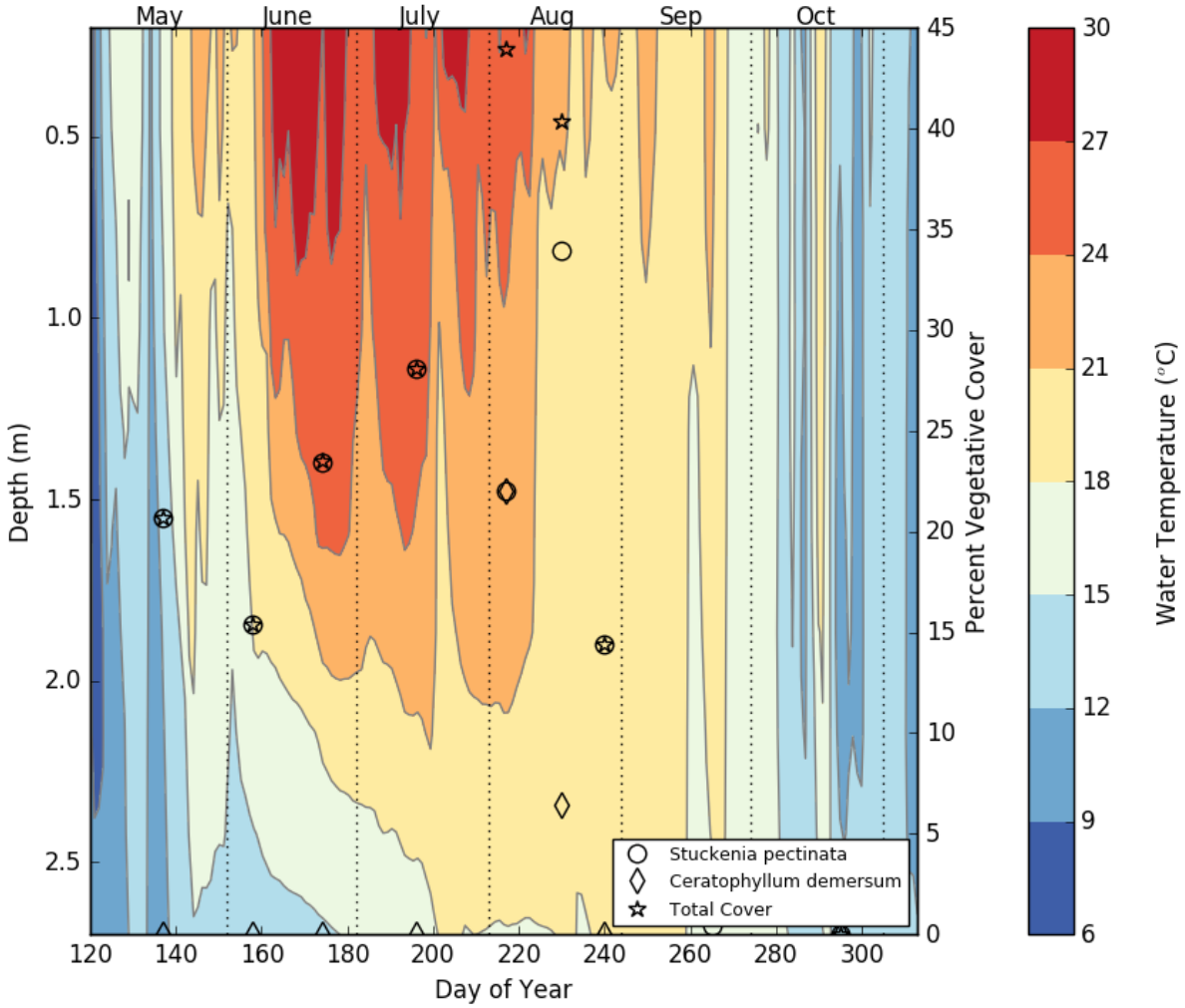

Figure 19A: Temperature contour plot showing daily average temperature as a function of water depth and submersed macrophyte percent cover throughout the observation period at the RS11 array.

APPENDIX B

MAPS OF INTERPOLATED VEGETATIVE COVER AND ARRAY LOCATIONS

This appendix contains maps of interpolated vegetative cover for each vegetation survey conducted at KS and RS. Temporal vegetation changes are shown as the growing season progresses. Patterns of growth, changes in distribution, and senescence can be observed throughout the growing season.

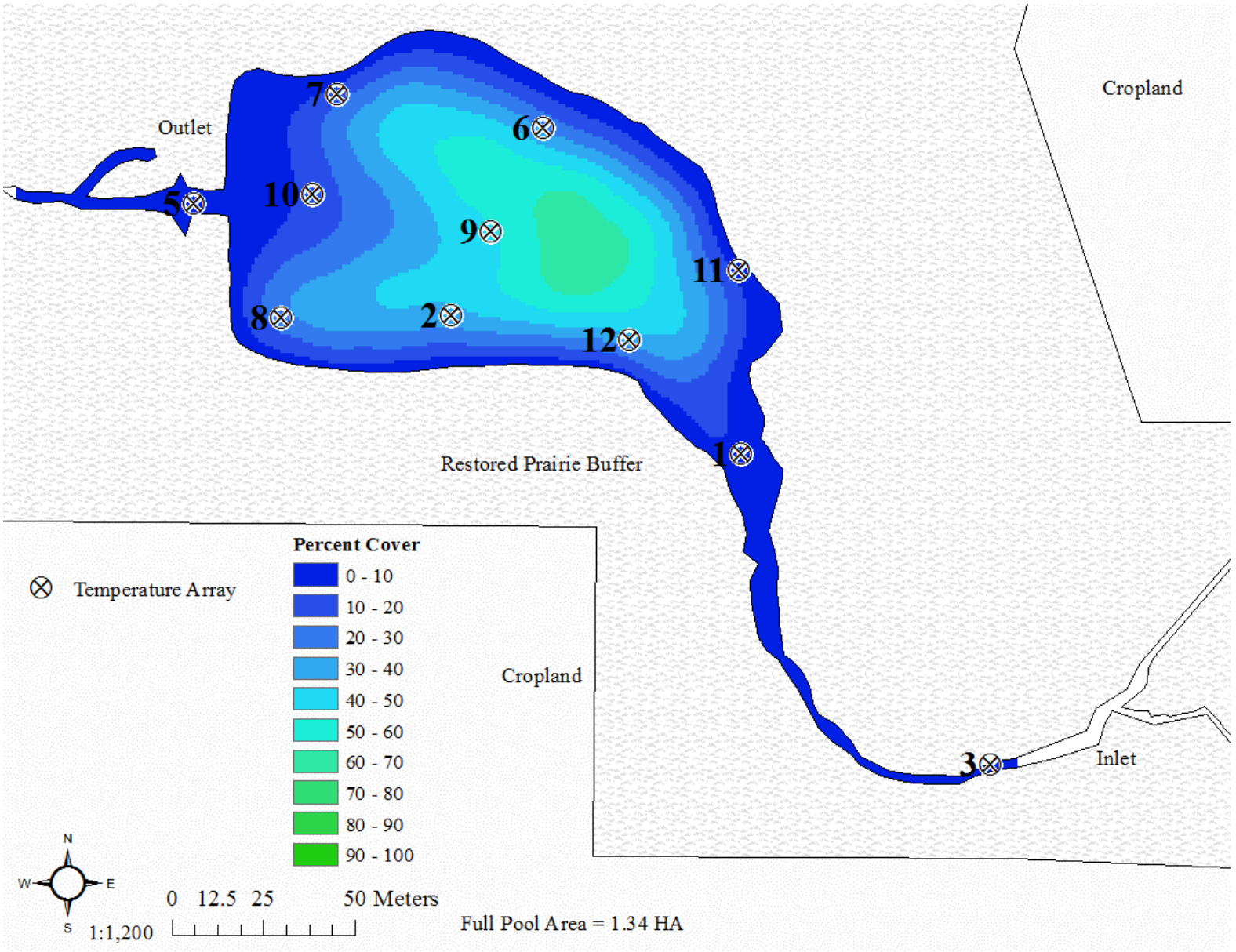

Figure 1B: Interpolated percent cover of submersed macrophytes based on survey conducted at KS on May 19, 2016.

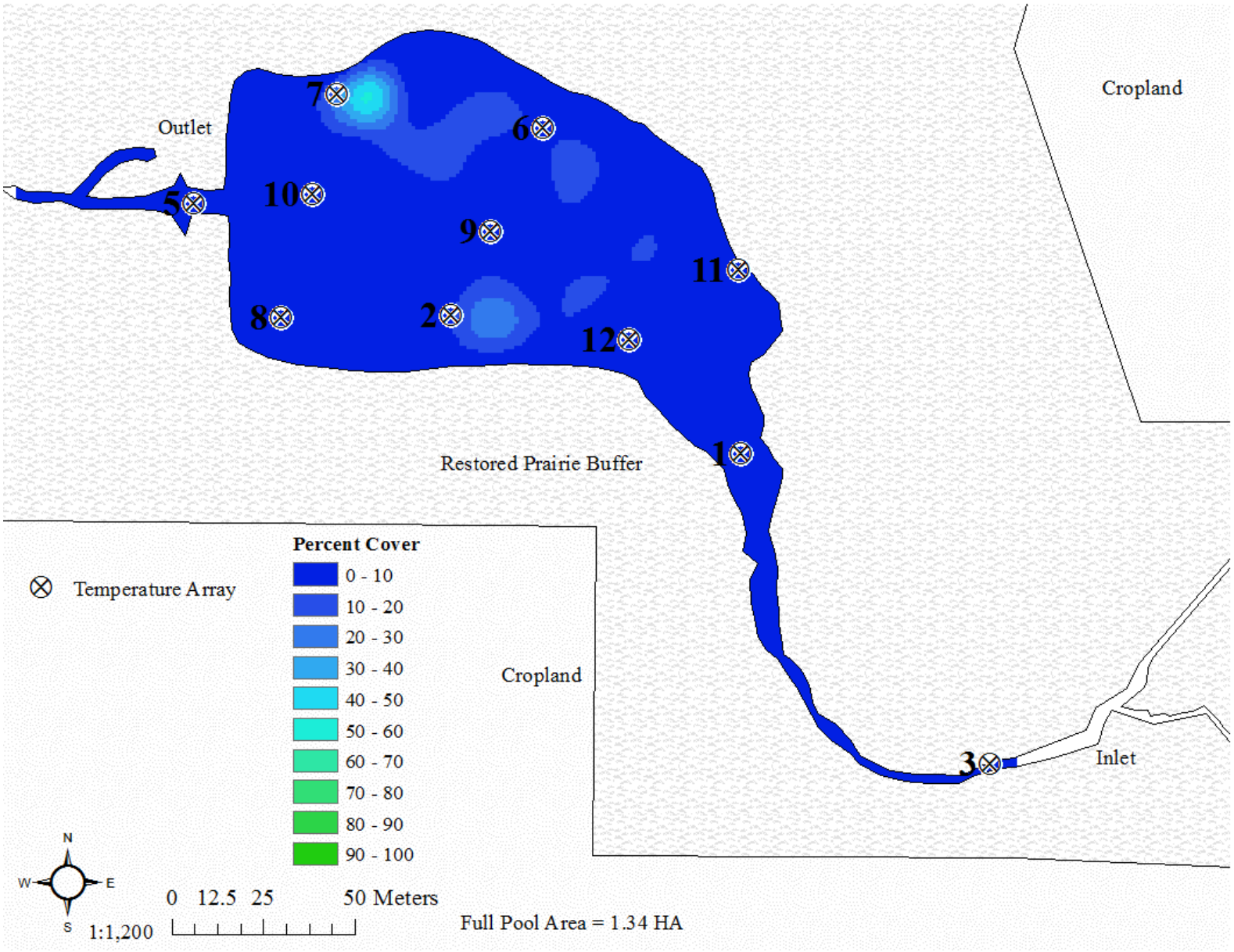

Figure 2B: Interpolated percent cover of submersed macrophytes based on survey conducted at KS on June 6, 2016.

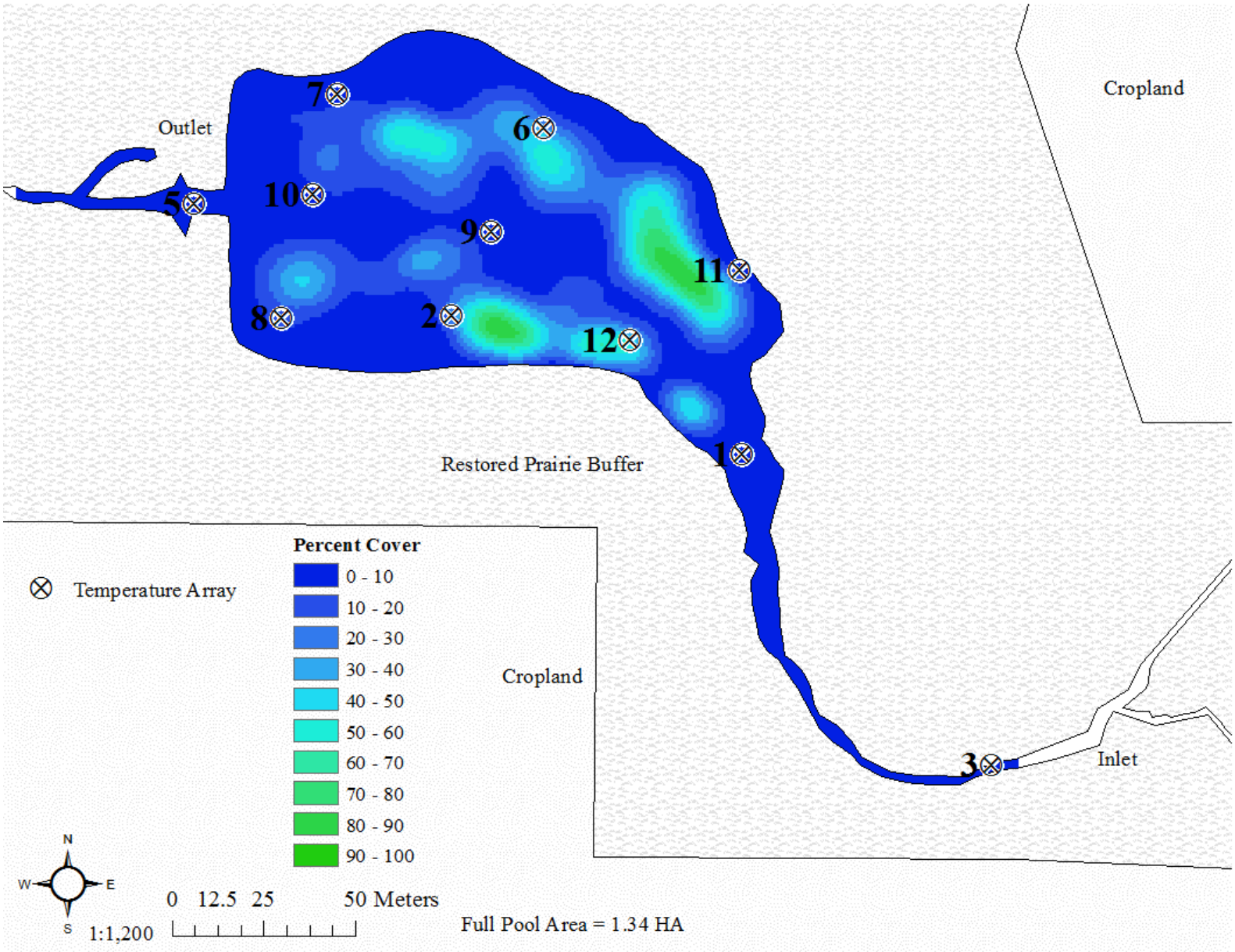

Figure 3B: Interpolated percent cover of submersed macrophytes based on survey conducted at KS on June 22, 2016.

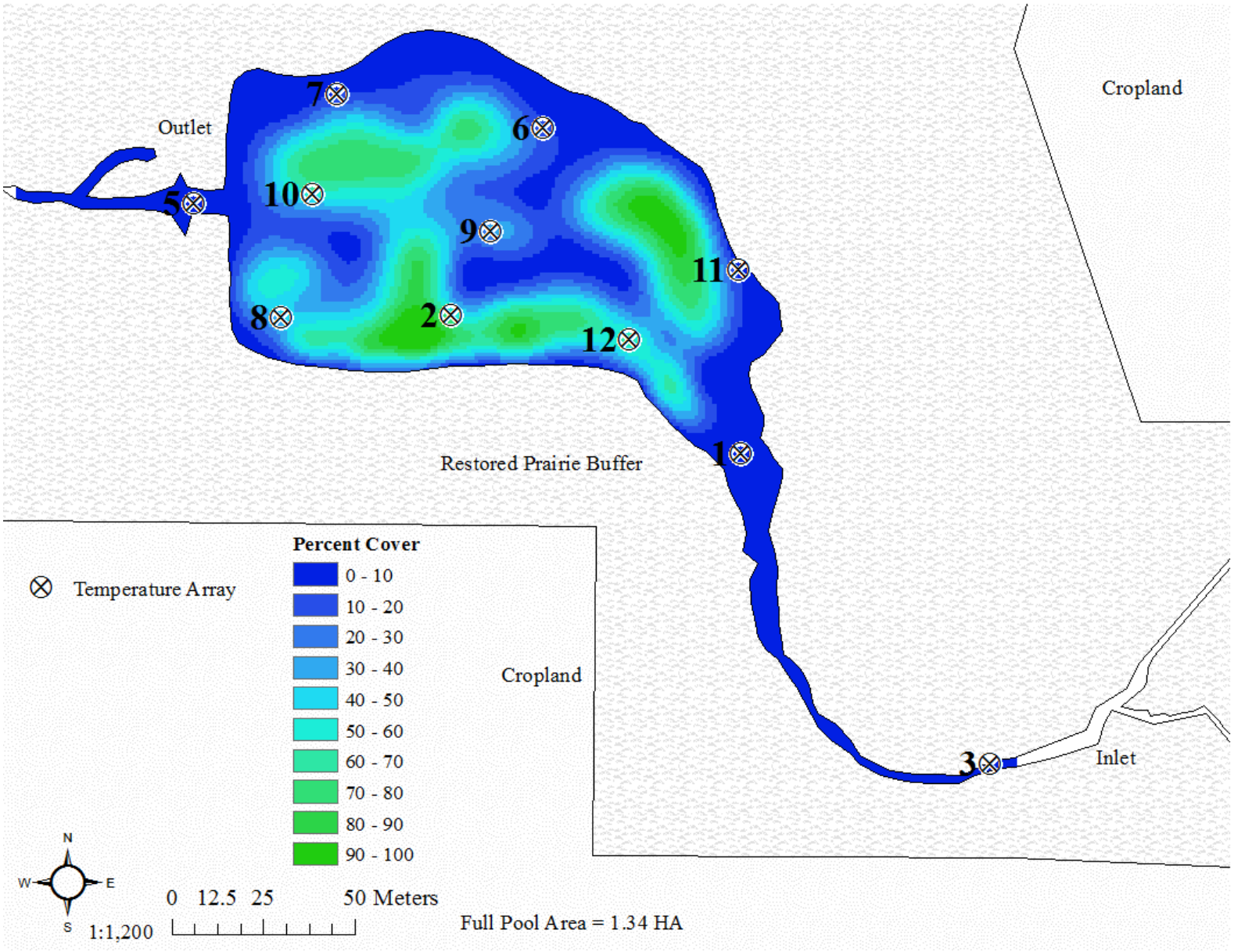

Figure 4B: Interpolated percent cover of submersed macrophytes based on survey conducted at KS on July 5, 2016.

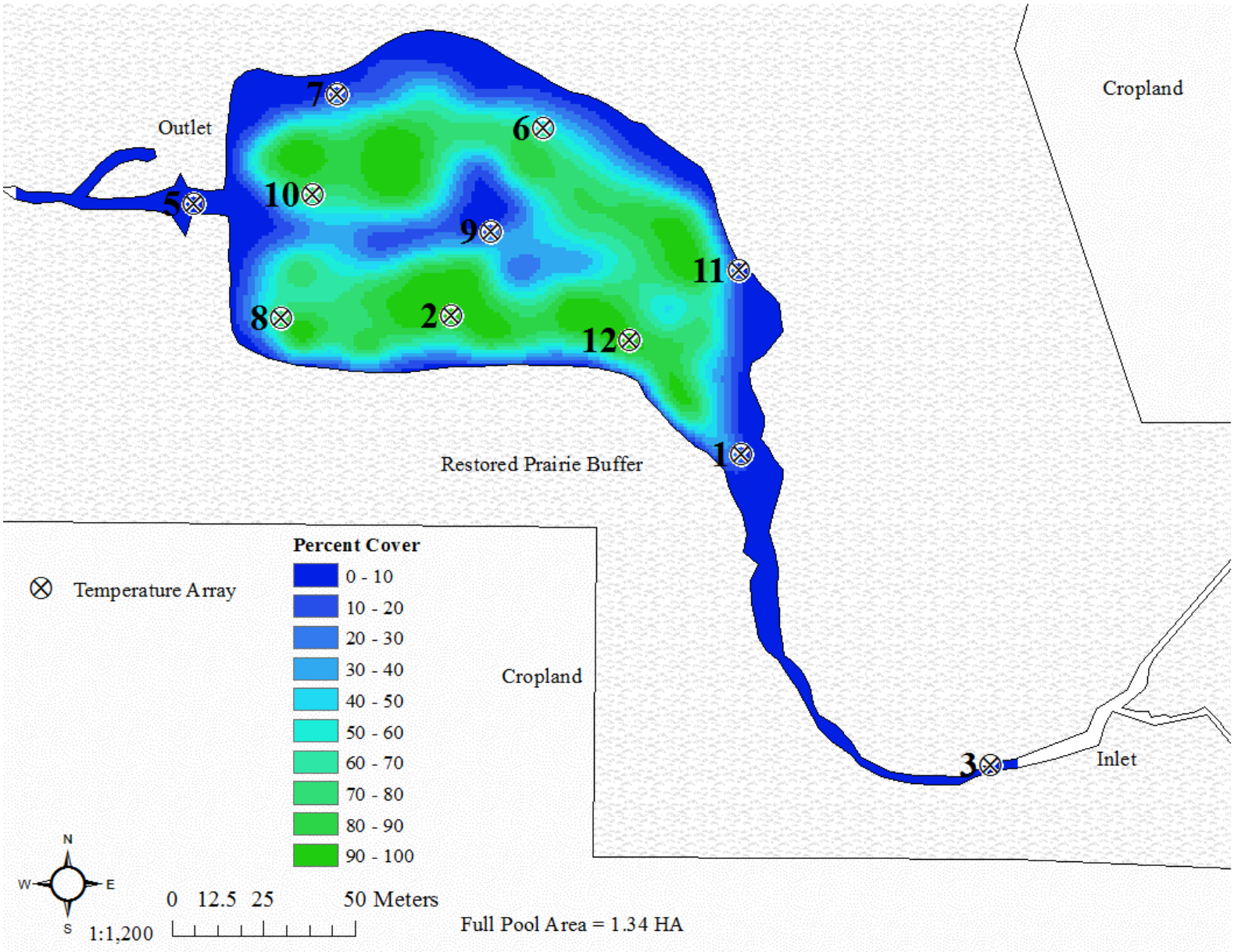

Figure 5B: Interpolated percent cover of submersed macrophytes based on survey conducted at KS on August 5, 2016.

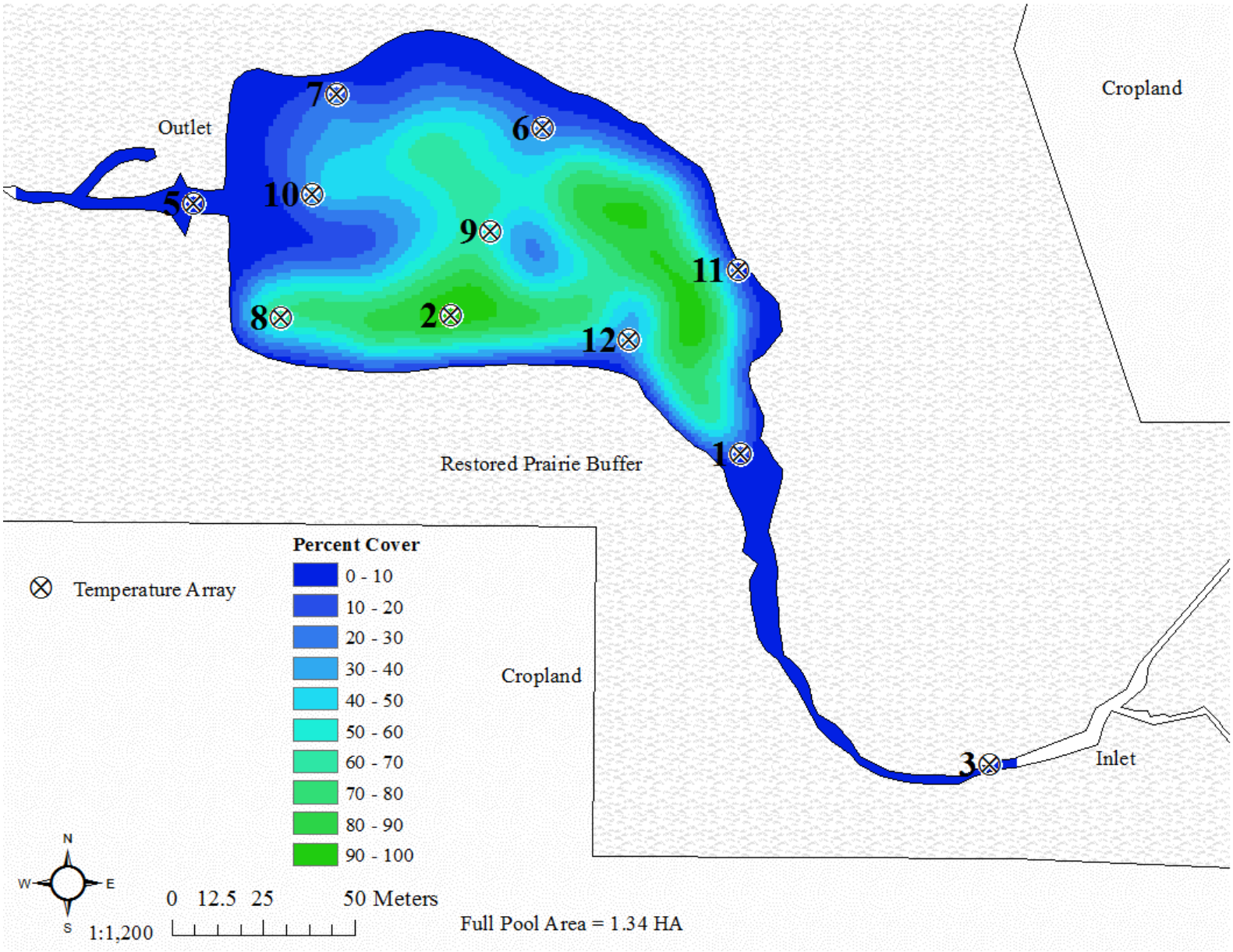

Figure 6B: Interpolated percent cover of submersed macrophytes based on survey conducted at KS on August 16, 2016.

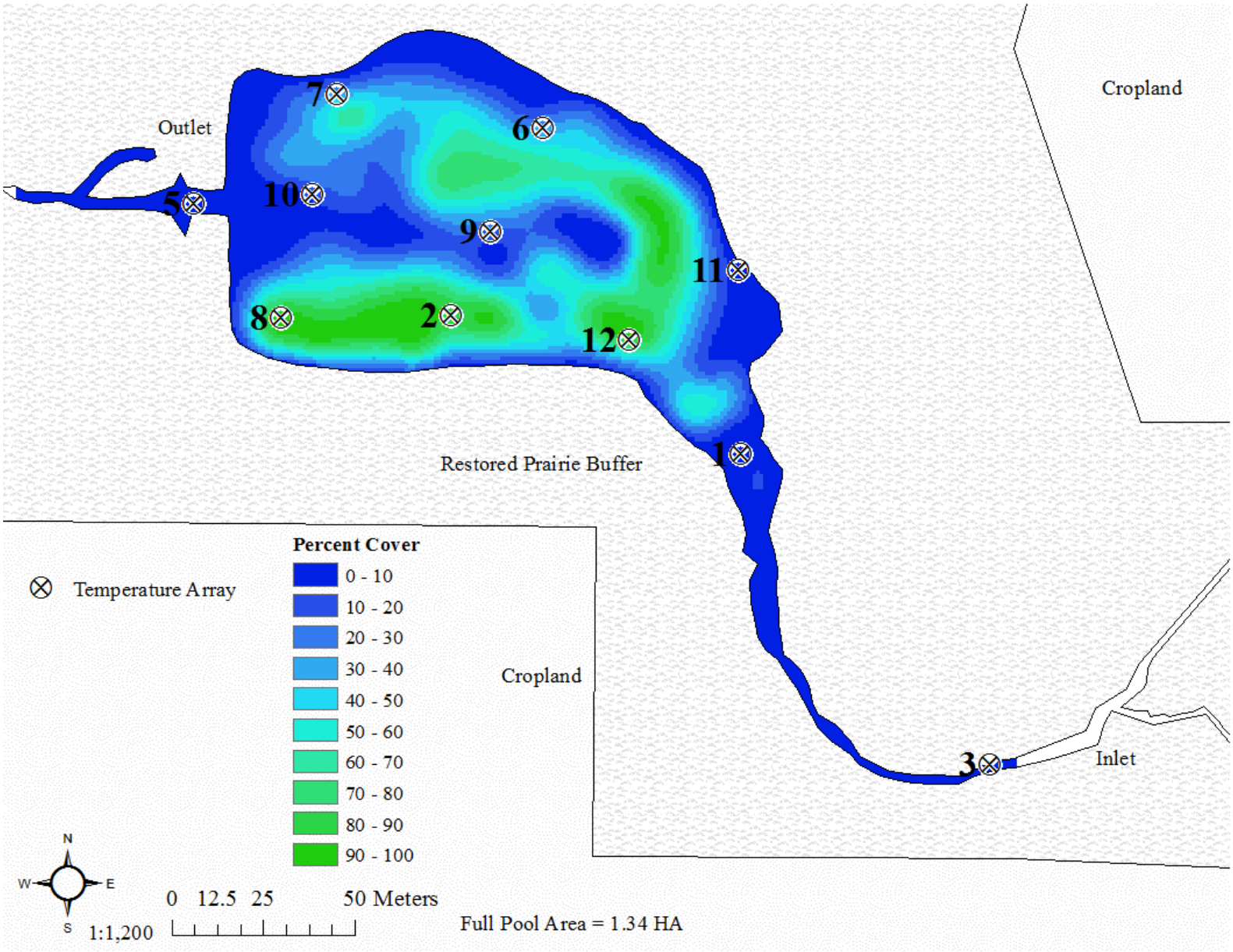

Figure 7B: Interpolated percent cover of submersed macrophytes based on survey conducted at KS on September 1, 2016.

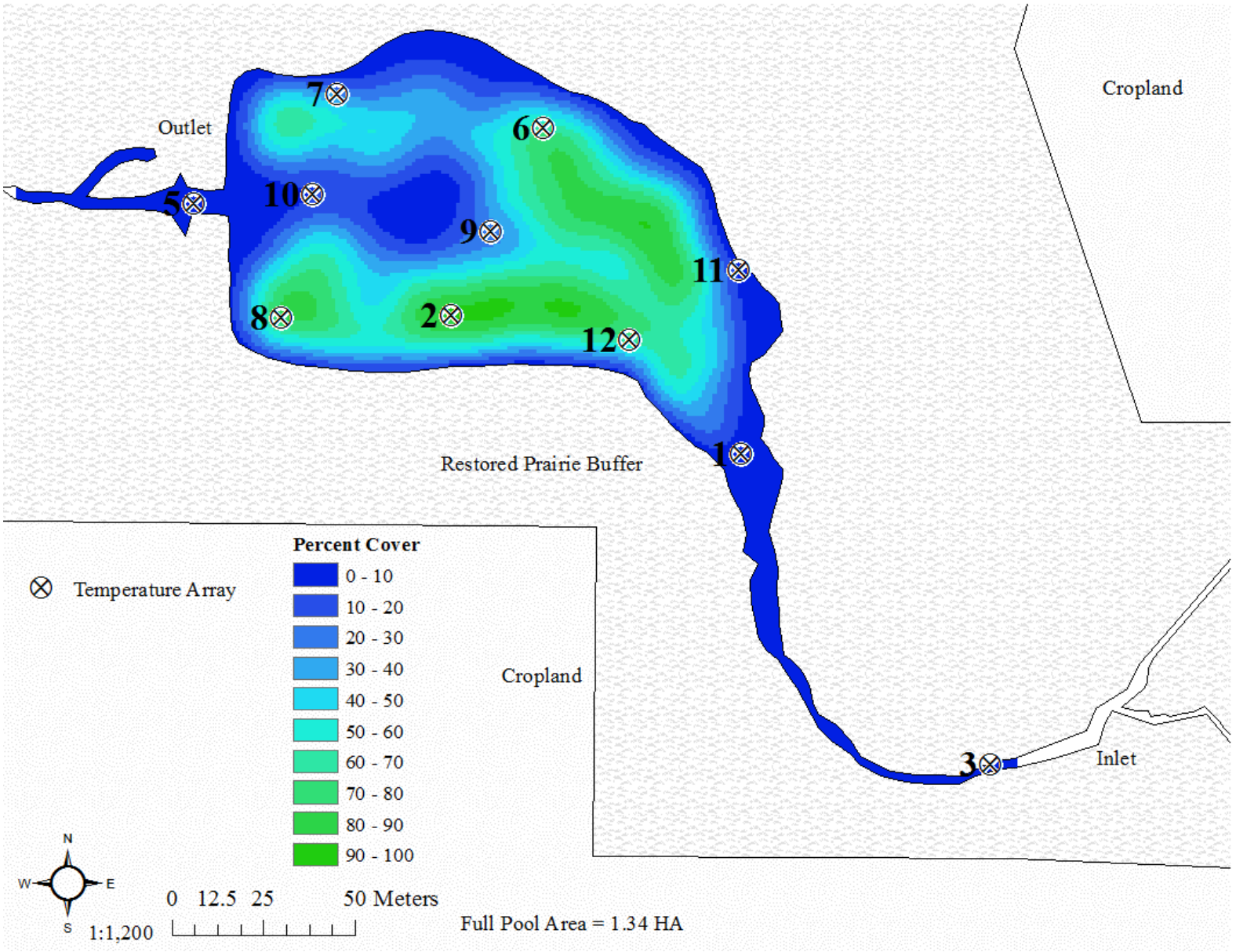

Figure 8B: Interpolated percent cover of submersed macrophytes based on survey conducted at KS on September 15, 2016.

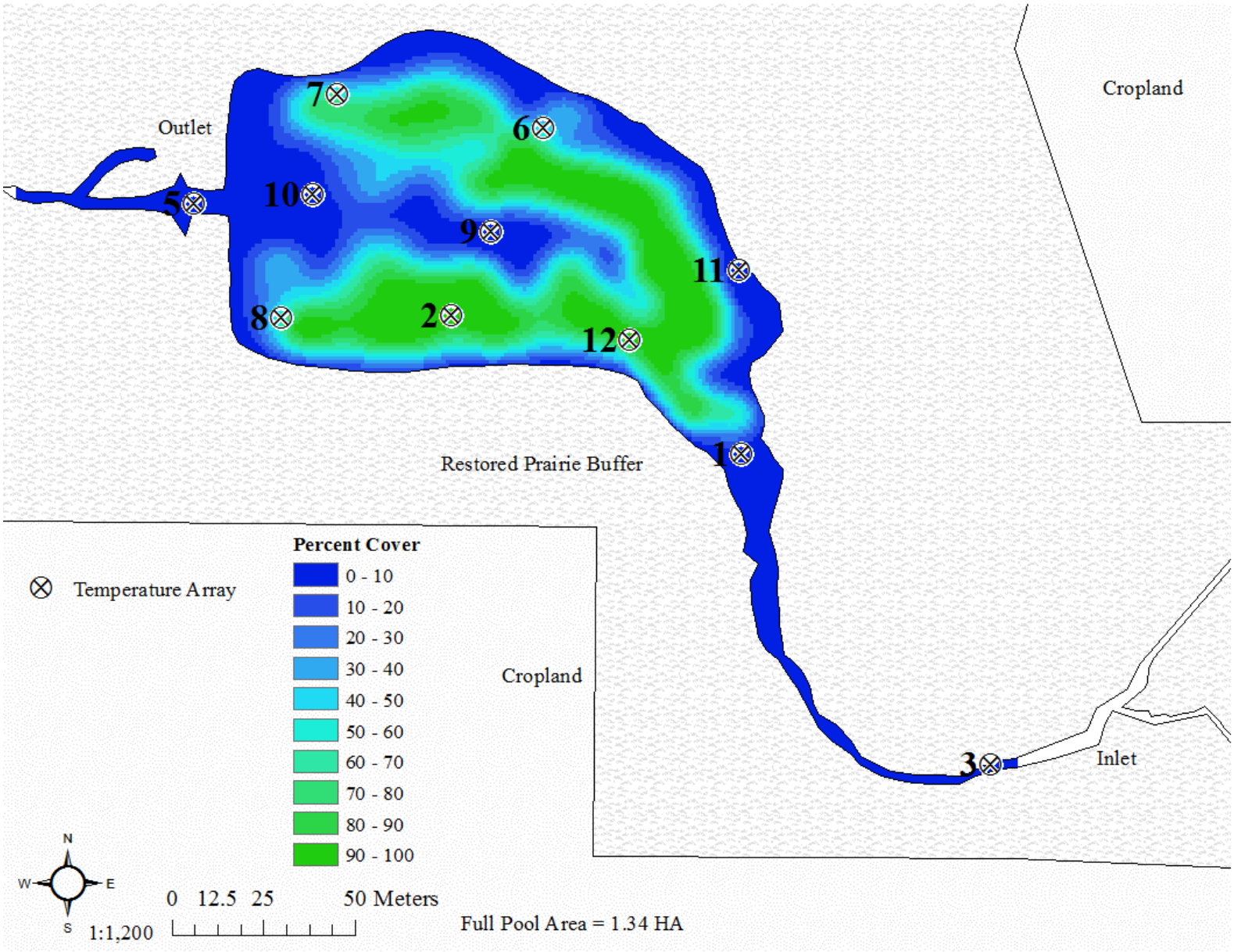

Figure 9B: Interpolated percent cover of submersed macrophytes based on survey conducted at KS on October 6, 2016.

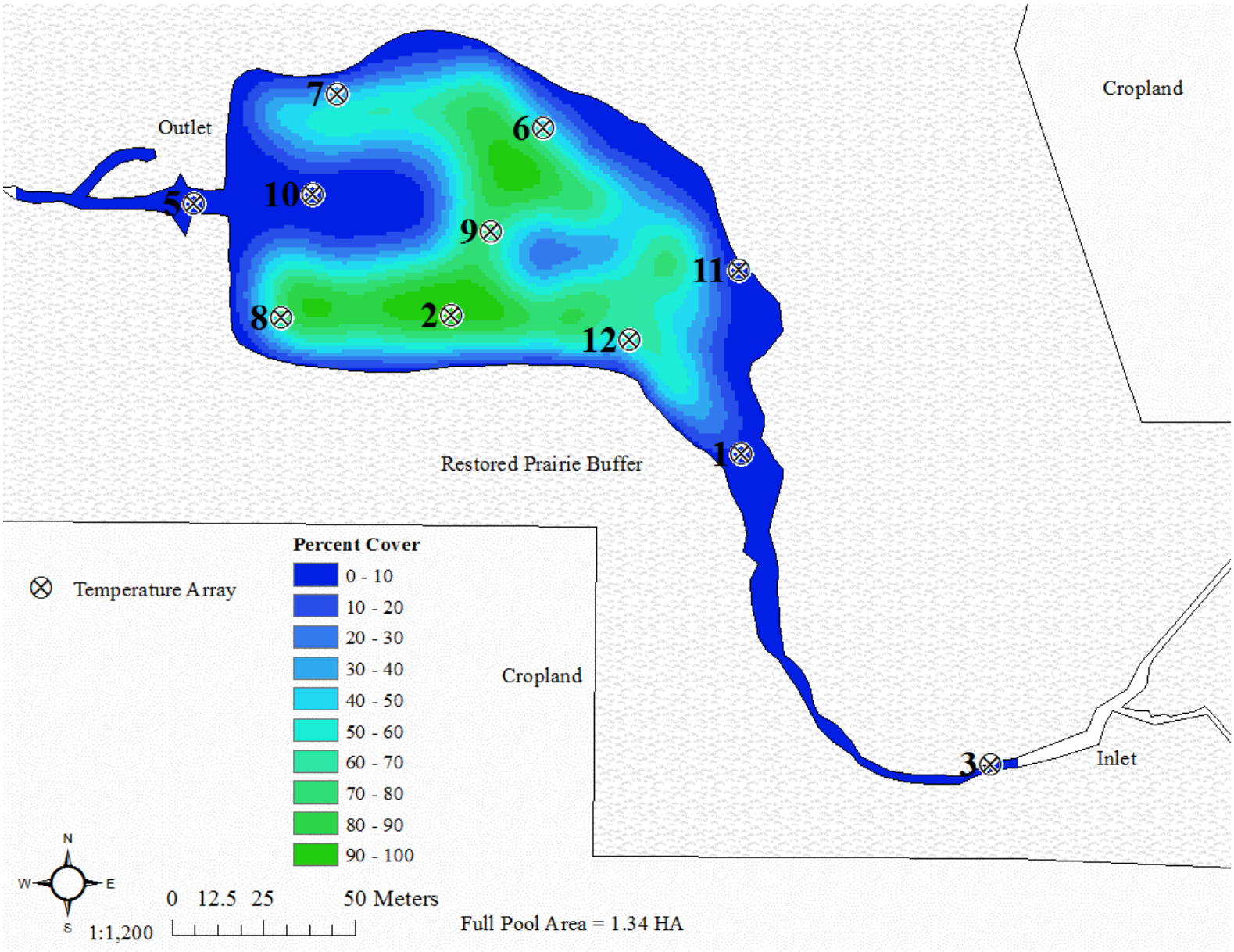

Figure 10B: Interpolated percent cover of submersed macrophytes based on survey conducted at KS on October 20, 2016.

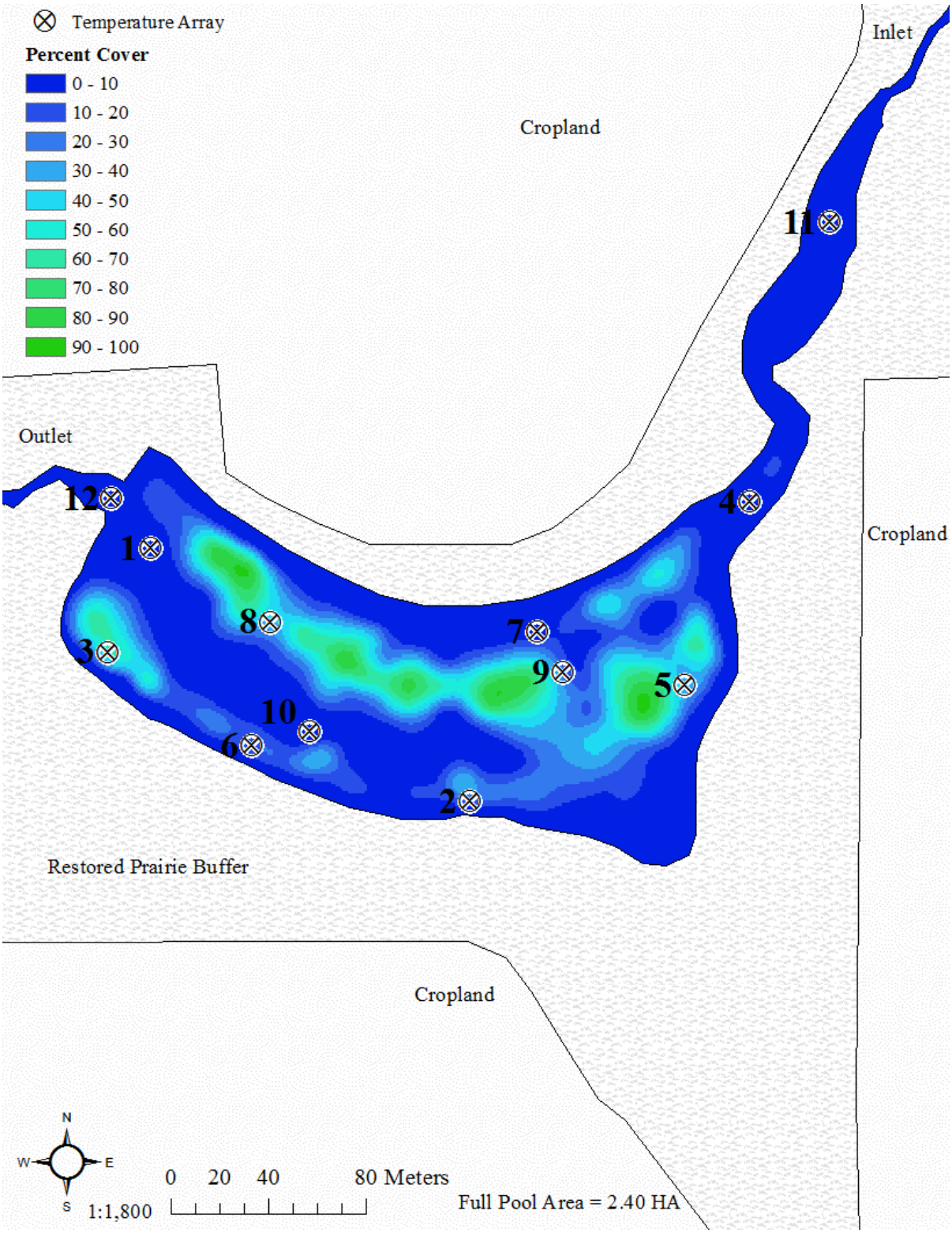

Figure 11B: Interpolated percent cover of submersed macrophytes based on survey conducted at RS on May 17, 2016.

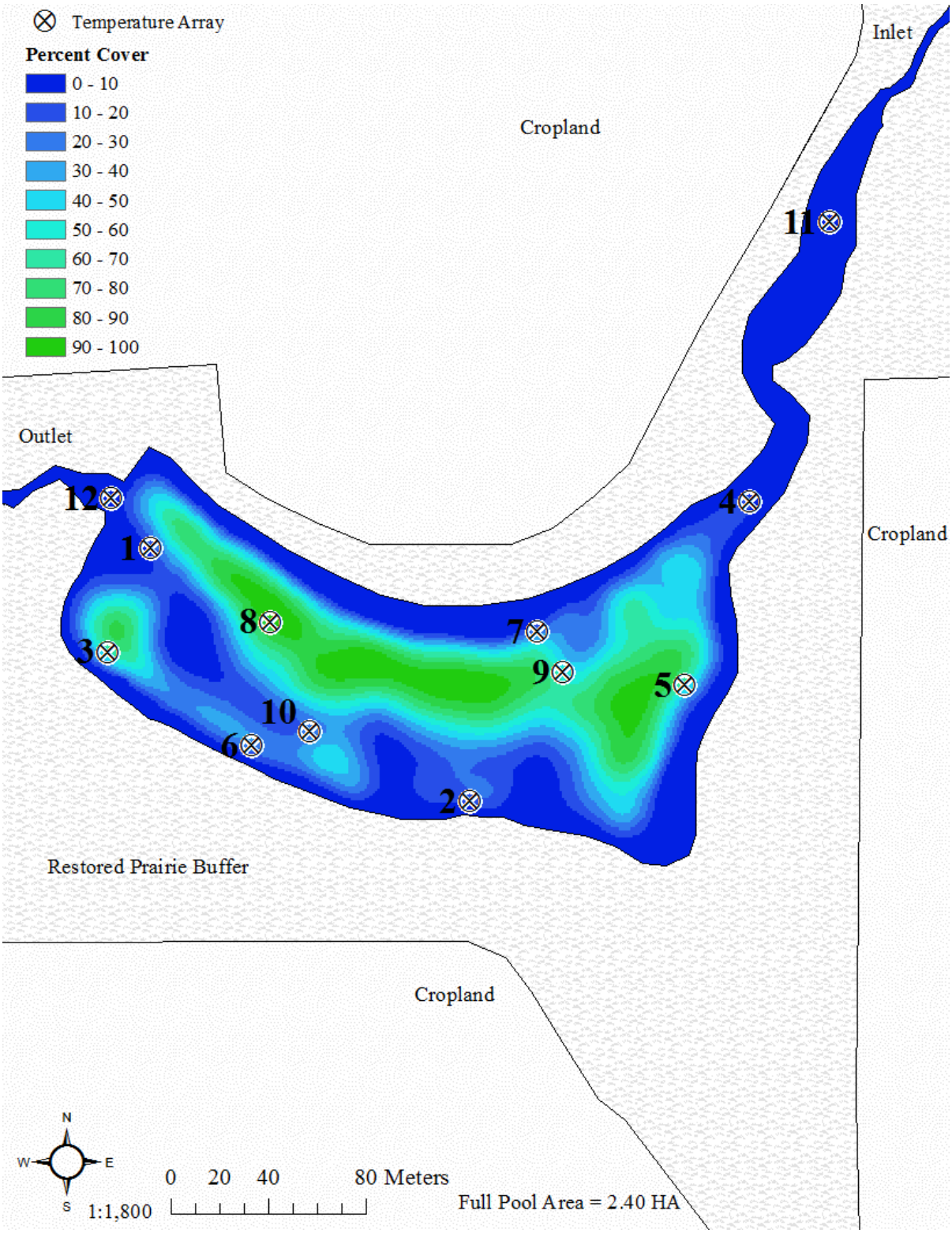

Figure 12B: Interpolated percent cover of submersed macrophytes based on survey conducted at RS on June 7, 2016.

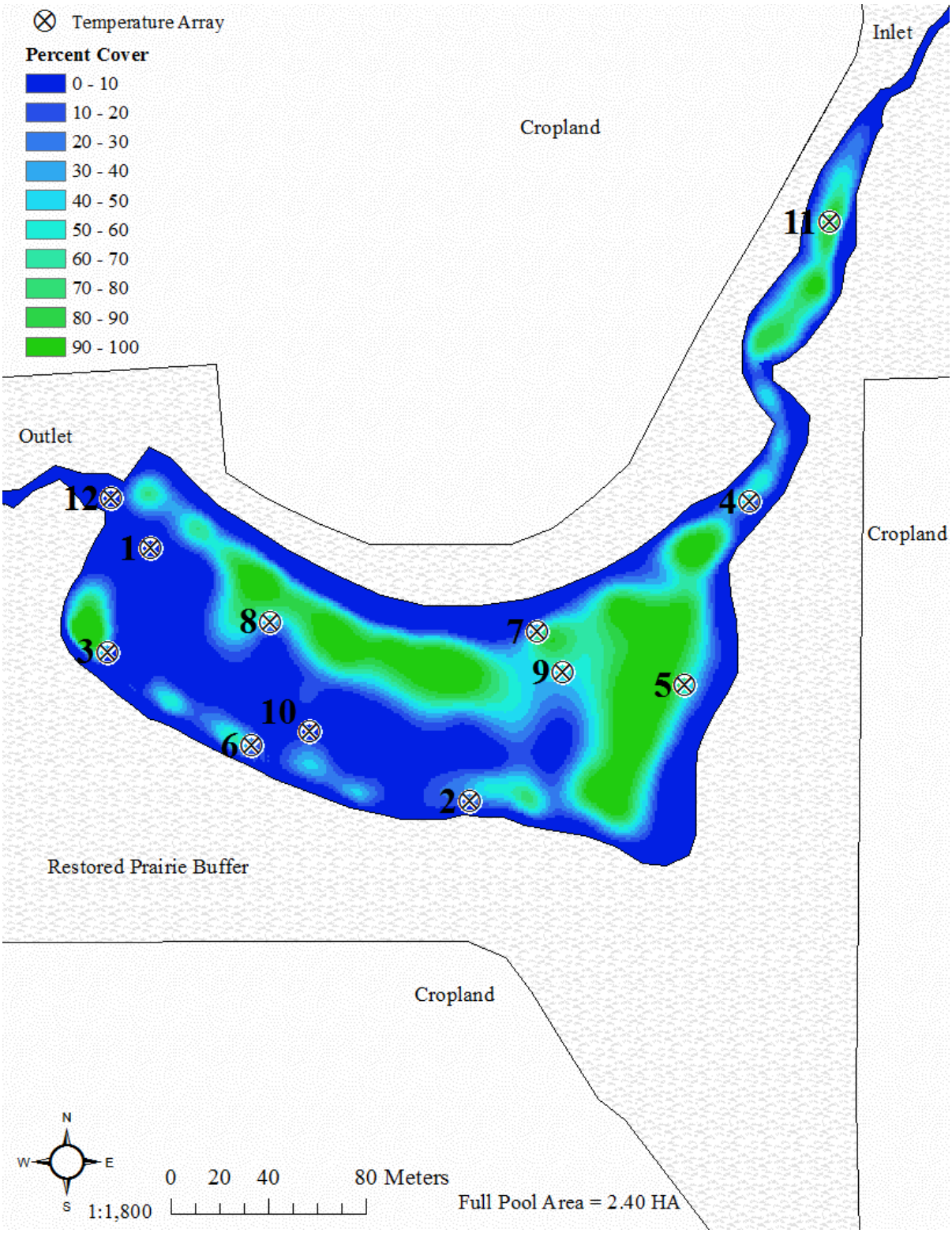

Figure 13B: Interpolated percent cover of submersed macrophytes based on survey conducted at RS on June 23, 2016.

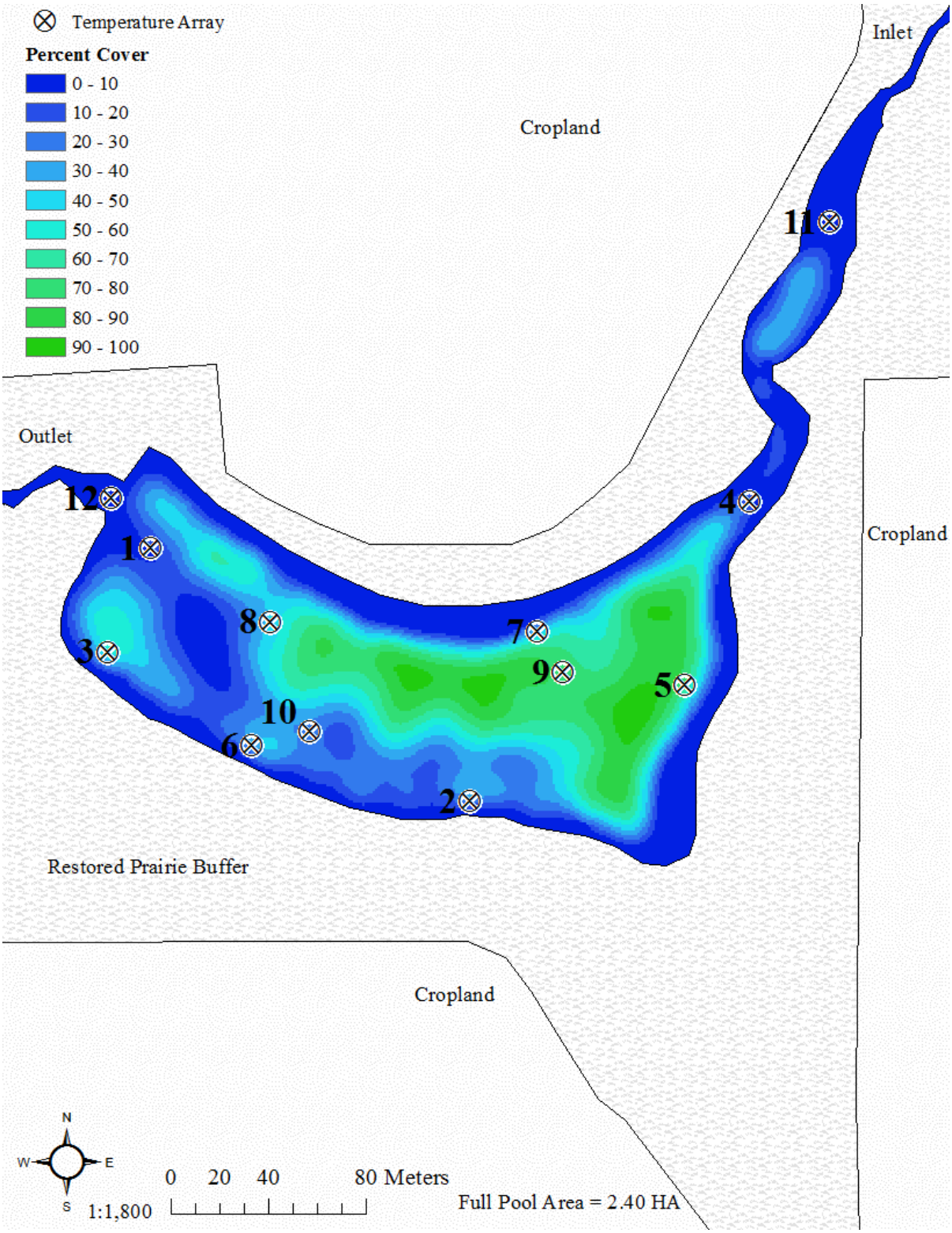

Figure 14B: Interpolated percent cover of submersed macrophytes based on survey conducted at RS on July 15, 2016.

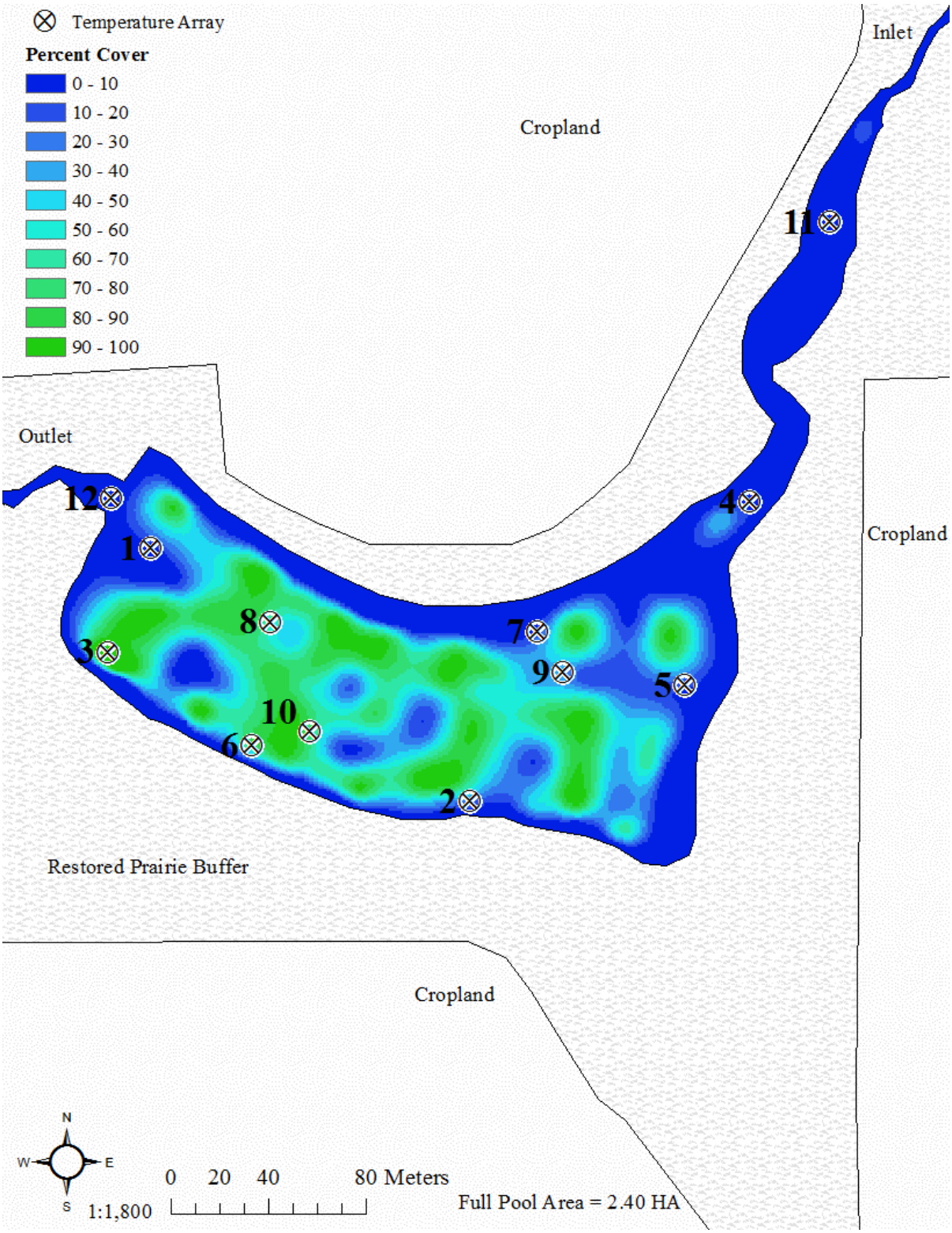

Figure 15B: Interpolated percent cover of submersed macrophytes based on survey conducted at RS on August 5, 2016.

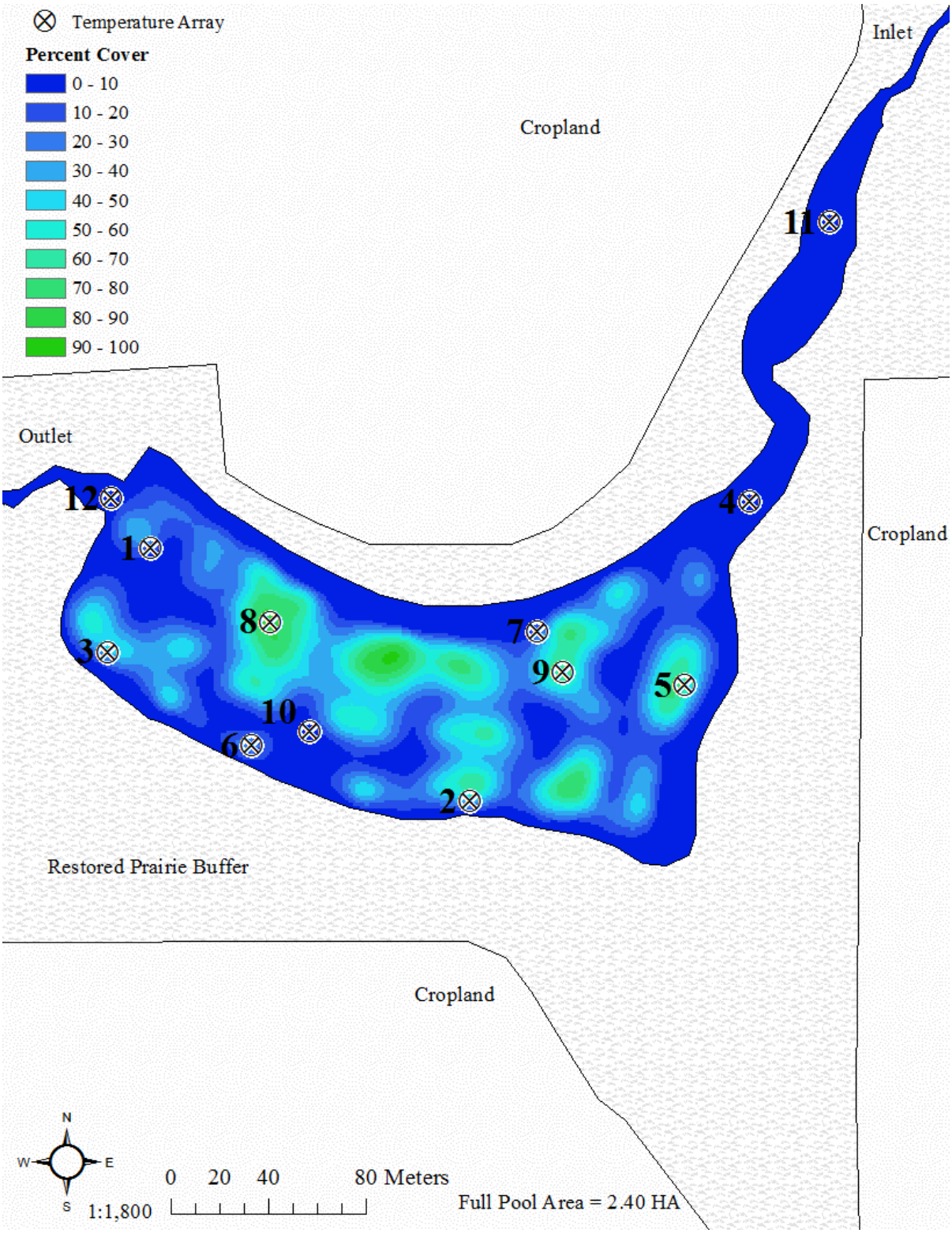

Figure 16B: Interpolated percent cover of submersed macrophytes based on survey conducted at RS on August 18, 2016.

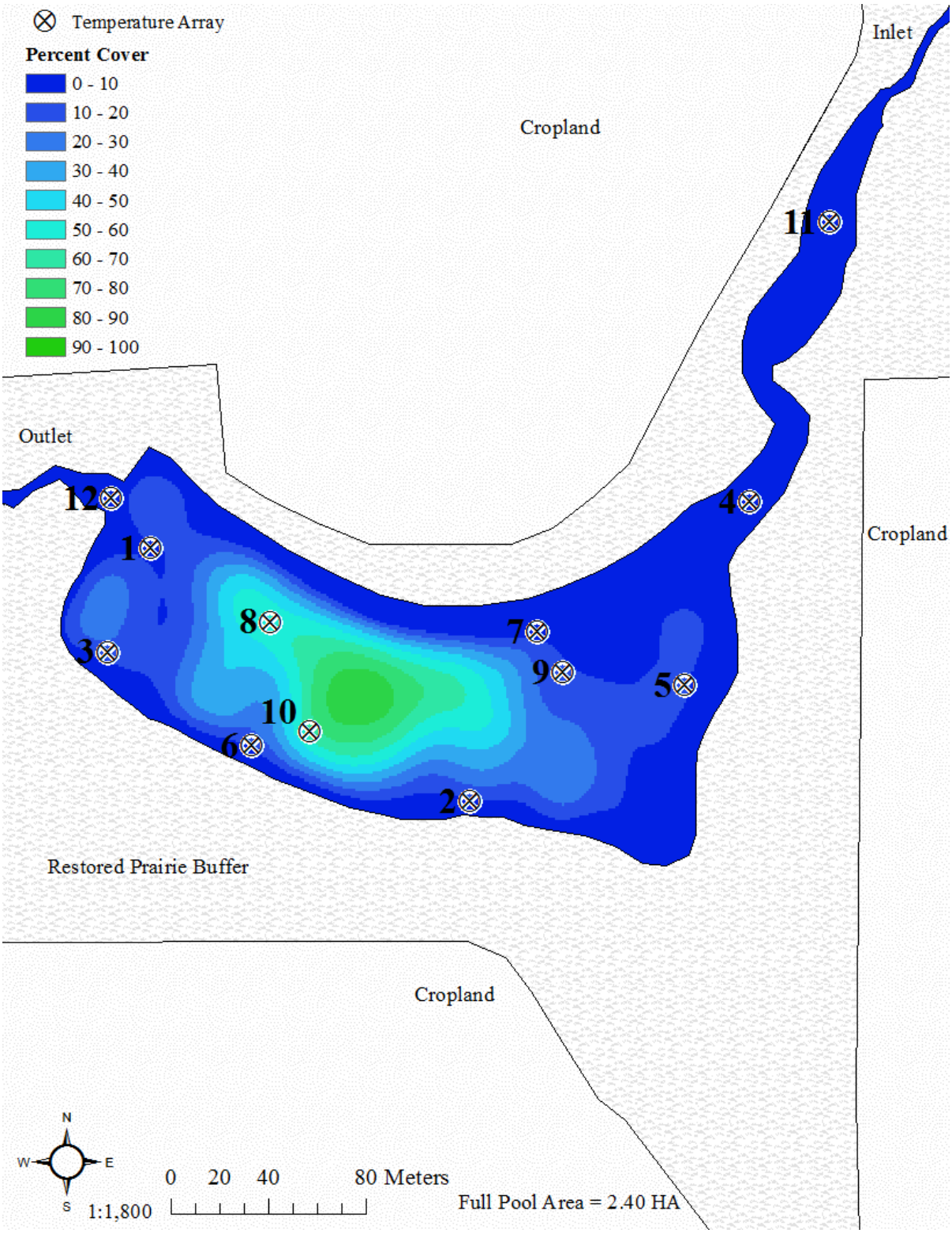

Figure 17B: Interpolated percent cover of submersed macrophytes based on survey conducted at RS on August 26, 2016.

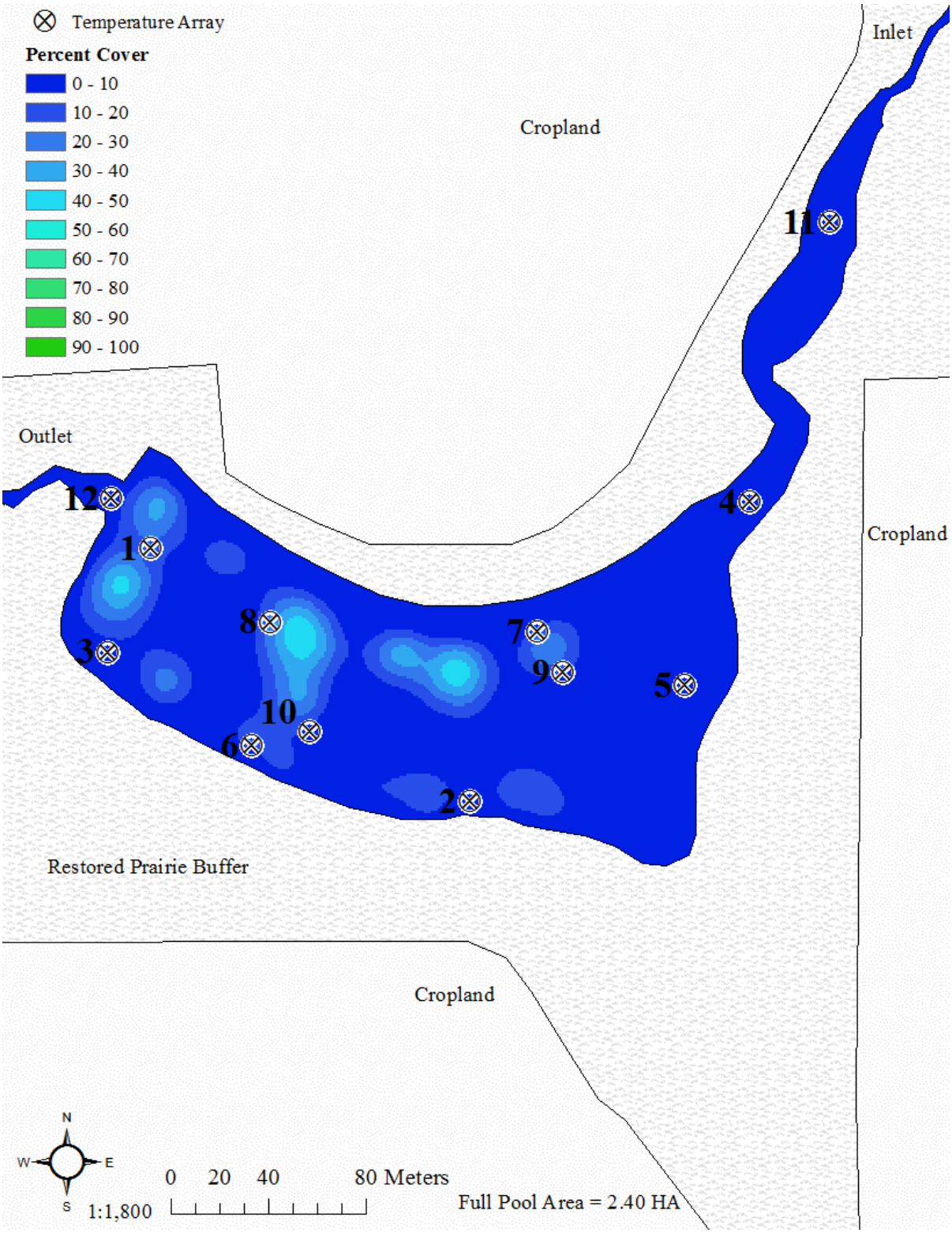

Figure 18B: Interpolated percent cover of submersed macrophytes based on survey conducted at RS on September 22, 2016.

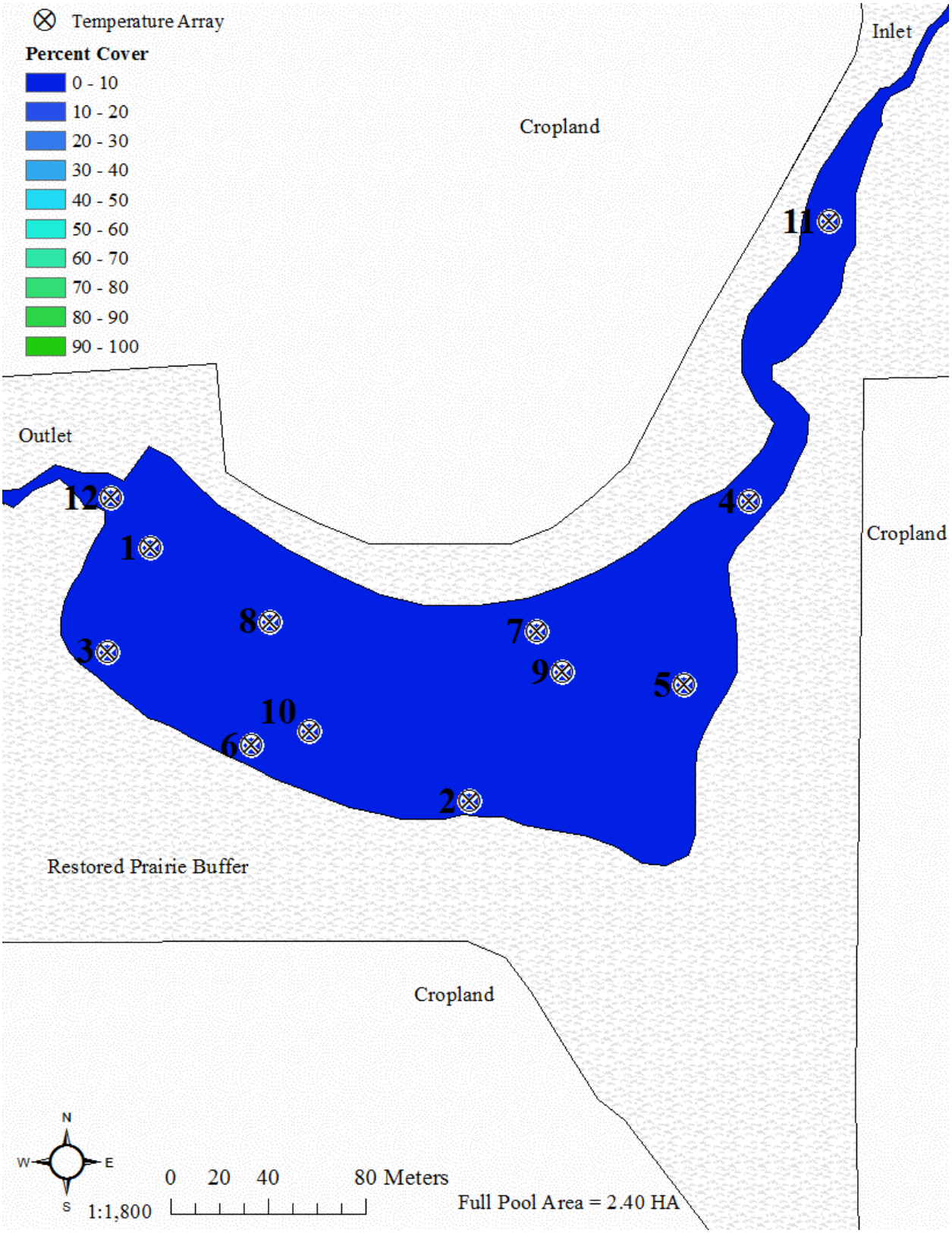

Figure 19B: Interpolated percent cover of submersed macrophytes based on survey conducted at RS on October 22, 2016.

APPENDIX C

PHOTOGRAPHS OF FIELD METHODS

This appendix contains photographs of field data collection methods of submersed macrophyte percent cover assessments and temperature sensor array installation are shown.

Figure 1C: Installation of galvanized steel pipe anchoring the temperature sensor array into the sediment with sediment sensor attached.

Figure 2C: Installation of PVC sleeve with attached sensors into the water column. The PVC sleeve was fitted over the anchored galvanized steel pipe.

Figure 3C: Fully installed temperature sensor array in the wetland. Topmost two sensors are visible through the water.

Figure 4C: 0.25 m^2 quadrat placed on the surface of the water with submersed macrophyte cover below. Percent cover was estimated using this method at 5% cover class intervals.

APPENDIX D

SEMIVARIOGRAMS OF VEGETATION SURVEYS

This appendix contains a semivariogram for each vegetation survey at KS and RS. These figures show how variance between points changes with distance. Each Kriging routine was based on the respective semivariogram.

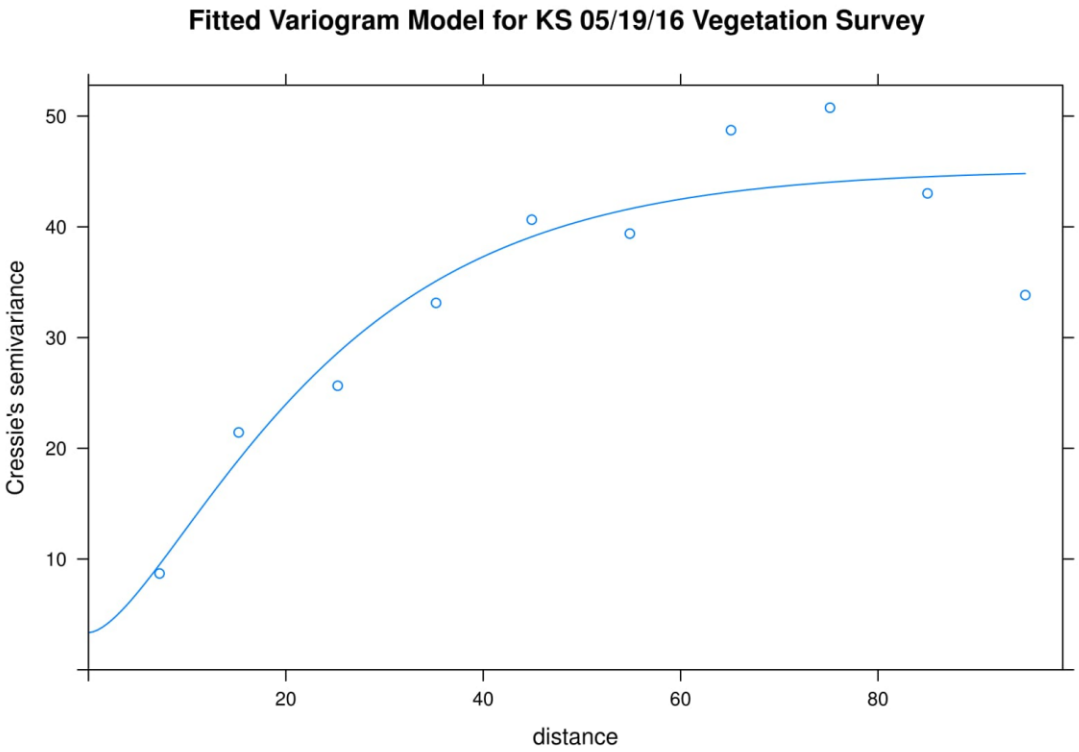

Figure 1D: Semivariogram model of the KS 05/19/16 vegetation survey.

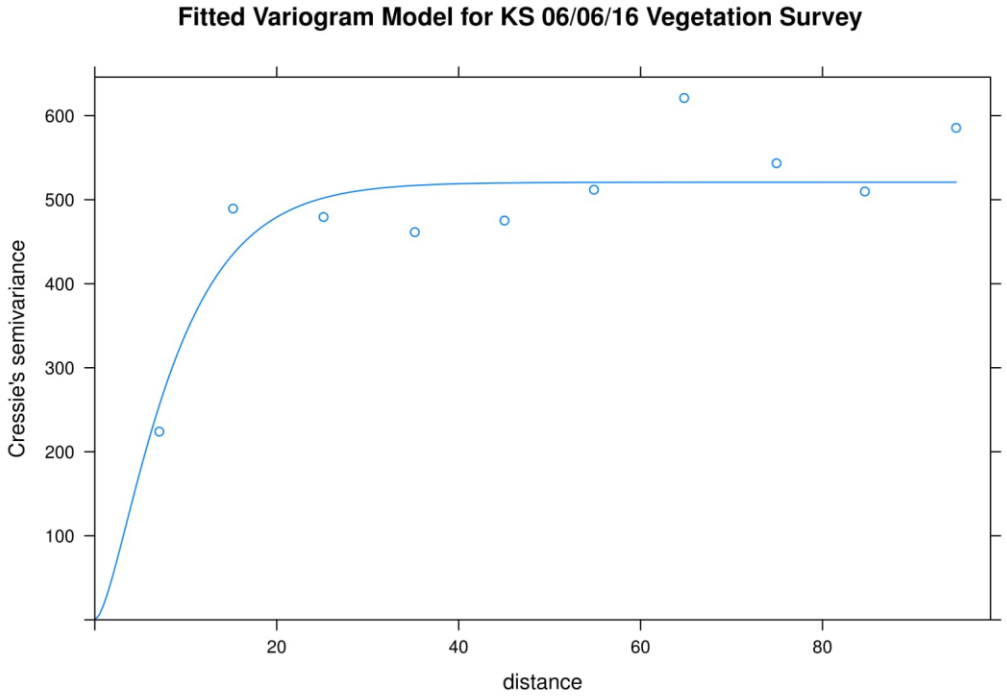

Figure 2D: Semivariogram model of the KS 06/06/16 vegetation survey.

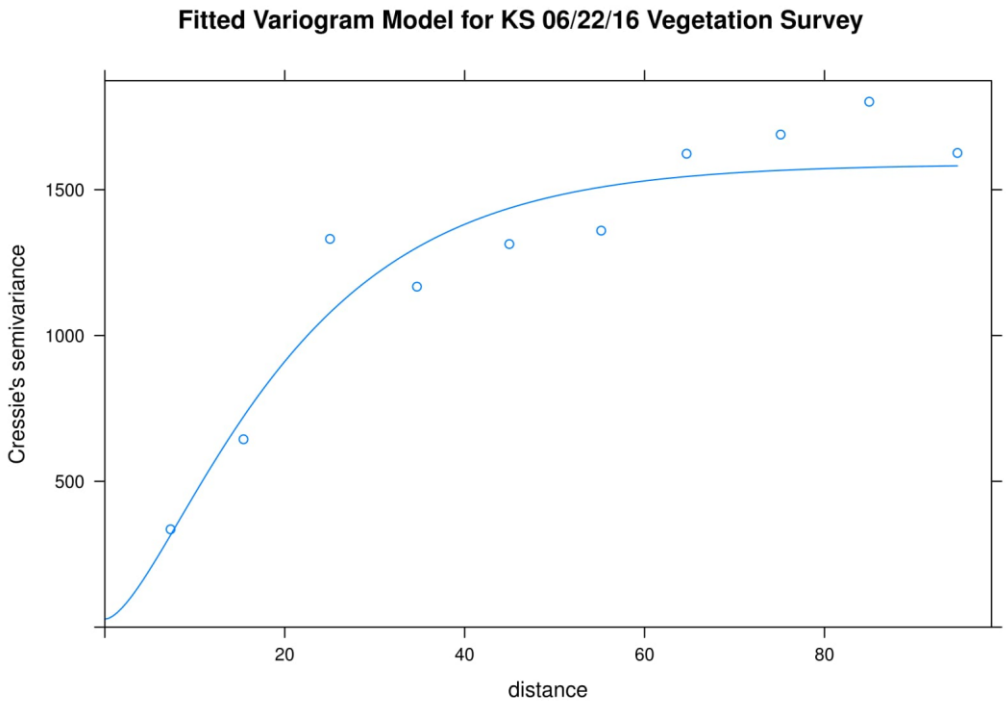

Figure 3D: Semivariogram model of the KS 06/22/16 vegetation survey.

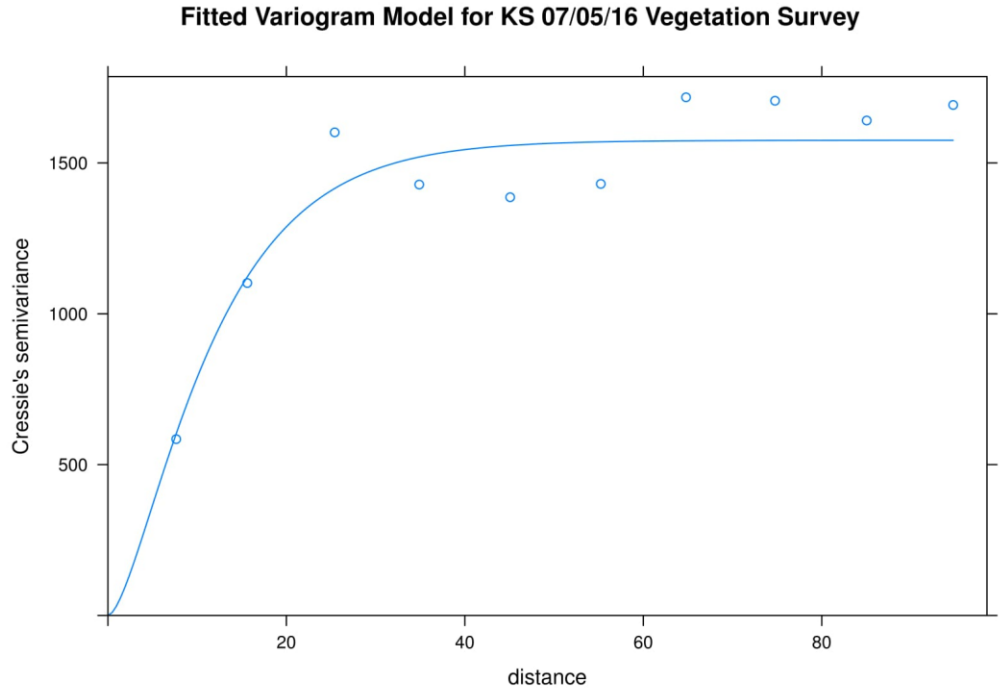

Figure 4D: Semivariogram model of the KS 07/20516 vegetation survey.

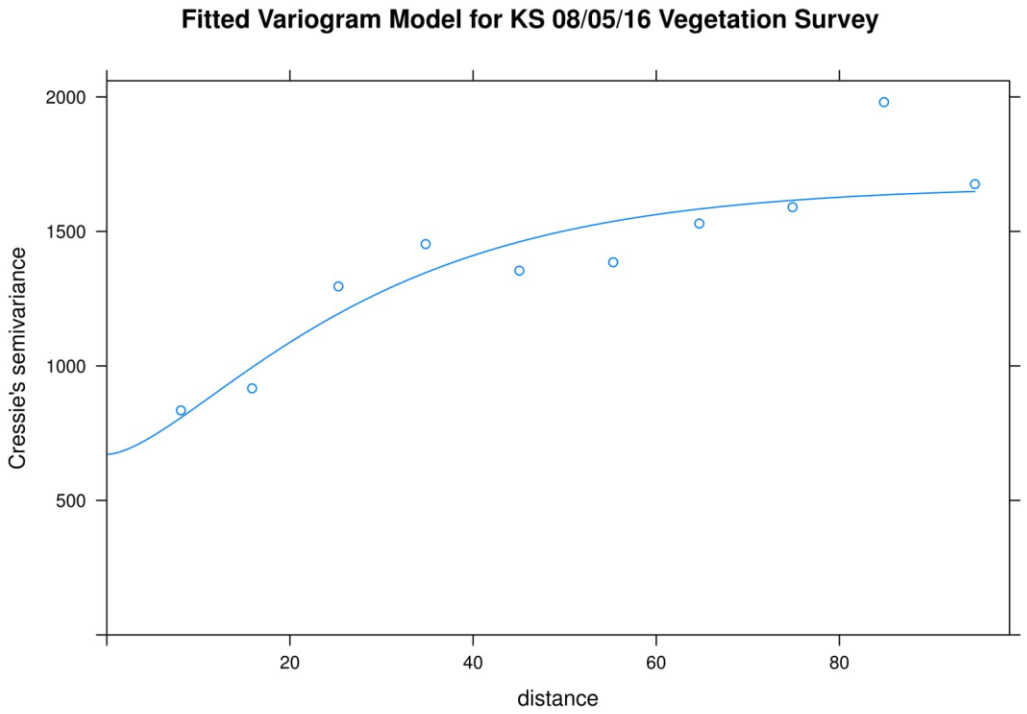

Figure 5D: Semivariogram model of the KS 08/05/16 vegetation survey.

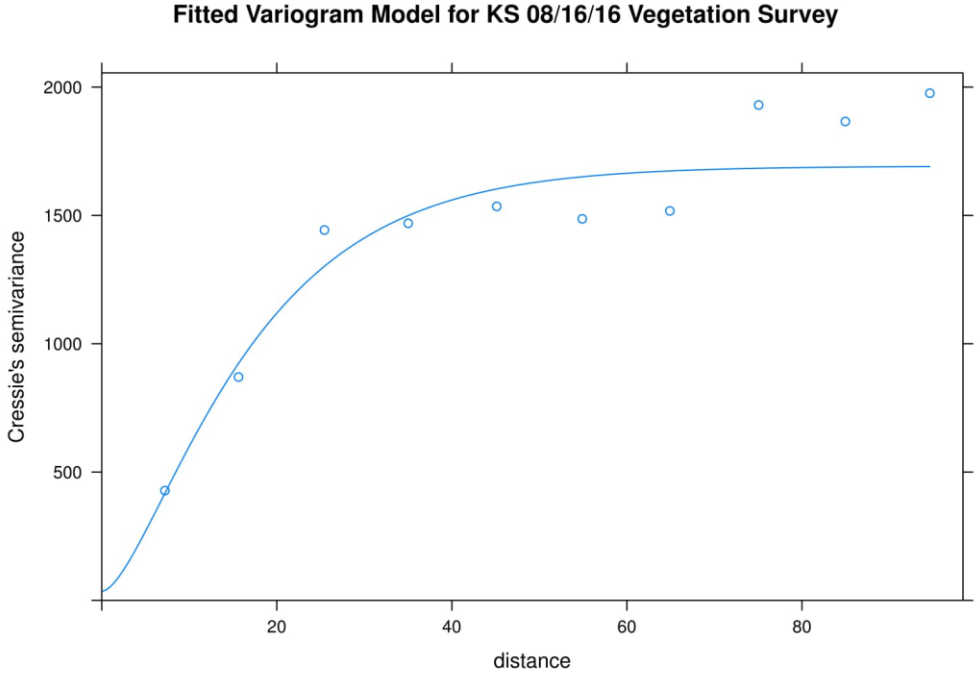

Figure 6D: Semivariogram model of the KS 08/16/16 vegetation survey.

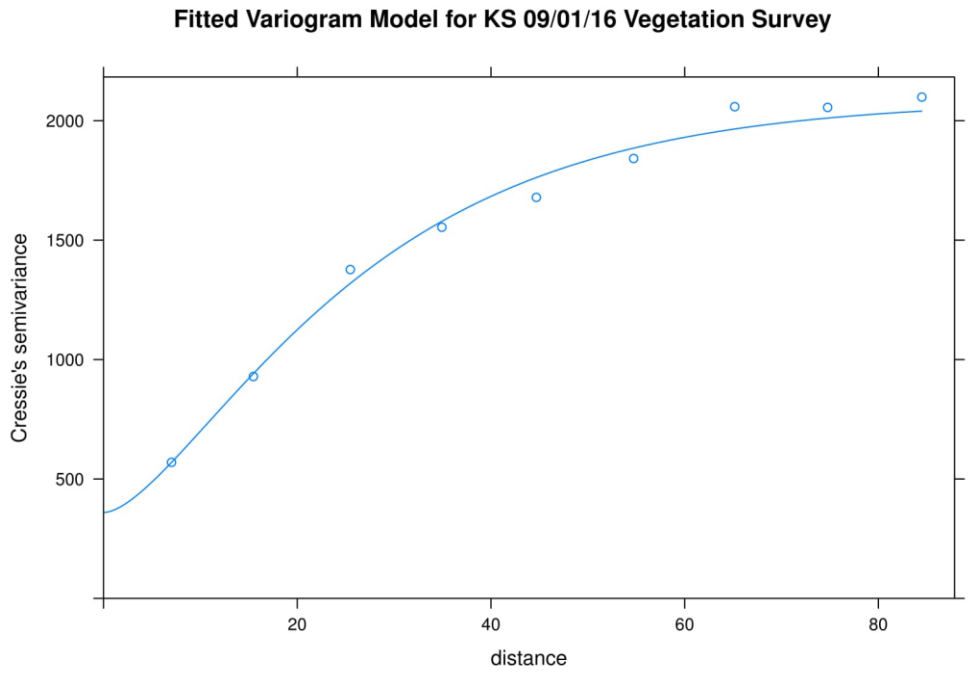

Figure 7D: Semivariogram model of the KS 09/01/16 vegetation survey.

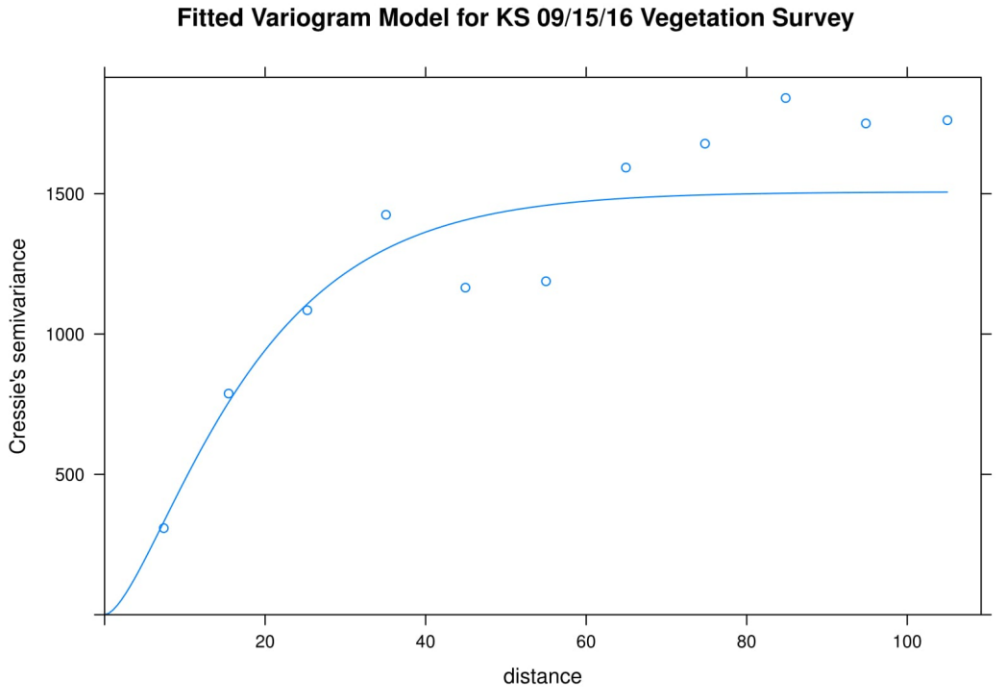

Figure 8D: Semivariogram model of the KS 09/15/16 vegetation survey.

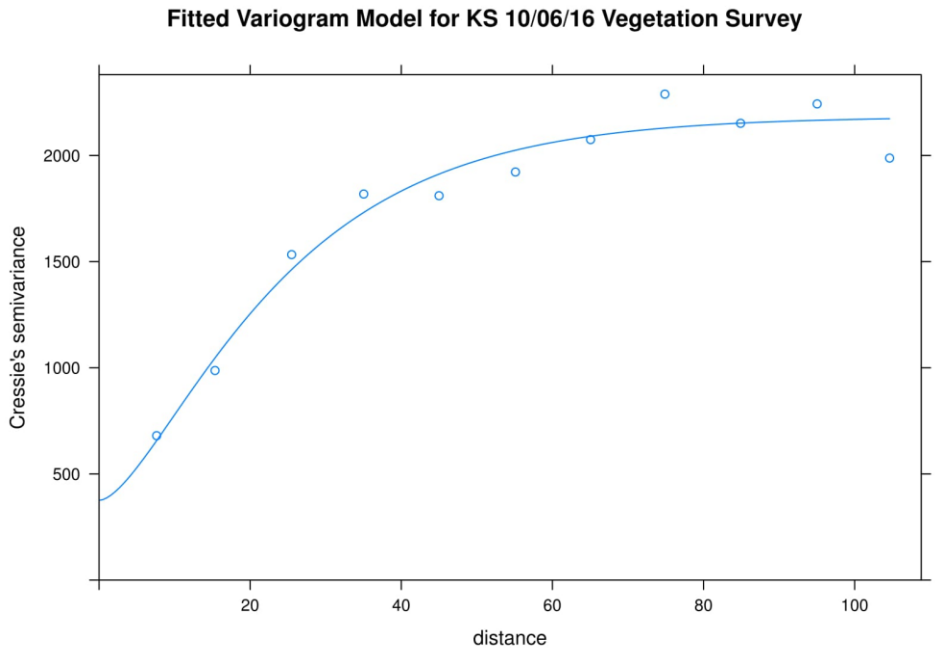

Figure 9D: Semivariogram model of the KS 10/06/16 vegetation survey.

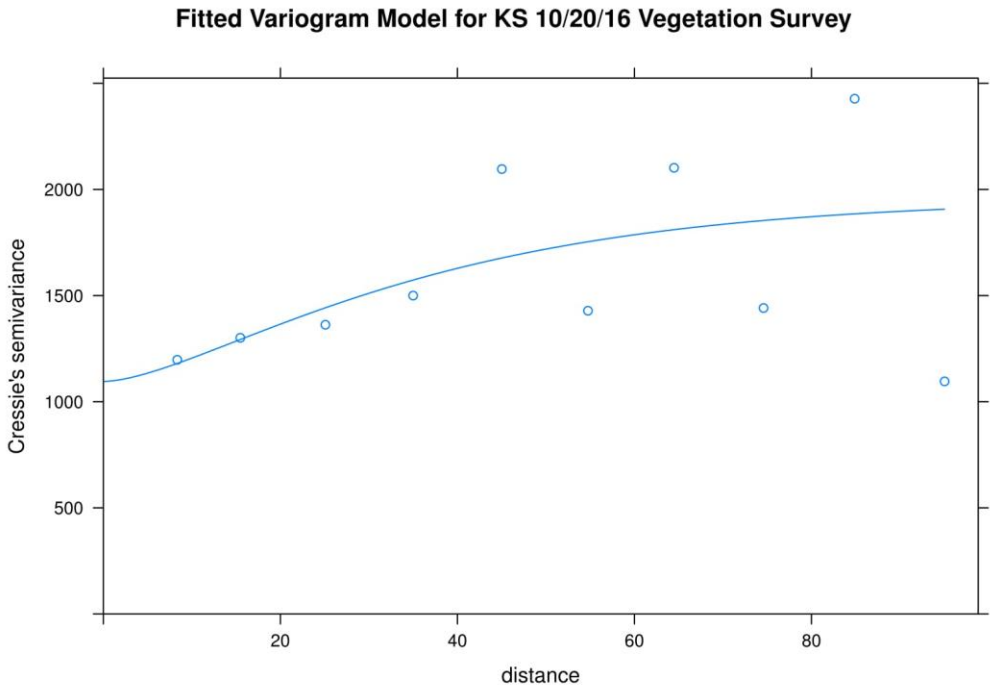

Figure 10D: Semivariogram model of the KS 10/20/16 vegetation survey.

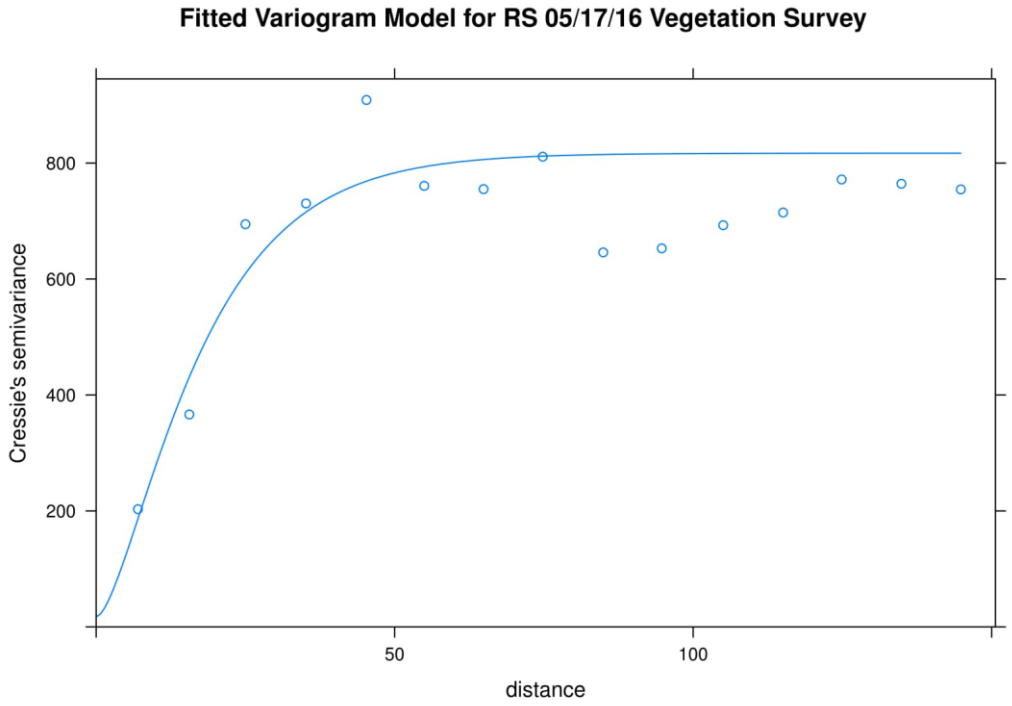

Figure 11D: Semivariogram model of the RS 05/17/16 vegetation survey.

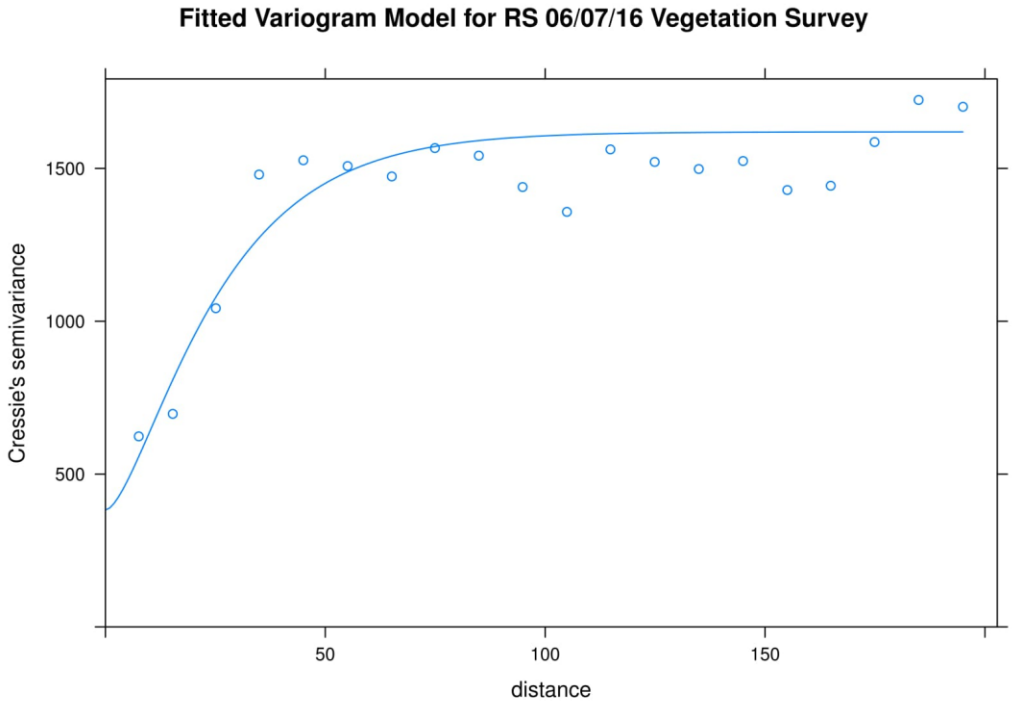

Figure 12D: Semivariogram model of the RS 06/07/16 vegetation survey.

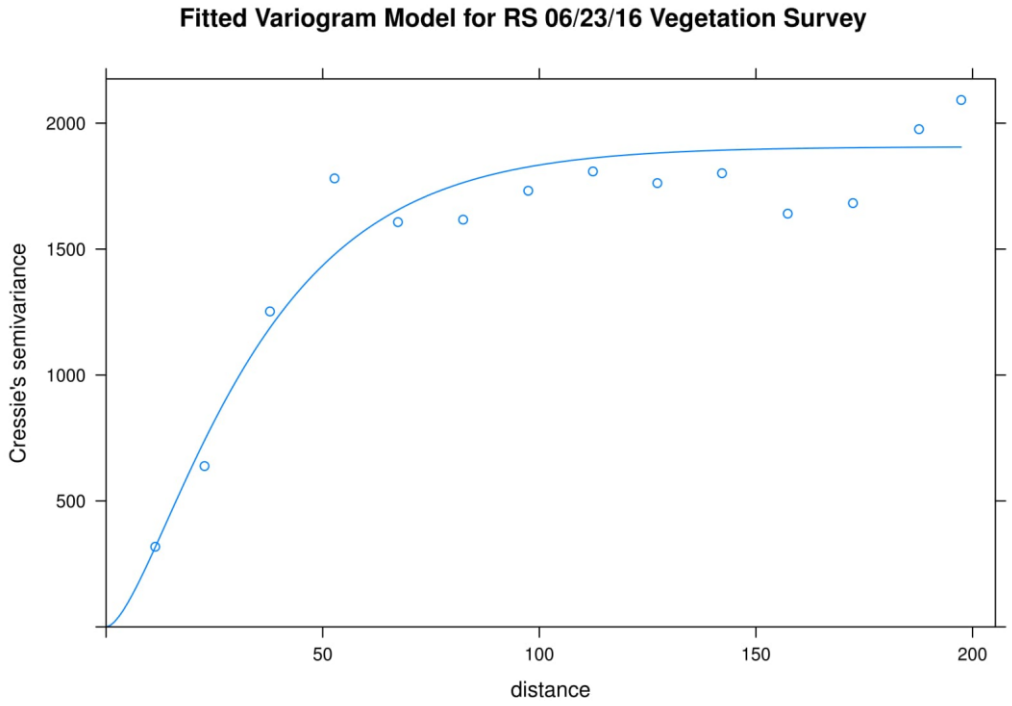

Figure 13D: Semivariogram model of the RS 06/23/16 vegetation survey.

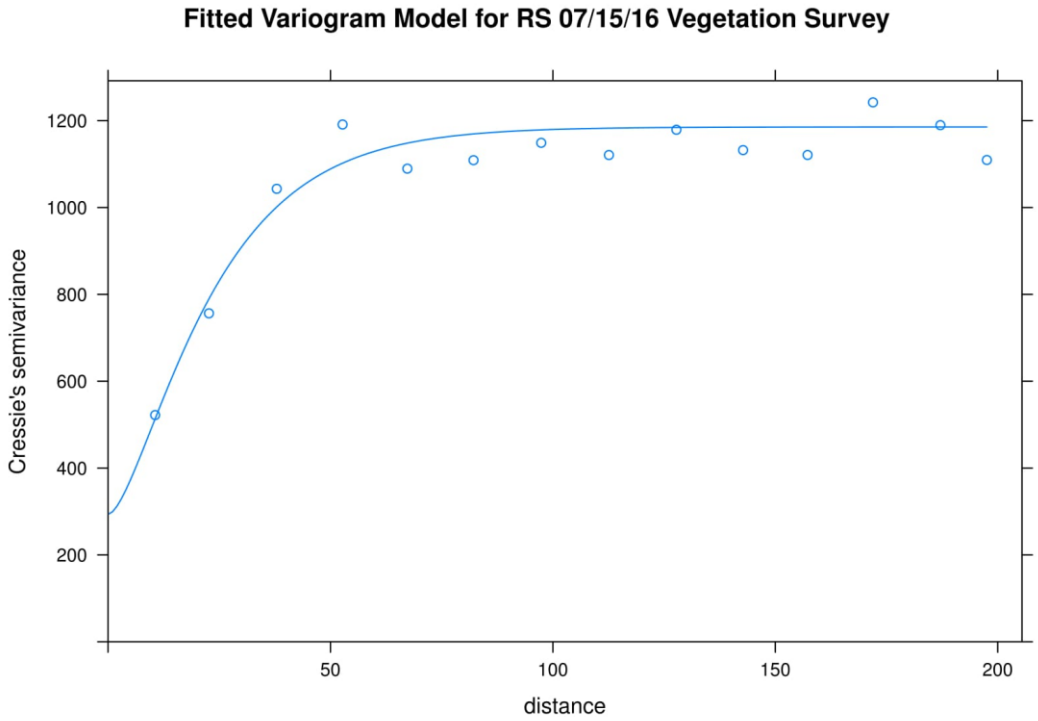

Figure 14D: Semivariogram model of the RS 07/15/16 vegetation survey.

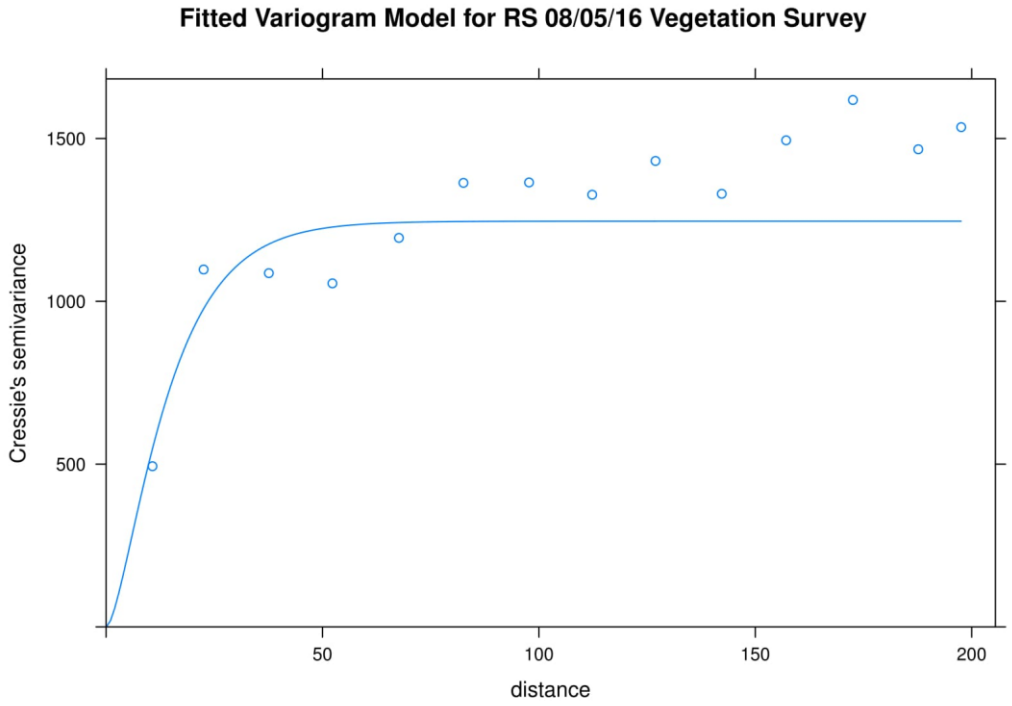

Figure 15D: Semivariogram model of the RS 08/05/16 vegetation survey.

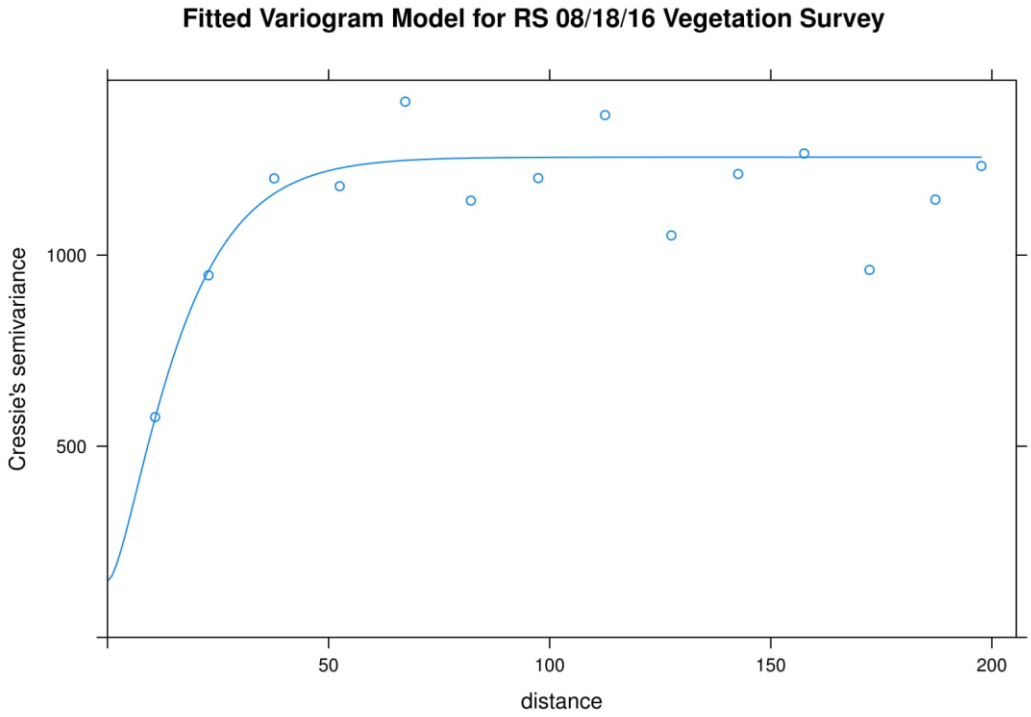

Figure 16D: Semivariogram model of the RS 08/18/16 vegetation survey.

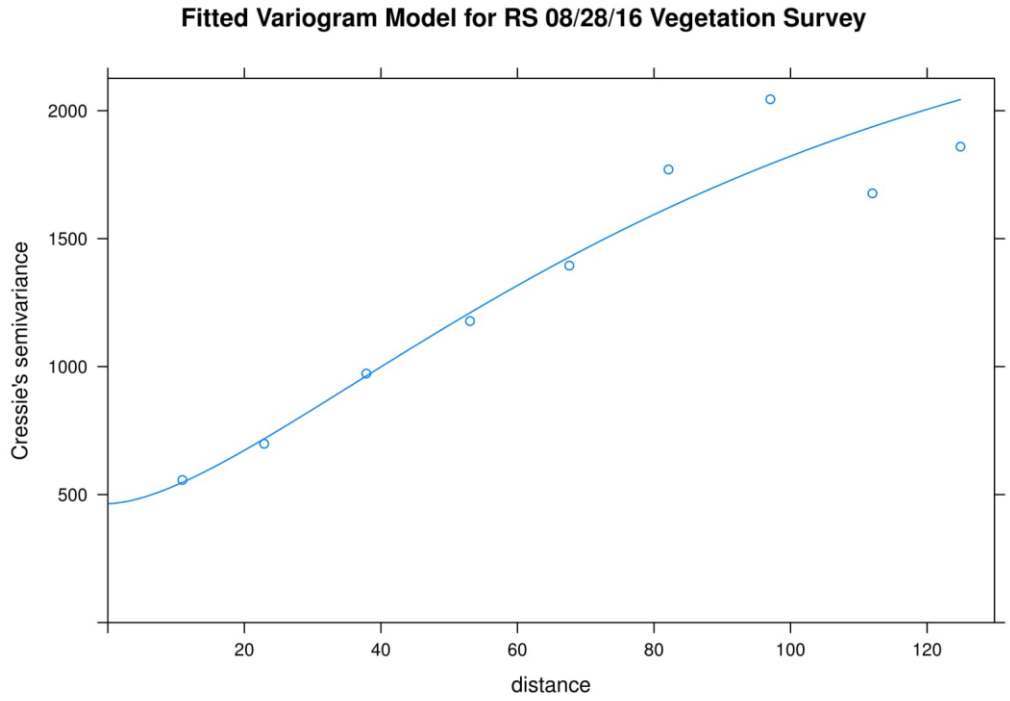

Figure 17D: Semivariogram model of the RS 08/28/16 vegetation survey.

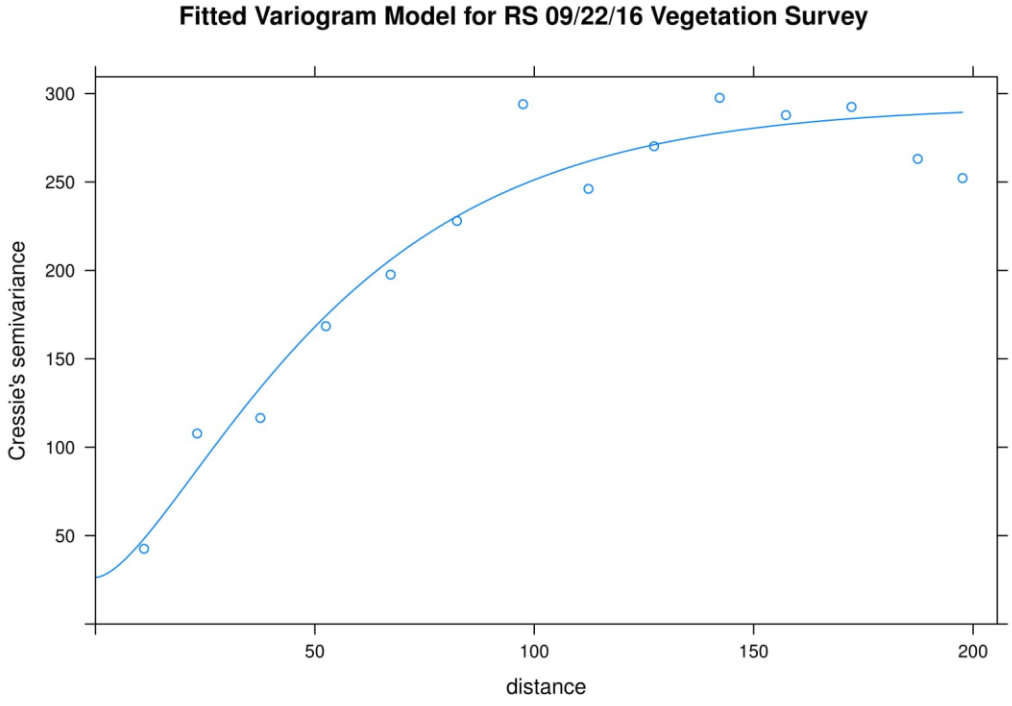

Figure 18D: Semivariogram model of the RS 09/22/16 vegetation survey.

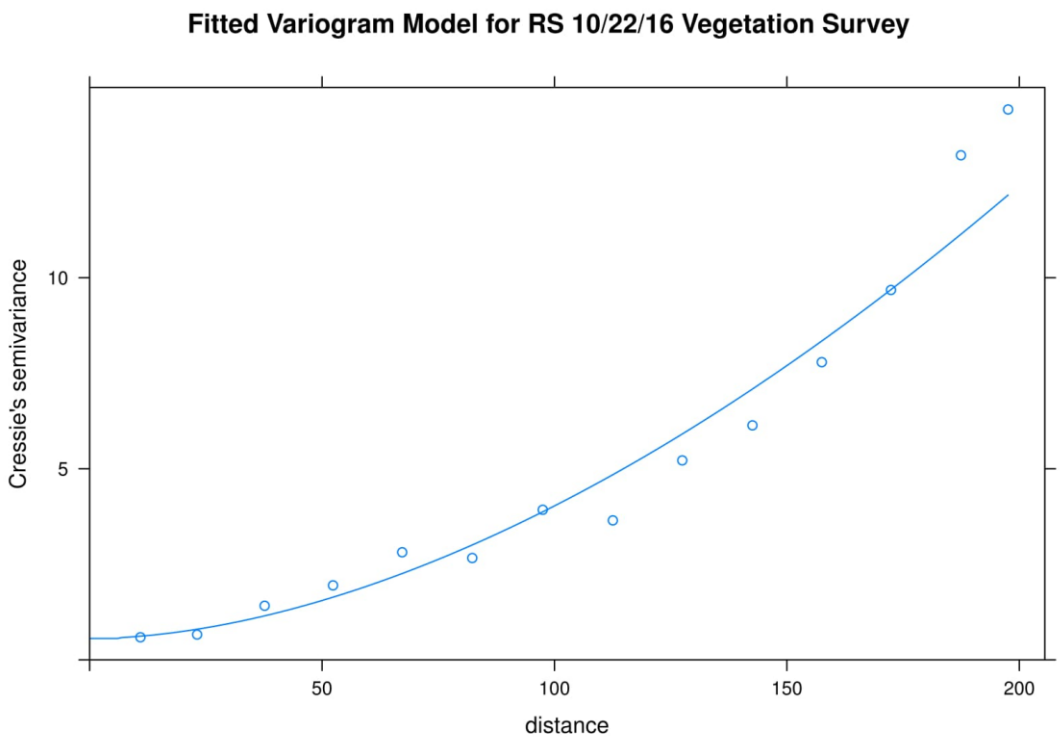

Figure 19D: Semivariogram model of the RS 10/22/16 vegetation survey.